Synthesis and Characterization of Ionomers andPoly(fullerene)sfor Promising Application in Organic Electronics.

Jéssyka Bittencourt

International Joint Doctorate Thesis

UNIVERSIDADE ESTADUAL PAULISTA "JÚLIO DE MESQUITA FILHO"
Programa de Pós-graduação em Ciência e Tecnologia de Materiais
and
UNIVERSITÉ DE PAU ET DES PAYS DE L'ADOUR
Ecole Doctorale Sciences Exactes et leurs Applications

Jéssyka Carolina Bittencourt

Synthesis and Characterization of Ionomers andPoly(fullerene)s for Promising Application in Organic Electronics

Brazilian supervisor: Profa. Dra. Clarissa de Almeida Olivati
French supervisor: Dr. Roger C. Hiorns

2023

Jéssyka Carolina Bittencourt

Synthesis and Characterization of Ionomers and Poly(fullerene)s for Promising Application in Organic Electronics

Thesis presented as a requirement to obtain the title of Doctor at the São Paulo State University "Júlio de Mesquita Filho" – Graduate Program in Materials Science and Technology, area of concentration of Polymeric, Hybrid and Nano-Structured Materials, under the supervision of Prof. Dr. Clarissa de Almeida Olivati and Dr. Roger C. Hiorns.

Presidente Prudente

2023

Acknowledgments

I would like to thank all those who contributed to the development of this doctoral research. I am especially grateful to those that helped me during the period when I was pregnant and could not work in the laboratory.

To thank my advisor, Prof. Dr. Clarissa de Almeida Olivati, who has been with me since my master's degree always helping me with all my difficulties working in this area of materials, thank you also for all the friendship.

To my advisor, Dr. Roger C. Hiorns, for accepting to guide a completely clumsy mathematician in a chemical synthesis laboratory, for always supporting and encouraging me by saying that I was a great chemist. Thank you so much!!!

My research group (LOFF – UNESP) and especially my brother Jefferson (Guto) and Maria Eduarda (Duda), because without them I would not have been able to.

To all my friends from Prudente (some are rich in Europe) who have always helped and supported me and often drank with me so I didn’t freak out.

All the friends I made when I was in France that made me feel closer to home.

To the Microfabrication Laboratory (LMF/LNNano/CNPEM – Brazil) for the manufacture of the interdigitated electrodes.

I would like to thank the committee members for their time in reading this thesis. I am sure that the suggestions and criticisms will contribute to improving the text and my scientific career.

My family, my husband Duber for all partnership, friendship, companionship, for always supporting and encouraging me, our baby Rafaela (our greatest achievement to date!) who has brought more joy to our lives, you are the loves of my life. To my parents and my brothers Sidmar, Clarice, Jeffrey and Guto who have always supported me, to my grandfathers Cidinha and Antônio for all the affection and love that is attributed to me until today and finally, but not least to my uncles, Cezar, Mariza, Dede and Cristina for the conversations and advice of always.

FAPESP, CAPES and the Eiffel Program of Excellence scholarships for their financial support.

O presente trabalho foi realizado com apoio da Coordenação de Aperfeiçoamento de Pessoal de Nível Superior - Brasil (CAPES) - Código de Financiamento 001.

This study was financed in part by the Coordenação de Aperfeiçoamento de Pessoal de Nível Superior - Brasil (CAPES) - Finance Code 001.

SUMMARY

LIST OF FIGURES

BITTENCOURT, Jessyka Carolina. **Synthesis and Characterization of Ionomers and Poly(fullerene)s for Promising Application in Organic Electronics: 2023.** PhD in Materials Sciences and Technology – UNESP, Faculty of Science and Technology, Presidente Prudente, 2023.

Abstract

The development of sensors goes through several parameters that must be analyzed systematically, among them: the potential for rapid detection, sensitivity, selectivity, and portability. For this, the processing of materials, which involves a sensory layer, deserves special attention so that the final performance is satisfactory. In addition to processing, the selection and synthesis of new materials as a sensor element is equally important in the development of versatile devices, bringing new possibilities for systems with reliability and durability. In this sense, polymeric materials are versatile, both in terms of synthesis and processing, opening up new possibilities for sensor devices. This work presents the application of polymeric materials, ionomers and a copolymer based on fullerene, as an ammonia gas sensor produced with different processing techniques, namely: Langmuir-Schaefer, Drop-cast and Spin-coating. The copolymer based on fullerene and Poly(ethylene oxide)-PEO was synthesized during the sandwich doctorate period at the Université de Pau et des Pays de l'Adour, France, at the Institute of Analytical Sciences and Physico-Chemistry for Environment and Materials - IPREM . The devices were characterized through the techniques of visible ultraviolet (UV-vis) spectroscopy, atomic force microscopy (AFM), DC electrical measurements and gas testing with monitoring of the electrical current as a function of the time of exposure to the ammonia gas, in which show that it is possible to apply the materials involved as a sensor element.

BITTENCOURT, Jéssyka Carolina. **Synthesis and Characterization of Ionomers and Poly(fullerene)s for Promising Application in Organic Electronics: 2023.** Doutorado em Ciência e Tecnologia de Materiais – UNESP, Faculdade de Ciências e Tecnologia, Presidente Prudente, 2023.

Resumo

O desenvolvimento de sensores passa por vários parâmetros que devem ser analisados sistematicamente, entre eles: o potencial de detecção rápida, sensibilidade, seletividade, preparação da amostra, e portabilidade. Para isso, o processamento de materiais, que envolve uma camada sensorial, merece atenção especial para que o desempenho final seja satisfatório. Além do processamento, a aplicação e síntese de novos materiais como elemento sensor é igualmente importante no desenvolvimento de dispositivos versáteis, trazendo novas possibilidades para sistemas com confiabilidade e durabilidade. Nesse sentido, os materiais poliméricos são versáteis, tanto em termos de síntese quanto de processamento, abrindo novas possibilidades para dispositivos sensores. Este trabalho apresenta a aplicação de materiais poliméricos, ionômeros e um copolímero à base de fulereno, como sensor de gás amônia produzido com diferentes técnicas de processamento, a saber: Langmuir-Schaefer, Drop-cast e Spin-coating. O copolímero à base de fulereno e poli(óxido de etileno)-PEO foi sintetizado durante o doutorado sanduíche na Université de Pau et des Pays de l'Adour, França, no Instituto de Ciências Analíticas e Físico-Químicas do Meio Ambiente e dos Materiais - IPREM. Os dispositivos foram caracterizados através das técnicas de espectroscopia no ultravioleta visível (UV-vis), microscopia de força atômica (AFM), medições elétricas DC e testes de gases com monitoramento da corrente elétrica em função do tempo de exposição ao gás amônia, nos quais mostram que é possível aplicar os materiais envolvidos como elemento sensor.

BITTENCOURT, Jéssyka Carolina. **Synthesis and Characterization of Ionomers and Poly(fullerene)s for Promising Application in Organic Electronics: 2023.** Thèse (Doutorado em Ciência e Tecnologia de Materiais) – UNESP, Faculdade de Ciências e Tecnologia, Presidente Prudente, 2023.

Résumé

Le développement de capteurs implique plusieurs paramètres qui doivent être systématiquement analysés, notamment: le potentiel de détection rapide, la sensibilité, la sélectivité, la préparation des échantillons, et la portabilité. Pour y parvenir, le traitement des matériaux, qui implique une couche sensorielle, mérite une attention particulière afin que les performances finales soient satisfaisantes. Outre le traitement, l'application et la synthèse de nouveaux matériaux en tant qu'éléments de détection sont tout aussi importantes dans le développement de dispositifs polyvalents, offrant de nouvelles possibilités pour des systèmes fiables et durables. En ce sens, les matériaux polymères sont polyvalents, tant en termes de synthèse que de traitement, ouvrant de nouvelles possibilités pour les dispositifs de détection. Ce travail présente l'application de matériaux polymères, d'ionomères et d'un copolymère à base de fullerène, en tant que capteur de gaz ammoniac produit avec différentes techniques de traitement, à savoir : Langmuir-Schaefer, Drop-cast et Spin-coating. Le copolymère à base de fullerène et de poly(oxyde d'éthylène)-PEO a été synthétisé lors du doctorat sandwich à l'Université de Pau et des Pays de l'Adour, France, à l'Institut des Sciences Analytiques et Physico-Chimiques de l'Environnement et des Matériaux - IPREM. Les dispositifs ont été caractérisés par spectroscopie ultraviolette visible (UV-vis), microscopie à force atomique (AFM), mesures électriques en courant continu et tests de gaz avec surveillance du courant électrique en fonction du temps d'exposition au gaz ammoniac, qui montrent qu'il est possible de appliquer les matériaux impliqués comme élément de détection.

Introduction

Conductive polymers, or conjugated polymers, and their derivatives have been used as the active layer of gas sensors since the early 1980s. [1] Their use has been growing more and more over the last decades [2]. This class of materials has many interesting characteristics for detection, and while less sensitive and slower in general than inorganic sensors, their sensitivity and response times can be tuned by synthetic variations [3]. Their excellent processing capabilities and good malleability opens up endless possibilities for the application of these materials [4,5].

To extend the functions or improve their performance, modifications are proposed in the chemical structure, through chemical synthesis or different forms of processing, seeking to circumvent the difficulties and improving the devices in termsof performance, durability, reliability, or manufacturing cost.

Through structural modifications polymers can be modified forming copolymers, joining two or more types of monomers in a polymeric chain, improvingthe properties of a sensory unit, that is, the development of copolymers is a considerable alternative that can have better properties and overcome limitations which their polymeric basic units are limited [6].

Due to the versatility in processability that polymers present, they can be easily manufactured in different ways and by various techniques, such as inkjet printing, drop-casting, Langmuir thin films, spin and spray-coating, *in-situ*polymerization. [7], among others, contributing to the improvement of gas detector systems on a nanometric scale.

Ammonia is a particularly dangerous gas being widely used in numerous industrial processes, such as the production of fertilizers, and therefore this work sought the study and development of an ammonia gas sensor. Specifically, we choseto use thin-films of polymers, to reduce the material requirements, and compared theimpact of processing on the sensor capabilities. The techniques of casting, spin- coating and Langmuir thin-film formation were examined. We decided to investigateionomers based on a block copolymer of sulfonated polystyrene and poly(methyl methacrylate) (PMMA), chosen for its combination of conductivity arising from the ionic groups, and flexibility and strength coming from the PMMA. We then chose toprepare a new and novel block copolymer based on fullerene (C_{60}) and poly(ethyleneoxide) (PEO). These materials were chosen for their ease of preparation and because good film formation was expected. Combining the highly hydrophobic fullerene and the water-soluble, hydrophilic PEO was expected to give amphiphilic materials thatmight self-organize to

give interesting structures with increased surface areas. Also,the strong electrophilic qualities of fullerene were expected to increase the sensitivity of the system towards ammonia. This work will demonstrate the first published example of an amphiphilic poly(fullerene) block copolymer prepared using the so- called stereochemically controlled azomethine ylide polymerization (SACAP) route.We then consider a very novel system, exploring the preparation of a 2- dimensional polymer made *in-situ* in the Langmuir trough. Although this material has not yet been investigated for its sensor properties, it was explored because it wasexpected to be an exceptionally interesting material for organic electronics, allowing a thin layer film to show simultaneously both hydrophilic and hydrophobic qualities,with each being exhibited on either side of the film. These initial studies should open the gate to future work, exploring this novel material for sensors, but also for use inorganic photovoltaics and other applications. It is, to our mind the first knownexample of an extremely thin (mono-molecular) material with opposing hydrophilic and hydrophobic faces.

The PhD is thus divided into the following chapters:

Chapter 1

Here we briefly review the relevant materials to the work performed in this thesis. We then look at fullerenes and their polymers, and poly(ethylene oxide) (PEO). Thesematerials are chosen for the reasons of the high electrophilicity of the fullerene (thusexpected improved sensibility to the gas ammonia), the hydrophilicity of the PEO tomake amphiphilic materials with the fullerenes and introduce interesting structures inthe films. By way of introduction to gas sensors we consider organic electronics in general, before focusing on the operation of gas sensors. We also consider the variousmethods of thin film processing.

Chapter 2

This chapter follows the preparation of the ionomer thin films, and the study of theiruse as gas sensors with ammonia.

Chapter 3

This chapter looks at the study of thin films made from the fullerene-based block copolymer.

Chapter 4

This chapter looks at the preparation of extremely novel thin films based on a light initiated polymerization of a product JB17 prepared in Pau, and performed in the Langmuir trough. The initial results are extremely promising, and this film would beexpected to be of interest for use in organic electronic devices where extremely thin films that can interface between inorganic and organic materials can be of use. In particular we are interested in this material because it presents the interesting propertyof being hydrophobic on one side, and hydrophilic on the other. .

Chapter 1 – Bibliographic Review

1.1 – Polymers

Polymers, known by society as plastics, revolutionized the area of materials, replacing many products that were produced using metals and ceramics, and their development began more quickly during the period of the two world wars [8]. The great advantage of polymers lies in their ability to synthesize, with the possibility of modifying various physical and chemical properties, and processing, using a range ofsolvents and at low temperatures, when compared to metals and ceramics and this has guided our decision to work with them.

The term Polymers, of Greek origin, Polys = many, Meros = repeating units, was created by the German chemist J. Berzelius in 1832, but only came to be used as it is known today, after 1922. Berzelius tried to create a term to differentiate organic molecules that had the same chemical elements but not necessarily the same chemical properties [9-11]

Polymers are synthesized from a simple molecule, which are monomers, by a process called polymerization, which can be done in two ways, step polymerization or chain polymerization. The first can be done through polyaddition or polycondensation, that is to say, respectively additions of small molecules without or with a loss of a small condensate like water to give a polymer. The second main type, chain polymerizations, include for example radical polymerizations that use an initiator to start a reaction of multiple monomers in one chain Figure 1 Monomers can give high or low molecular weight polymers that can be linear or branched.

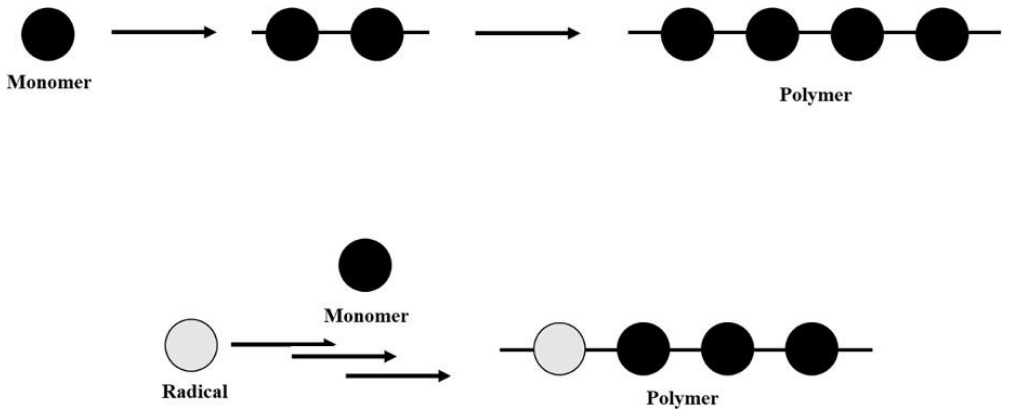

Figure 1-Representation of the two main classes of polymerizations. Above, a step polymerization where small oligomers are made first. Step polymerizations can also

be called polycondensations or polyadditions, depending on whether they lose small molecule durin.

Due to the different properties that polymers can present, they have different classifications in engineering, either by their chemical structure, method of preparation, behavior or mechanical performance, crystallinity, amongst others. [12] The enormous number of polymers, and their exceptional range of qualities, all tied directly to their structure makes them an exceptionally interesting class of materials to work with. While their chemical structure can determine their qualities such as electrophilicity, (semi)conductivity etc., often the molecular weight of the polymer can have the greatest impact. High molecular weights (> 100 000 g mol^{-1}) lead to rigid materials, while low molecular weights (<10 000 g mol^{-1}), tend to give materials which are mechanically weak.

Polymers can also be referred to as homopolymers and copolymers, as shown in Figure 2. Homopolymers are formed from a single type of monomer, whereas copolymers are formed from two or more types of monomers. [13,14].

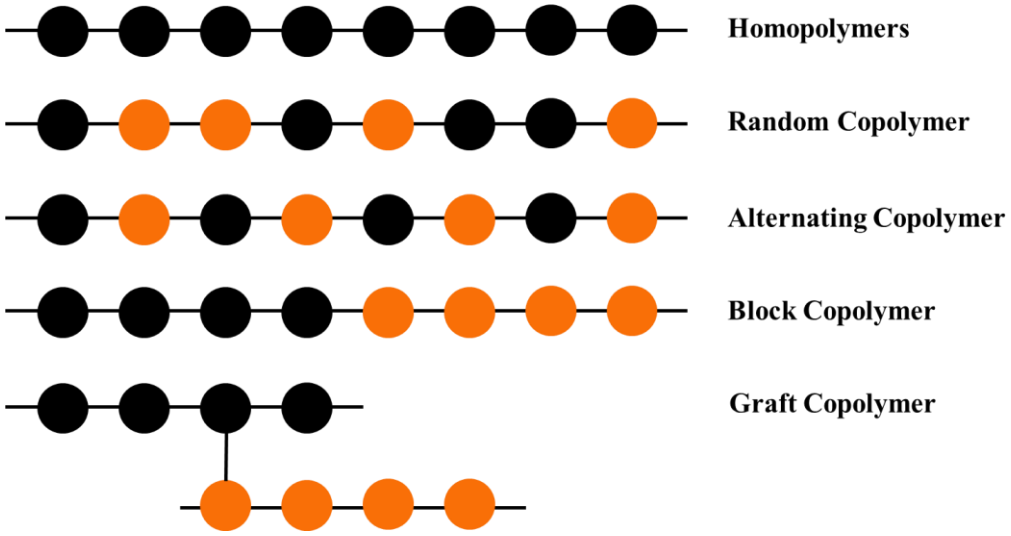

Figure 2-Representation of different types of polymer structure, in accordance with IUPAC terminology.

These materials are widely used in all areas of engineering, as they are extremely versatile, practical and mostly economical products. Some examples of polymer applications are: paint bases, tires, car parts, adhesives, fibers and coatings for optical fiber and high voltage wires, among others. Such multiplicity of applications derive from the ease of synthesis and processing, combined with its low cost compared to other materials, in addition to important electrical, optical, thermal and biochemical properties. [15].

In addition to all the revolution caused by polymers, being called "the era of

plastics" by various sectors of society, this class of material came to prominence again at the end of the twentieth century and opened new fields for scientific research, due to the discovery electrical and electronic conductive properties similar to those of inorganic semiconductors [16], expanding the range of applications to sensors and photovoltaic devices, for example.

1.1.1-Ionomers – their structure and properties

Here we consider ionomers as we expect them to be of particular interest to sensors given their ionic nature, of use for interesting with gases, and in allowing conductivity. The term ionomer was first used in 1964 [17]. They are structures in which a polymer is combined with an ionic group, at a low concentration of charged units along the chain [18]. Figure 3 shows the various known structures of ionomers. These variations in structure can impact on the electronic conductivities of the materials, but also on their physical qualities, such as malleability, and solubility in the solvents used. Furthermore, more variations can be introduced by changing the ionic groups from sulfonic, to carboxylic or phophosphoric acid, for examples, and the counterions from protons to monovalent or multivalent ions [19].

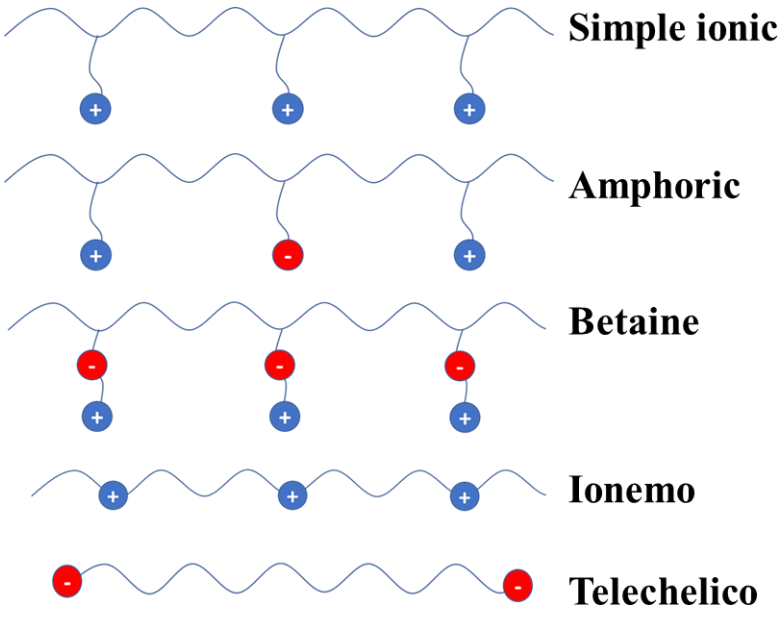

Figure 3-The various common architectures taken up by ionomers.

The presence of these ionic groups in the polymer drastically alters some of its properties, such as the increase in viscosity of several orders of magnitude and changes in the glass transition of hundreds of degrees.

Ionomers differ from polyelectrolytes due to long electrically neutral groups

and small ionized groups, at a concentration of no more than 15 mol% [20], while polyelectrolytes are polymers containing large amounts of densely packed ionic groups [21]. To differentiate, an example of a polyelectrolyte might therefore be polystyrene sulfonate with more than 15 mol% of sulfonate groups along the polymer chain.

In addition, the diffusion coefficients can be modified drastically, mainly due to the presence of reversible ionic cross-linkages in these materials. Due to the low dielectric constant of most organic polymers, ions or ionic dipoles tend to aggregate. This aggregation process, however, is limited, because the ionic groups are covalently linked to the organic chain, therefore limiting the impact on polymer processing and solubiliization[22].

Ionomers are insoluble in water but can be dissolved in low- and high-polarity polar solvents. When dissolved in low-polarity solvents, the ionic groups are not dissociated, and the polymers exhibit intermolecular aggregation between the ion pairs. In highly polar organic solvents, e.g., dimethylformamide and dimethylsulfoxide, the ionomers behave like polyelectrolytes [23], due to the Coulomb repulsive forces of the ionic groups, as the dissociation of ionic groups in the main chain leads to the formation of macroions.

Interactions between the pendent ionic groups, either in solution or in solid films, can impact heavily on the electronic and physical processing properties of ionomers. This also widens the range of applications for which they can be used, such as fuel cells, water purification, batteries and sensors [19]. While there are many that are widely used, this short review will focus on the ionomers used in this work.

1.1.1.1-Sulfonated Polystyrene (SPS)

Sulfonated polystyrene (SPS) is a derivative of polystyrene (PS), containing ionic groups covalently linked to its polymeric chain [24,25]. The degree of sulfonation impacts heavily on the processing properties and solubility of the polymer, and therefore controlling the degree of sulfonation of the SPS is of fundamental importance to obtain an adequate product that can formed into thin-films.

Figure 4 shows the structure of PS and SPS, where the units of x and y change depending on the degree of sulfonation. When the value of y increases, we have a greater degree of sulfonation with a consequent reduction in the value of x.

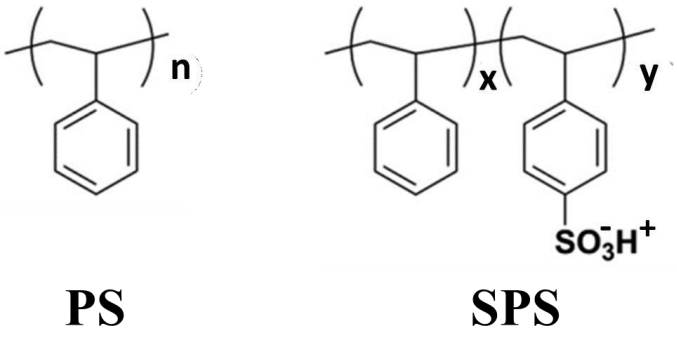

Figure 4-Structure of polystyrene (PS) and poly(sulfonated styrene) ionomer (SPS).

In the sulfonation of PS, a hydrogen is replaced by a sulfonic acid group (-SO3H) that will be covalently bonded to a carbon atom of the chain, thus modifying the chain [26]. Sulfonation reactions are typically electrophilic substitutions, in which the oxygen atoms in the -SO3H group are more electronegative, attracting the electron density of the sulfur atoms, acting as an electrophilic region. [27]. This electrophilic region can react with the delocalized π electrons of the aromatic ring in the position of highest electron density. [28].

Sulfonated products have different characteristics in relation to the respective homogeneous chain, such as better ionic conductivities, greater hydrophilicity, consequently better solubility in aqueous or high polarity systems [29].

1.1.1.2-Poly[styrene-*mod*-(sulfonated styrene)-*co*-(methyl methacrylate)], more commonly called SPS-*co*-PMMA

As shown in Figure 5, poly[styrene-*co*-(methyl methacrylate)] (PS-*co*-PMMA) can be sulfonated at the PS groups, to produce poly[styrene-*mod*-(sulfonated styrene)-*co*-(methyl methacrylate)] (SP-*mod*-SPS-*co*-PMMA). The sulfonation is performed at a relatively low temperature of around 40 ˚C using a well-known protocol [29,30].

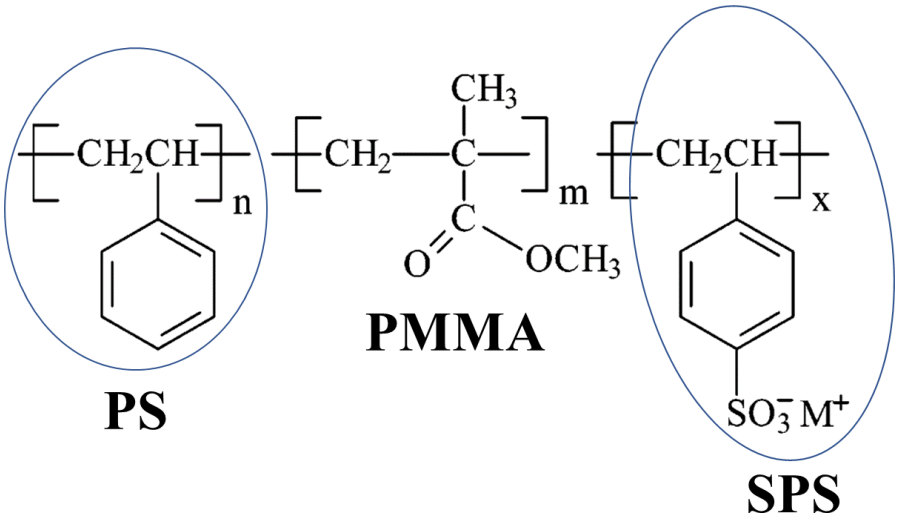

Figure 5-Structure of the SPS-co-PMMA ionomer formed by the SPS and PMMA copolymer.

Selective sulfonation occurs through an electrophilic aromatic substitution reaction that attacks the PS aromatic rings to modify them with a sulfonic acid group. The sulfonation occurs directly for aromatics, although the dissociation energy of the C-H bond is higher in aromatics (428 kJ/mol) than in aliphatics (374 to 384 kJ/mol), and only one sulfonic acid group (-SO3H) can be attached to each aromatic ring [30]

Briefly, the sulfonation reaction occurs in two main steps: the first step corresponds to the addition of the strongly electrophilic sulfonic acid group, which reacts with the electron system π delocalized from an aromatic ring. In the second step of the reaction, a hydrogen atom is abstracted by an oxygen atom (anion, produced in the first step) and produces acetic acid as a byproduct [31].

1.1.2-Fullerenes

Here we consider fullerenes as they are one of the materials that will be used in our work on thin-films sensors. Fullerenes were discovered in 1985 by a group of scientists who obtained several structures ranging from 20 up to around 90 carbon atoms, and where the most stable was found to be that formed by 60 carbons (C60). This was a major discovery of the 20th century, as it broadened the range of allotropic forms of carbon, [32] and won the 1996 Nobel Prize for chemistry for Robert Curl, Harold W. Kroto and Richard Smalley.

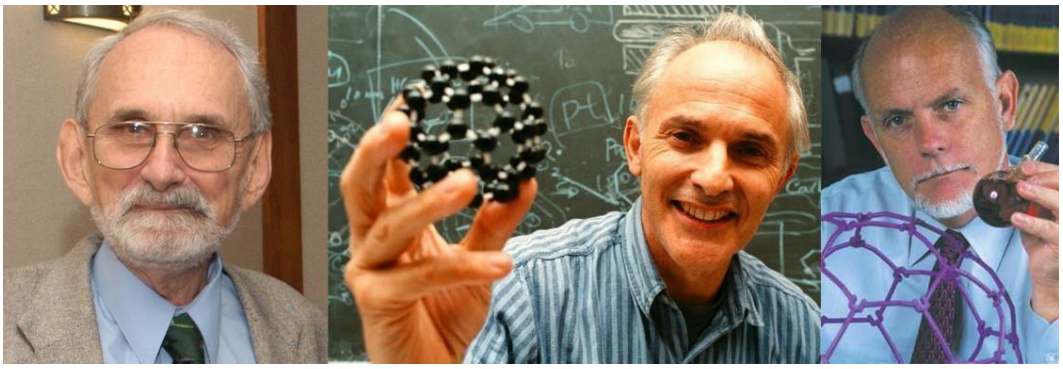

Figure 6-The 1996 Nobel Prize winners for chemistry: Robert Curl; Harold W. Kroto and Richard Smalley, from left to right, respectively.

Buckminsterfullerenes, as fullerenes are also known due to their resemblance to architectures designed by Buckminster Fuller, are part of a large family of symmetric molecules, composed of several carbon atoms distributed at the vertices of an Archimedean solid. The most common form of fullerene is C_{60}, which resembles a football, but other forms composed of more or less carbon atoms can also be found or calculated, such as C_{20} and C_{70} as shown in Figure 7 [32].

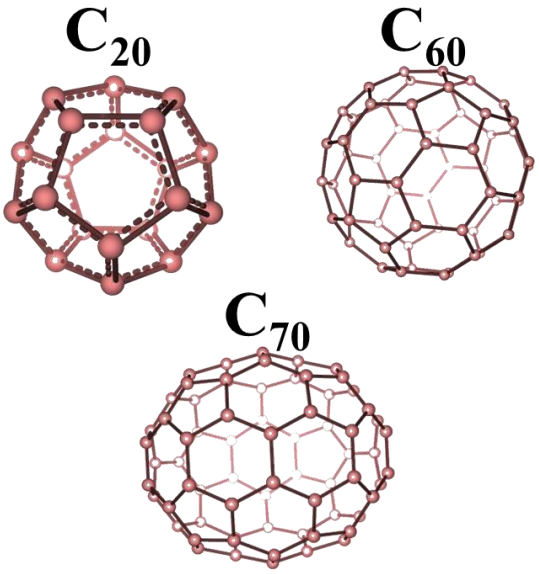

Figure 7-Some forms of fullerenes that can be synthesized, such as C_{20}, C_{60} and C_{70}.

Since their discovery, fullerenes have attracted the attention of researchers from different areas due to their three-dimensional nanostructure, in addition to their electrochemical, electrocatalysis and photocatalysis properties [33]. Fullerenes also have good semiconductivity, high surface area, and chemical stability, which facilitates electron transport. [34,35].

Recently, research using fullerenes as a modifier material has been growing and with that it is being considered a new attraction for the development of sensors and biosensors. The low solubility ends up being a problem for the processing of this

material, for this reason, research has been carried out around the synthesis of fullerene derivatives to increase the range of solvents that can be used [36,37], facilitating the processing of these compounds.

Since the first study on the light-induced charge transfer of a conjugatedpolymer to a fullerene (C_{60}) in 1992 by Sariciftci *et al*. [38], the polymer-fullerenefield for organic photovoltaics (OPVs) has undergone a major revolution [39,40].Generally, fullerene is used as a modified adduct, which is phenyl-C_{61}-butyric acidmethyl ester (PCBM), as it has a higher solubility. However, PCBM still suffers from C_{60}'s tendency to aggregate and form crystals which can lead to thermal degradation. The fullerene derivative, PCBM is used as an electron acceptor (type n)
[41,42]. Its exceptional property of transferring charges through heterojunctions in the bulk (bulk-heterojunction - BHJs) [43,44] demonstrates its wide applicability, showing a tendency to self-organization to favor the collection and percolation of

electrons in lateral and vertical directions [45]. The PCBM, however, has some behaviors that are detrimental to the stability of a device. For example, its processing on thin films is sensitive, often leading to excessive aggregation [46].

Fullerenes are exceptional electron acceptors, with each molecule accepting up to 6 electrons, however, their exploration and chemistry are limited by the need to functionalize them to adjust their properties [47-49], to make them soluble and improve their malleability and physical stability. The synthesis of fullerene-based polymers with the use of an appropriate comonomer increases their solubility in organic solvents, raises their ability to form thin-films, and can be used to vary their properties.

Polymers incorporating C_{60} are classified as shown in Figure 8. Various structures can be used to bring C_{60} into a polymer. For example, it can be incorporated as a side-group or into the main chain. In general, side-groups tend to give less control over the properties of the material because the fullerene aggregates strongly. Therefore we prefer to use main-chain fullerene polymers because they generally show higher solubilities [50]. We can further change their properties by incorporating fullerenes into block copolymers (BCs). BCs have been the focus of broad scientific interest, both experimental and theoretical, due to their properties and numerous applications involving pharmaceuticals, biology, biomaterials, microelectronics and photovoltaic materials [51]. Interestingly, a BC can combine the properties of both blocks, to express both properties, for example, one block can be a semiconductor

and the other an insulator or a hydrophilic materials.

Also, because of different solubilities of each block, they can give rise to nano-dispersions in liquids, where one block might be soluble and the other not. These objects can range in scale from tens to several hundred nanometers, dependingon their structure and the dispersion matrix in which they are formed.

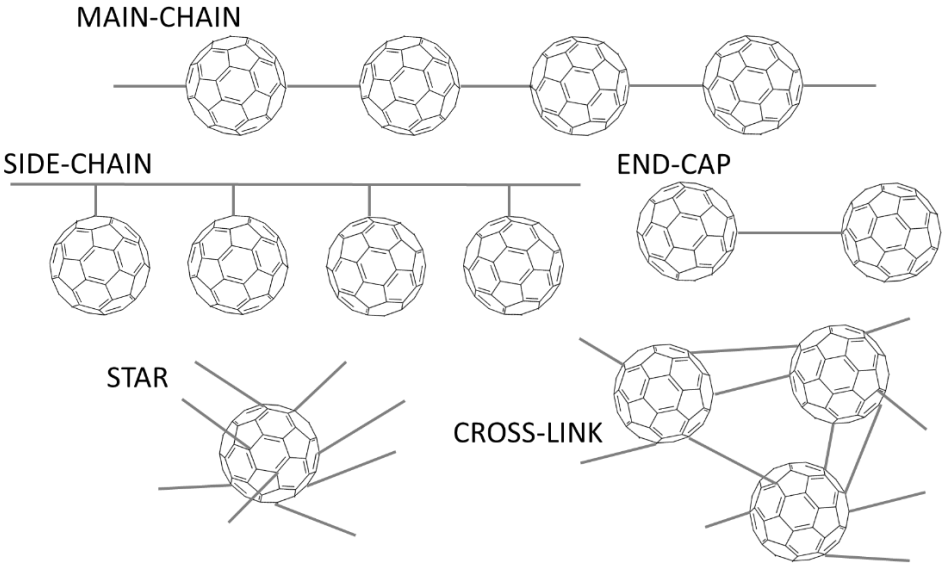

Figure 8-Copolymers classification based on C_{60}.

In our work we are particularly interesting in studying poly(fullerene)s due to their ability to combine the forementioned properties of fullerenes and polymers. There are only very few examples of BCs containing main-chain fullerenes [52-55]. While there are several different routes to make poly(fullerene)s, such as the atom transfer radical addition polymerization (ATRAP) route based on radical additions to C60, the so-called BAP route based on azide addition chemistry, we will exploit the the stereochemically controlled azomethine ylide polymerization (SACAP) of fullerene as it leads to the most robust poly(fullerene)s due to the strong cycloaddition between the comonomer and the fullerene.

1.1.3-Poly(ethylene oxide) (PEO)

We chose to work with poly(ethylene oxide) (PEO) because it is non-toxic, low-cost, and completely soluble in water. It was thought that this material would allow us to make a hydrophilic surface to the film to improve contact with the air. Also, it was thought that by combining PEO in a BC with the aforementioned poly(fullerene)s, it would give the resulting materials a more hydrophilic character, making their contact with the substrate and air easier. Also, given that BCs with the poly(fullerene)s would

result in amphiphilic materials, it means that they would form interesting film structures in the Langmuir trough that might be better organized than the poly(fullerene)s alone. It was expected that they might make materials with large surface areas that would increase the air-solid intereface, and thus improv ethe sensitivity of the device.

PEO is a polymer formed from the polymerization of cyclic ethylene oxides to give a synthetic polyether. This chemical compound is also known by other names such as poly(ethylene glycol) (PEG) or polyoxyethylene. In general, materials with molecular weights lower than 20 000 g/mol are called PEGs and those with molecular weights above 20 000 g/mol are called PEOs [56].

The polymerization of PEO is performed through a substitution reaction [57] starting from the ethylene oxide monomer [58], as shown in Figure 9 this reaction was first performed in 1859 by the French chemist Charles Adolphe Wurtz.

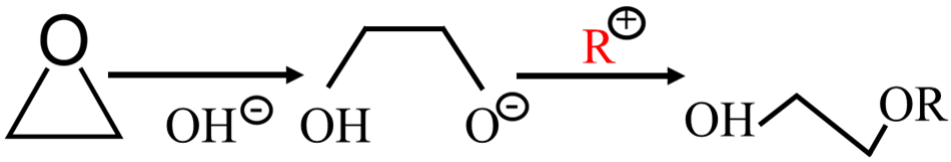

Figure 9-The polymerization reaction leading to poly(ethylene oxide). The metallic ion, typically, Na^+, K^+ or Cs^+ is not shown for simplicity.

PEO modified with chain-ends has an amphiphilic nature that means a hydrophobic syrup formed by carbons and a hydrophilic ionic head as in Figure 10 [59]. The high presence of oxygen atoms in the chain facilitates its solubilization in either in water or even organic solvents (ethanol, acetonitrile, toluene, acetone, dichloromethane, hexane and chloroform), colorless, odorless, clear and another advantage is the fact that it is a non-toxic material and with this is widely used in the pharmaceutical, cosmetic and food areas [60].

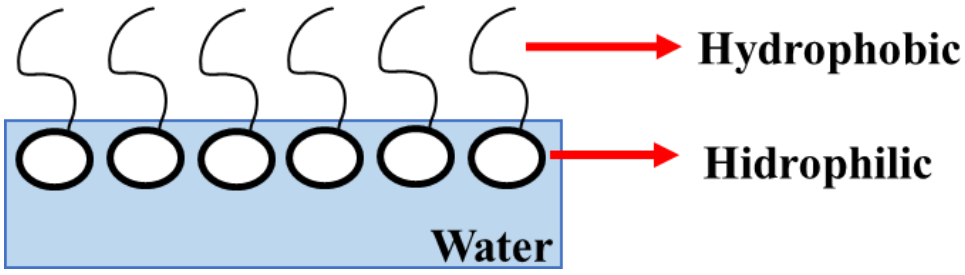

Figure 10-Behavior of PEO modified with chain-ends in water giving rise to amphiphilic behavior.

While PEO has been used for the formation of copolymers with C_{60}, to improve electronic and solubility properties, to better the processability of the final compound for various applications such as electronics and medical [61], as far aswe are aware, polymers of PEO and poly(fullerene)s have not been published before.

1.3-Gas sensors and "Electronic noses"

One of the first gas sensors was developed in 1925. It was an interferometer, which worked by measuring the interference of light waves. Since then, and especially in recent years, the demand and need for the detection of toxic substances has increased more and more [62], and as a result, different types of sensors have been developed and improved year after year [63,64] with technological advances, to satisfy the need for improvements. This has occurred in a wide number of areas, such as: the agricultural industry, bioscience, medicine, dentistry, etc. Especially important areas are the use of gas detectors to sense the presence of diseases and as essential safety equipment in industry, especially those involving the production of potentially toxic substances due to the mass production of artifacts and the confinement of large quantities of materials for industrial activity. There is a clear need to monitor dangerous gaseous products, to avoid possible leaks. This has given rise to the so-called electronic nosepiece and the gas sensor.

Electronic noses are sensors that can also detect gases, the term this name is more used for more complex detection systems that aim to imitate or replicate the human sense of smell. This implies the ability to identify and distinguish between different odors or volatile chemical compounds.

Typically, these devices are more specific, and can be used for analyzing aromas in foods [65], medical diagnosis based on body odors, such as detecting lung cancer through exhaled air [66], and other situations where odor discrimination is necessary, Figure 11 and Figure 12 exemplify two different types of electronic nose.

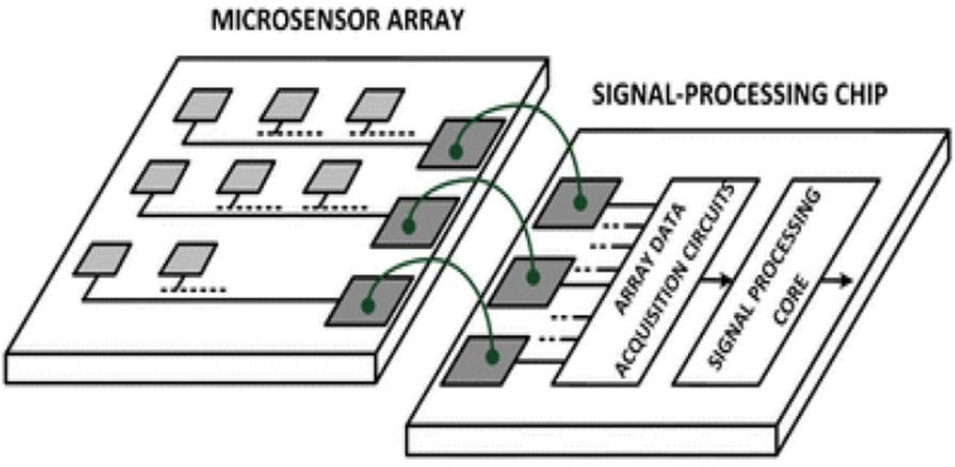

Figure 11-A two-chip solution for E-nose system, comprising a front-end sensor array and a back-end low-power signal-processing chip in 2014[67]

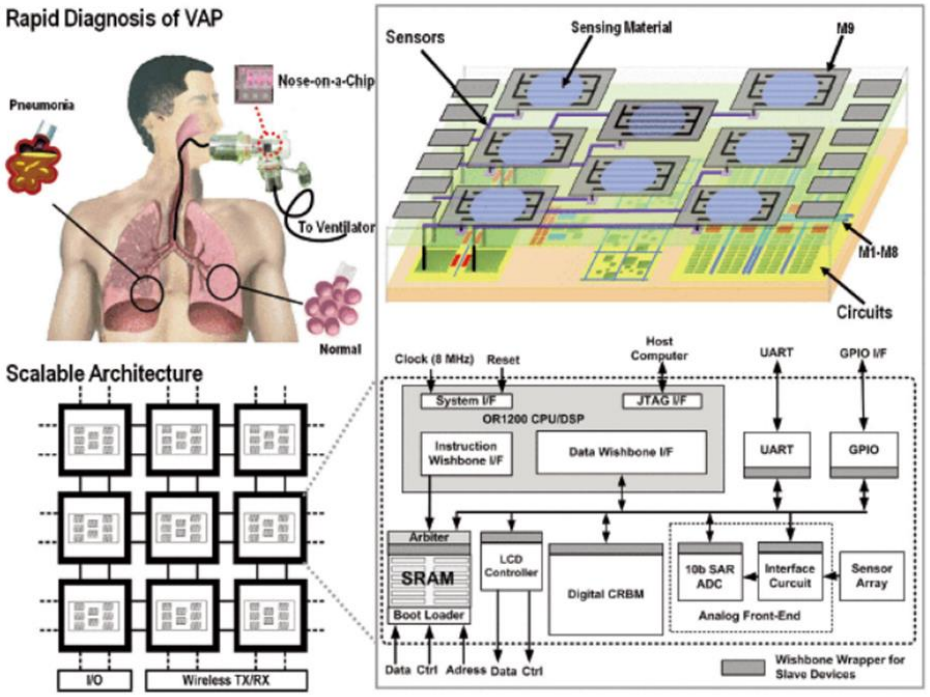

Figure 12-Target application scenario and top-level system view of the nose-ona-chip in 2014 [68].

Figure 12 microprocessor was adopted to perform the KNN algorithm (it is a classical supervised and instance-based learning algorithm. It is a non-parametric statistical method widely used in classification and regression [69] as a gas recognition circuit. The overall system had 100% classification accuracy when testing five alcoholic products [70]. Next we have figure Y with a system slightly different from the previous figure, in this case we have this fully integrated chip, which consisted of eight sensors on the chip, a reading interface circuit and a gas recognition circuit. The gas recognition circuit integrated two cores: (1) a restricted continuous digital Boltzmann machine (CRBM) core loaded with a probabilistic neural network for data dimension reduction; (2) a RISC core as a KNN classifier to generate recognition results. This device was used for rapid detection for ventilator-associated pneumonia with 95.73% accuracy.

The electronic nose has a variety of sensors that can include technologies such as gas sensors, but often involves a more sophisticated combination of methods such as mass spectrometry, optical spectroscopy and other methods for detailed odor analysis.

Gas sensors are broader devices that detect the presence of specific gases in the environment. These sensors can be used to monitor various types of hazardous gases including CO, CO_2, NO_x (x = 0.5, 1 and 2), SO_x (x = 2 and 3) and NH_3 as environmental and human health concerns grow. Just like the electronic nose, gas sensors can operate in different areas

such as: industrial production [71]; automotive industry [72]; medical applications [73]; indoor air quality supervision [74]; environmental studies [75]. Sensors can easily be used in different technologies, such as semiconductor gas sensors, fuel cells, infrared detectors, among others, depending on the type of gas to be detected.

Among the gas sensor applications is the detection of ammonia gas (NH_3), the detection of which has attracted substantial attention in the field of gas sensors, which is important because NH_3 is one of the most common chemicals manufactured and applied in several areas around the world. Around the world in society it is common to classify a sensor by the analyte to be detected, however in the field of research and development gas detectors are generally classified according to the operating mechanism [76], such as semiconductor, oxidation, catalytic, photoionization, infrared, among other classifications. Fundamentally, gas detection technologies can be divided into two groups; i) methods based on the variation of electrical properties and ii) other properties [77], as shown in Figure 13.

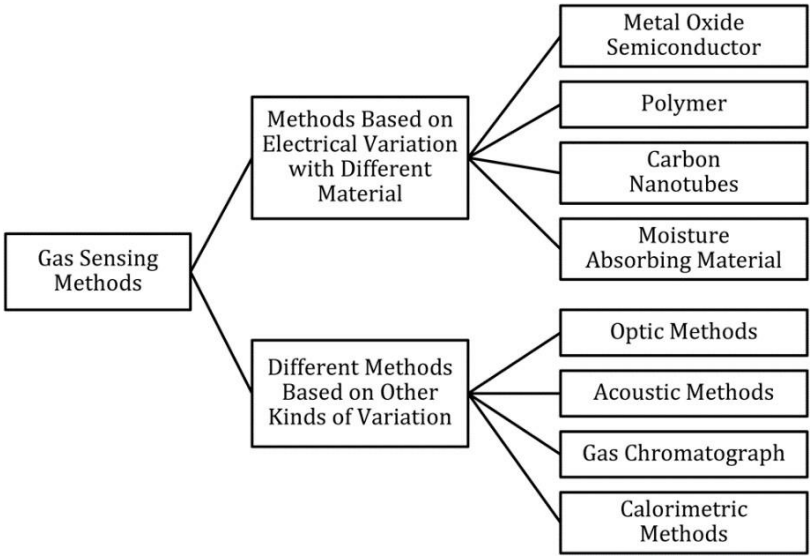

Figure 13-Classification of gas sensing methods, reproduced from reference.[77].

Ammonia is a gas that serves as a raw material for various applications. It is used in the manufacture of agricultural fertilizers, fibers and plastics, cleaning products and explosives. Being continuously monitored in industrial refrigeration processes and biological degradation processes [78], including exhaled air. Human perception in the air is from 53 ppm, however an amount of 25 ppm in the air can already cause lung problems. Another problem related to the excessive amount of ammonia in the air occurs in poultry farming centers [79], where this compound is produced by animal waste, harming the production of

eggs and poultry meat. Another latent problem is the leakage of ammonia gas, reported on the International Space Station (ISS) [80] and in industries [81], for example in refrigerators.

Gas sensors generally operate with a lower exposure limit of 25 ppm; however, ammonia detection for industrial safety requires continuous monitoring above the 0.1% fatal exposure limit [82]. Depending on the required sensitivity, different types of sensors are used, for example, flame ionization detector, semiconductor, electrochemical, photonic membranes [83].

Currently, there are different types of ammonia gas sensors, such as: i) electrochemical sensors: these are sensors that work through chemical reactions that occur in an electrochemical cell when ammonia is present. The resulting change in electrical current is measured and interpreted as an ammonia concentration. ii) thermal conductivity sensors: which measure changes in the thermal conductivity of air when ammonia is present. The presence of the gas affects the air's ability to conduct heat, and this change is converted into an electrical signal. iii) optical sensors: use optical technology to detect the presence of ammonia. The absorption of light at certain wavelengths is measured, and this absorption is related to the concentration of ammonia in the environment. iv) semiconductor sensors: which are based on semiconductors detect ammonia through changes in the electrical properties of a semiconductor material when exposed to gas [84,85].

Devices that use polymers with electrical properties, such as polypyrrole, polyaniline, polythiophene, etc. have the advantage of flexibility, low cost and, above all, being able to work at room temperature, as this is not possible in other types. of sensors. The detection mechanism of the conducting or semiconducting polymer for ammonia gas depends mainly on the oxidation-reduction reaction between the ammonia gas and the conducting polymer [86,87]. This sensor can be classified as a “chemical sensor”. There are several types of classifications of chemical sensors, for example, based on the type of output signal, chemical sensors can be classified as optical, magnetic, mass, thermal or electrochemical [88]. Knowledge of the gas detection mechanism plays an important role in the design of a gas sensor [89]. In this work, the sensors developed were classified as “electrochemical sensors”, as the interactions result in a measurable electrical signal. Due to the way the electrical property is measured, electrochemical sensors can have a more specific classification, such as Chemiresistive or Amperometric sensors [90].

Shi and Bai [91] carried out intense literature review in order to seek an explanation for the mechanism of interaction between ammonia and conducting polymers, in which they concluded that p-type conducting polymers dedope under an ammonia atmosphere, but some different phenomenon was observed in the polycarbazole thin film sensor [92], in which it

was observed that a decrease in electrical resistance occurred when it reacted with ammonia, concluding that further studies are still needed to clarify the interaction mechanisms between a conjugated polymer and the analyte.

For a better understanding, conducting polymers are composed of conjugates, these polymers in a neutral state have weak conductivity and can be modified into conducting or semiconducting states through chemical or electrochemical doping. [93]. Its conjugated double bonds comprise a σ bond and a π bond. The electrons in σ bonds form the backbone of the chain, which provides the mechanical properties of the conducting polymer. The π electrons delocalize along the entire chain due to overlapping π orbital molecules of neighboring conjugated structure. This contributes to the conductive and semiconducting properties [94]. Understanding the charge conduction mechanism of the conductive polymer is an essential step before understanding the gas sensing mechanism of the conductive polymer. [95].

Figure 14 makes it easier to understand the interaction of the polymer with ammonia.

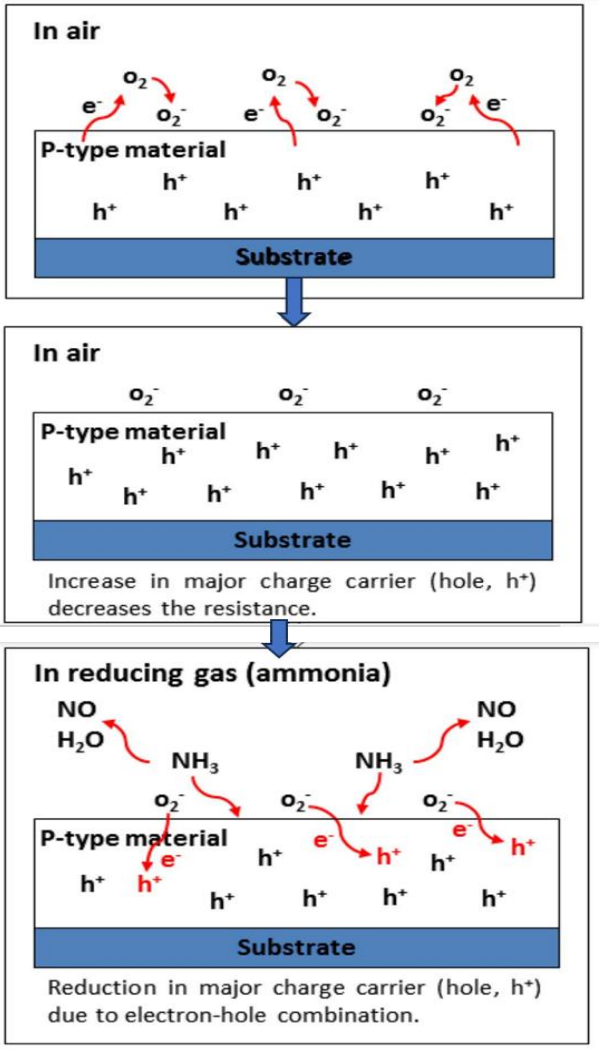

Figure 14-Sensing mechanism of p-type material in air and reducing gas environments.[96].

Holes and electrons are responsible for conduction in p-type and n-type semiconductors, respectively [97]

Figure 14 shows the typical gas detection mechanism of the p-type gas sensor in response to air and ammonia, respectively.

Doping and dedoping play vital roles in the gas detection mechanism of conductive polymer sensors [98] Doping with oxidizing agent, which is known as 'p-type doping', introduces charge carriers into electronic structure and forms p-type conductive polymer. On the other hand, the use of reducing agent corresponds to n-type doping [99]. Specifically, the detection response to various analytes is affected by the level of oxidation of the conducting polymer, which is also easily influenced by chemical or electrochemical doping/dedoping (oxidation/reduction) mechanisms between the interacting analytes and the conducting polymer. [100]. The doping and dedoping of most conducting polymers are achieved by redox reactions or protonation, where the latter only applies to polyaniline. The doping level is changeable by the transport of electrons to or from the target analytes. Electron transport can induce changes in the resistance and work function of sensing materials

Comparing gas sensor and electronic nose we can point out some advantages of gas sensors, such as; (i) simplicity and cost: they are often more accessible and easier to implement. If detection of specific gases is the only application requirement and it is not necessary to distinguish between different odors or compounds, a direct gas sensor may be more cost-effective and simple. [101] (ii) continuous monitoring: for applications that require continuous monitoring of gas levels in an environment, gas sensors may be more suitable as they are designed to provide real-time readings without the need for more complex analysis associated with electronic noses [102]. (iii) detect specific gases: are designed to detect specific concentrations of gases, which can be crucial in industrial or laboratory environments where the presence of specific gases needs to be closely monitored [103] (iv) operation in hostile environments: they can be designed to operate in adverse or extreme environments, such as places with high temperatures, high humidity or the presence of aggressive chemical substances. This robustness can be important in certain situations [104] (v) Power requirements: In some cases, gas sensors may be more power efficient, which can be an important consideration, especially in battery-powered applications [105]

1.4-Processing polymers into thin films

In order to better consider the use of polymers, it is worth considering that their processing has a high impact on their behaviors, changing their bulk and surface structures and film-thickness. The processing of nanostructured materials in thin films plays a fundamental role, aswell as the synthesis process, in the development of high-performance devices and materials, making the connection between active regions, acting as a structural element, isolating conductive layers, protecting surfaces from the external environment. Among the polymer processing techniques for organic electronics, we highlight the drop-cast, spin-coating and Langmuir techniques, which will be described below. These three techniques are key to polymer processing, and are known to give widely different film morphologies and surfaces. We describe each briefly here to show why we have chosen them.

1.4.1-Drop-casting

The drop-cast technique is very simple compared to other thin-film deposition techniques and has the advantage of being low-cost and not requiring sophisticated equipment. [106]. This method basically consists of the deposition of the solution of the material in a suitable solvent on the interdigitated electrodes as shown in Figure 15, taking due care so that the material does not overflow the surface of the substrate. And once this is done it is only necessary to wait for the solvent to evaporate for the formation of the film [107].

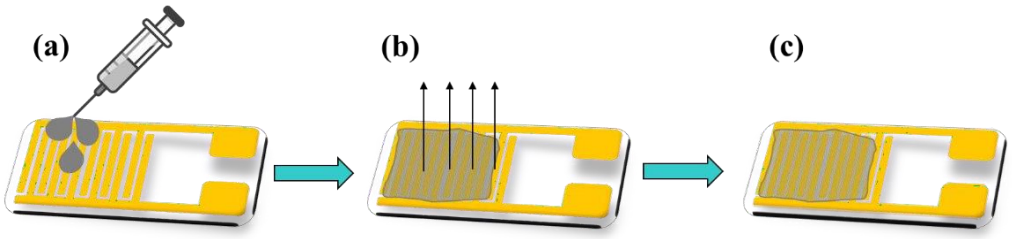

Figure 15-Drop-cast technique presented, in which we can see the production process of the thin film (a) deposition, (b) evaporation of the solvent and (c) formation of the film, respectively.

1.4.2-Spin-coating

Spin-coating is a method of coating surfaces widely used in the preparation of thin films. This is a film deposition technique on flat substrate that is used both in laboratories and in industry, such as in the production of LEDs, transistors and polymer film capacitors. From this technique thin (> 200 nm) and ultrathin (< 200 nm) films can be obtained [108].

Basically, its operation consists of the rotation (at controlled speed) of a solid substrate on which the solution of the material of interest is deposited Figure 15.

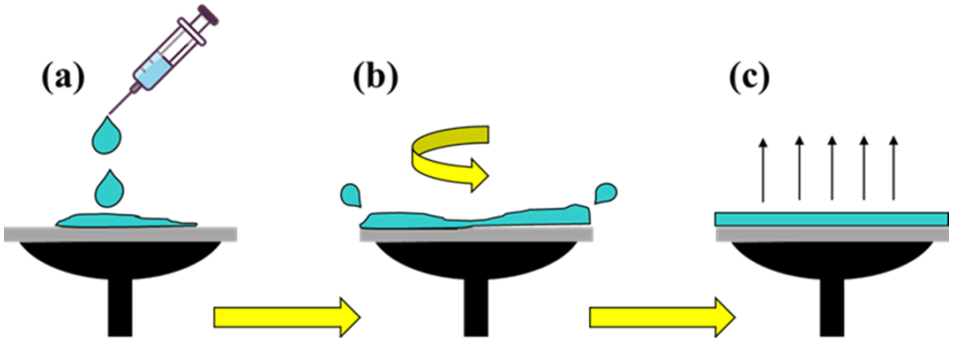

Figure 16-Deposition of films through the spin-coating technique, being (a) deposition of the solution on the substrate, (b) rotation to unify the film and (c) fabrication of the film.

In the process of obtaining the film, operating parameters such as speed and rotation time can be varied, in addition to the characteristics of the solution, such as concentration, type of solvent, etc. These variables are factors that directly influence the final properties of the film such as roughness, uniformity, and thickness.

1.4.3-Langmuir

The improvement in the manufacture of Langmuir's thin films, over the years, has led to new techniques being developed in order to improve the optical, electrical, magnetic properties, among others. The Langmuir-Blodgett technique can transfer (macro)molecules in an organized and controlled way to the substrate, and it allows the study of monolayers in some substances [109].

The study of thin-films started around 1891, when Agnes Pockels developed equipment capable of measuring the exact area of an oil film. However, it was not until the 1930s that more complete and in-depth works emerged. Irving Langmuir was the first to initiate research with thin-films, specifically oil films on water, as wellas developing a theory of adsorbed films. The name Langmuir monolayer was givenin his honor, because this work was what founded this area of research. His assistants,as also shown in Figure 17 , Katharine Blodgett and Vicente Schaefer, continued their work, where together they developed the theory of films transported to solid supports by means of immersion and emersion[110]. Due to the immense contribution to thin-film technology, this technique is generally known as Langmuir [111].

Figure 17-Irving Langmuir, Katharine Blodgett and Vicente Schaefer.

Of the many advantages that this technique provides, we can highlight, for example, the organization of the films that is extremely high and the thickness control rate that are very sensitive. This is a very important factor and with technological advancement many of the devices tend to get smaller and more efficient [112].

The films are produced by spreading a quantity of solution of the study material, over an aqueous subphase. The materials usually used in the formation of Langmuir films are amphiphilic, with well-defined polar (hydrophilic) and non-polar (hydrophobic) parts. The hydrophobic part, usually consisting of aliphatic carbon chains, decreases the solubility of the molecules in the aqueous subphase. The hydrophilic part is responsible for the scattering of the film on the surface of the water due to its greater interaction with the aqueous subphase [113].

The compression of the barriers causes the molecules to get closer and closer to the point where they begin to interact with each other on the surface of the subphase, characterizing a surface pressure isotherm. The study of isotherms was based on a common thermodynamic system that is equivalent to the isotherm π-A, pressure versus volume curve, referring to the average molecular area occupied by the molecules present at the interface for different values of surface pressure, SP (surface *pressure*) [114].

In analogy to thermodynamics, three distinct phases characterize the compression of the Langmuir film: (A) gas phase, in which the molecules do not interact with each other; (B) liquid phase, in which the molecules show some interaction, and (C) the condensed phase, where the molecules are relatively well oriented and packed forming a monomolecular thickness film (Langmuir film). The isotherm π-A for the stearic acid material was obtained, so that in the condensed phase

we find the area per molecule. This area is found through the tangent line to the condensed phase as shown in Figure 18.

To perform the deposition of the film it is necessary that the material is in the condensed phase, because it is in this phase that the molecules are at a minimum distance from each other forming a monolayer indicated in Figure 19 (a) and (b).

For the Langmuir-Schaefer films the initial experimental procedure is the same as the LB, but the deposition is done by the horizontal contact of the substrate with the monolayer, Figure 19 (b), the process must be careful, because it is done manually. The substrate is slowly approached the interface with the stabilized Langmuir film and, soon after, the substrate is slightly elevated, thus a hydrophobic part of the molecule is in contact with the substrate.

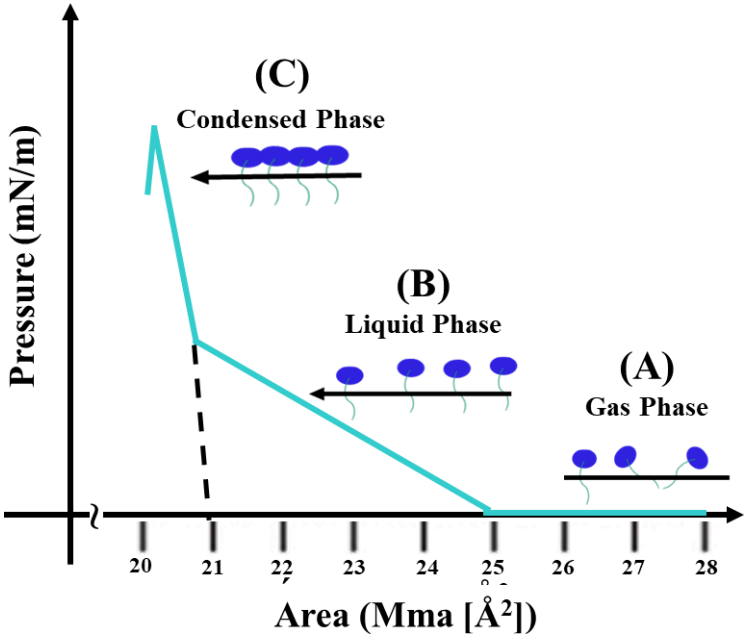

Figure 18-Isothermal π-A for stearic acid[113].

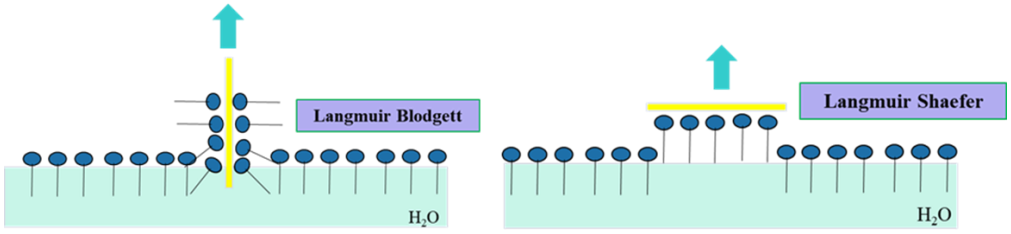

Figure 19-Langmuir-Blodgett (a) and Langmuir-Schaefer (b) deposition scheme.

Some parameters must be analyzed in order to obtain a satisfactory deposition and transfer of the LB film. The stability of the film, characteristics of the substrate, properties of the scattered molecule among other factors such as pressure and speed

of deposition must be analyzed, data that are provided by the software. Through pressure isotherms we can determine what would correspond to the solid phase, that is, when the area under a given pressure remains constant. The speed of deposition can be controlled and determined with the aid of the TR *transfer rate* obtained, where it must be kept at a value close to 1, which corresponds to the rate of material being transferred to the substrate. The transfer rate is the ratio between the area of the monolayer removed from the subphase at a constant pressure and the area of the immersed substrate.

Chapter 2 – Ionomers

This chapters presents the results of the preparation of SPS and SPS-*co*- PMMA (different degrees of sulfonation), Additionally, we will explore Langmuir and LS films, as well as spin-coating films performing morphological and electrical characterization and its performance as a gas sensor.

2.1-Introduction

Ionomeric polymers are a special class of polymers that exhibit unique properties due to the presence of ionic groups in their molecular structure. These polymers combine characteristics of traditional polymers with the properties of ionic materials, resulting in a set of properties useful in various applications.

The structure of ionomeric polymers is composed of main polymer chains, generally derived from organic polymers, in which ionic groups are covalently incorporated. These ionic groups give the polymer the ability to interact with ions, water and other polar compounds, which makes these materials especially interesting in various areas such as chemistry, materials engineering and polymer science. A distinctive feature of ionomeric polymers is their ability to form ionic complexes and electrostatic interactions in solution or in the solid state. These ionic interactions contribute to properties such as ionic conductivity, which is particularly useful in applications related to conductive materials, such as membranes for electrochemical fuel cells. Furthermore, ionomeric polymers are also widely used in biomedical applications, as materials for controlled drug release, due to their ability to interact with ions present in biological fluids. Continuous development in this area aims to overcome these challenges and further explore the potential of these innovative polymers in diverse technological and scientific applications.

2.2-Materials

The ionomers studied in this work were obtained in collaboration with Prof. Dr. Antônio J.F. Carvalho of EESC-USP, in which the starting polymers were prepared by the copolymerization of styrene and methyl methacrylate *via* a free radicalpolymerization, and the sulfonation reaction was performed using the Makowski method in homogeneous medium using as sulfonating agent the acetyl sulfate obtained *in-situ* by the reaction acetic anhydride with concentrated sulfuric acid [115]. The degree of sulfonation was controlled so that for SPS-*co*-PMMA we obtained 3, 6, and 8 molar % of ionic groups, and for SPS we had 3, 6, and 20% ionicgroups. The ionomers of SPS Figure 4 and SPS-*co*-PMMA (see Figure 5) were dissolved at a concentration of 0.2 mg/mL in xylol for all the techniques used in thiswork, i.e., Langmuir Schaeffer (LS), drop-casting and spin-coating.

2.3-Results and Discussion.

The techniques used are described in the Appendix

2.3.1 - Surface Pressure Isotherms for the Production of Langmuir Films

The study of surface pressure isotherms is essential to obtain information about the molecular organization of thin films in the aqueous subphase. Through these curves it is possible to estimate at what pressure the Langmuir film has a higher ordering for the transfer in solid substrates and, consequently, excellent morphology and better performance of the final device.

The Figure 20 shows the results obtained from surface pressure isotherms per area (π-A) for the Langmuir films of the SPS-*co*-PMMA ionomers, in different degrees of sulfonation. It is possible to observe the condensed phase of the Langmuir film at a pressure around 30 mN/m, being the ideal surface pressure for SPS-*co*-PMMA deposition, another data observed is that the Langmuir film of the studied materials has the melting point between 60-70 mN/m.

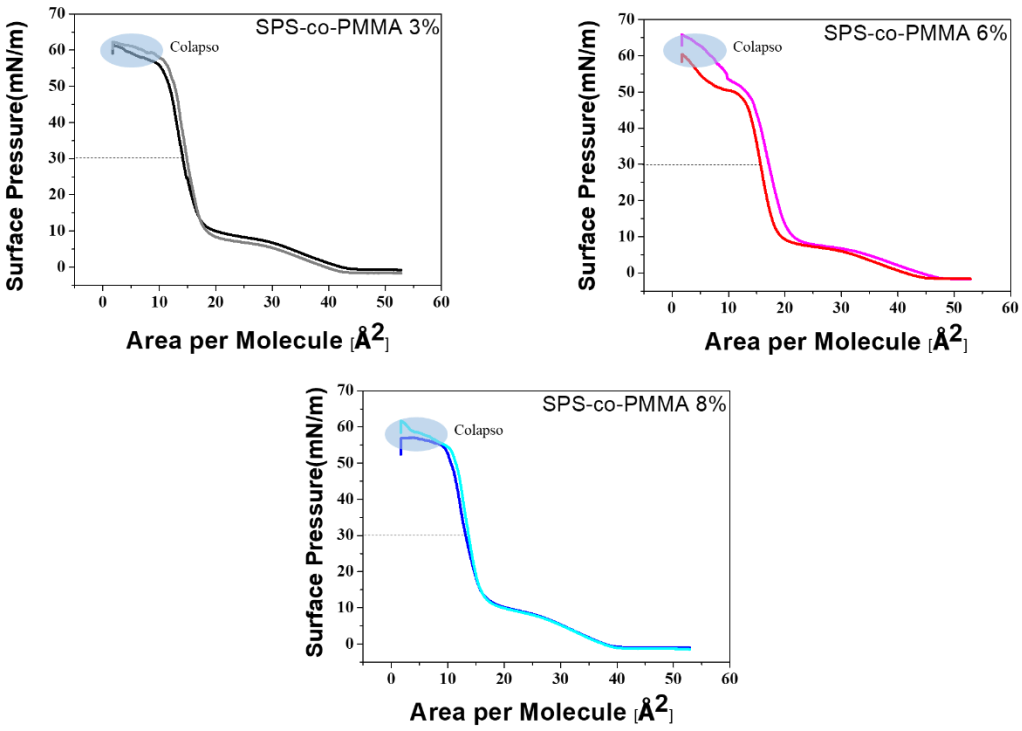

Figure 20- Surface Pressure isotherms by molecular area of Langmuir S PS-co-PMMA films 3, 6 and 8%, respectively.

Through the graphs it was also possible to express the curve in the condensed phase of the pressure isotherm of a Langmuir film, where we can estimate the average molecular area of the materials, being 18.7 Å² for SPS-*co*-PMMA 3%, 22.3 Å² for SPS-*co*-PMMA 6% and 18 Å² for SPS-*co*-PMMA 8%, as shown in Table 1 [116].

Table 1-*Average Molecular Area of SPS-co-PMMA films 3, 6 and 8% in the faif condensed.*

SPS-co-PMMA	3%	6%	8%
Area per Molecule (Å²)	18.7	22.3	18

For the study of Langmuir films of SPS ionomers with degrees of sulfonation of 3, 6 and 20%, the isotherms were made by spreading 500 µL of the solutions in the aqueous subphase. Through the analysis of the graphs in *Figure 21*, we can see that the ideal surface pressure for SPS depositions at 3 and 6% is 30 mN/m (condensed phase), collapsing at 70 mN/m. For SPS 20% the ideal surface pressure for the deposition of the films was 20 mN/m, collapsing at 40 mN/m, which indicates a greater aggregation of the films in the aqueous subphase.

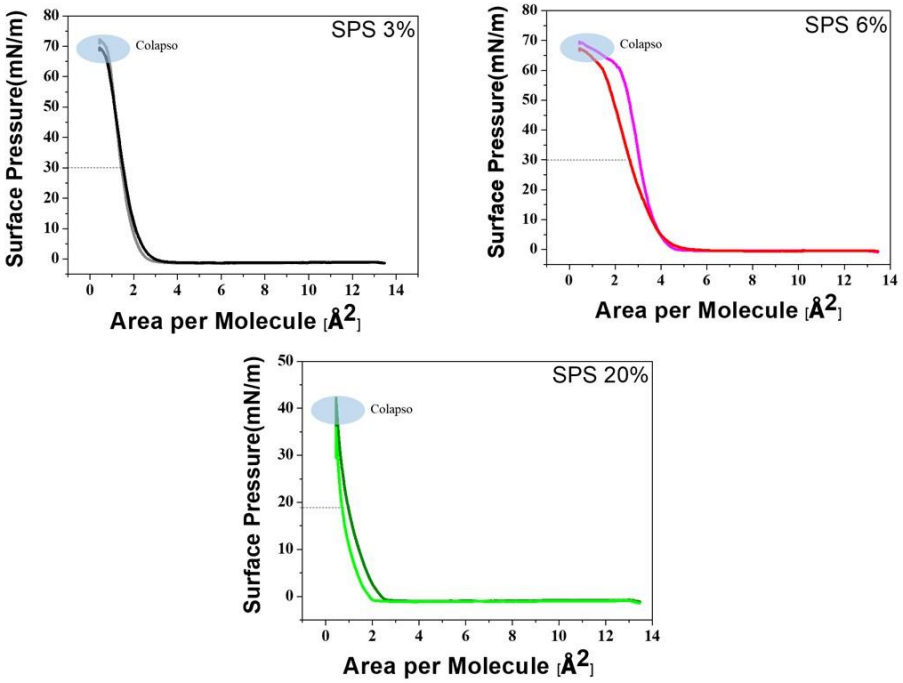

Figure 21- *Surface Pressure isotherms by molecular area of SPS 3, 6 and 20%.*

The average molecular area of the materials was estimated, being 2.2 Å² for SPS 3%, 3.8 Å² for S PS 6% and 1.7 Å² SPS 20% and as shown in Table 2 [104].

Table 2- Average Molecular Area of ionomers PS 3, 6, 8 and 20%

SPS-co-PMMA	3%	6%	8%
Area per Molecule (Å²)	18.7	22.3	18

A small change in the behavior of SPS 20% can be observed, in which studies carried out by Yu[117] showed that ionomers have a strong tendency to form aggregates or *clusters* through their ionic groups, facing processing difficulties when the ion content becomes higher

than 10%, which is corroborated by [LANTMAN, C. W. et al. Light scattering studies of ionomer solutions. Macromolecules, v. 20, n. 5, p. 1096-1101, 1987.], in which he reported that aggregation occurs at higher levels of sulfonation.

Both materials, SPS-*co*-PMMA and SPS, with different degrees of sulfonation, presented well-defined phases during compression in the Langmuir vat, being possible to identify the condensed phase, which enables the transfer of these films to solid substrates, due to their molecular organization during processing. Through the isotherms (π-A), it was possible to verify the i) conformation of the material, ii) the molecular area that ionomers occupied in the Langmuir vat and iii) ideal pressure for deposition of the films, this being the fundamental parameter for the development of thin films of Langmuir-Schaefer with morphology and satisfactory quality for application in gas sensing devices.

2.3.2- Atomic Force Microscopy (AFM)

The images containing the nanoscale morphology of the films were obtained by an Atomic Force Microscope in contact mode, for an area of 10 μm x 10 μm. Through the images in Figure 22 it is possible to see a linear roughness with well-defined peaks, with the Rms value of 3.33 and 1.73 nm, respectively, as shown in Table 3.

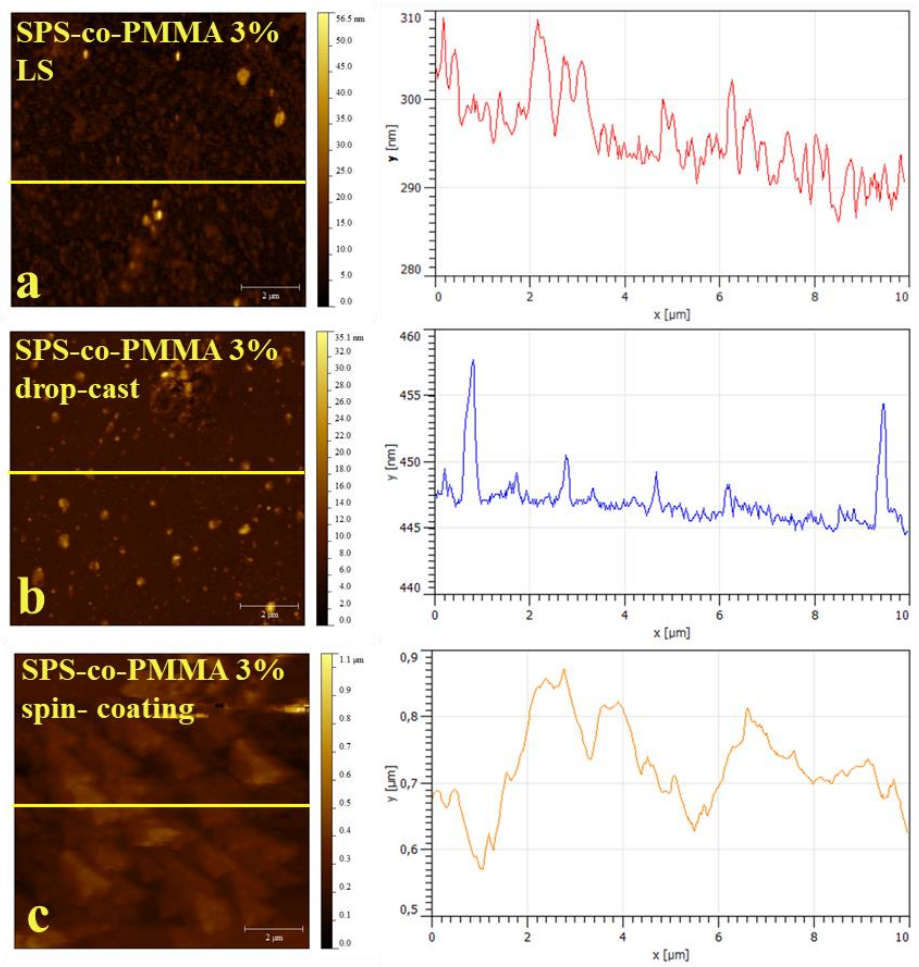

Figure 22- AFM topographic images of SPS-*co*-PMMA films with 3% ions deposited by: (a) LS; (b) drop-cast and (c) spin-coating techniques.

On the other hand, Figure 22 (c) presents the AFM images for the films obtained by spin-coating, which presented an irregularity in its morphology and with the roughness value of 10.04 nm, Table 3, being higher when compared with the other techniques (LS and Drop-cast). For the films of SPS-*co*-PMMA 6% we can observe a slightly different morphology in relation to the previous material, that the films of SPS-*co*-PMMA 6% Figure 23 (a) LS; (b) drop-cast , (c) spin-coating presented an irregular morphology with Rms values of 8.36 nm, 14.25 nm and 5.46 nm, respectively, shown in Table 3.

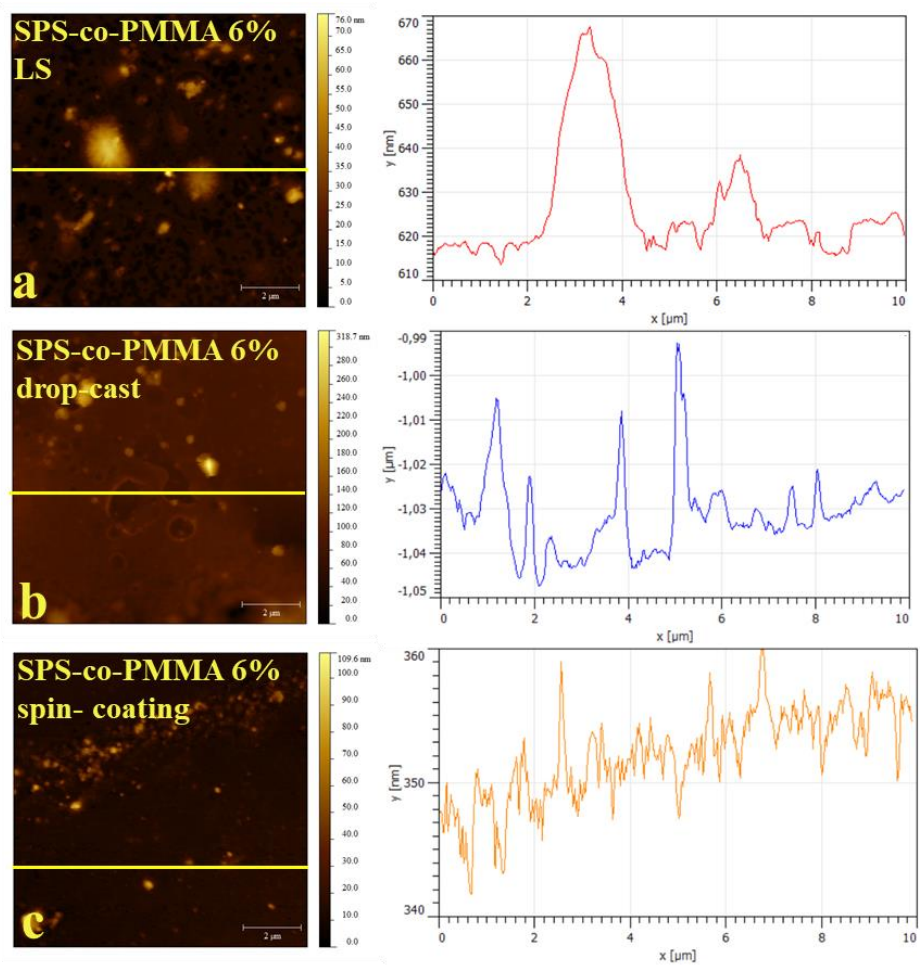

Figure 23- Topographic AFM images of SPS-co-PMMA films with 6% ions deposited by the technique of: (a) LS; (b)drop-cast; and (c) spin-coating.

The Figure 23 (c) shows that the spin-coated films that presented a reduced and more uniform roughness when compared to the other techniques.

Figure 24 shows the images obtained by AFM of SPS-co-PMMA 8% for the films obtained by the techniques of (a) LS and (b) drop- cast, (c) spin-coating. There was a significant improvement in relation to the morphology of the samples, when compared with the samples with sulfonation degree in 3 and 6%, with an emphasis on the films obtained by spin (c).

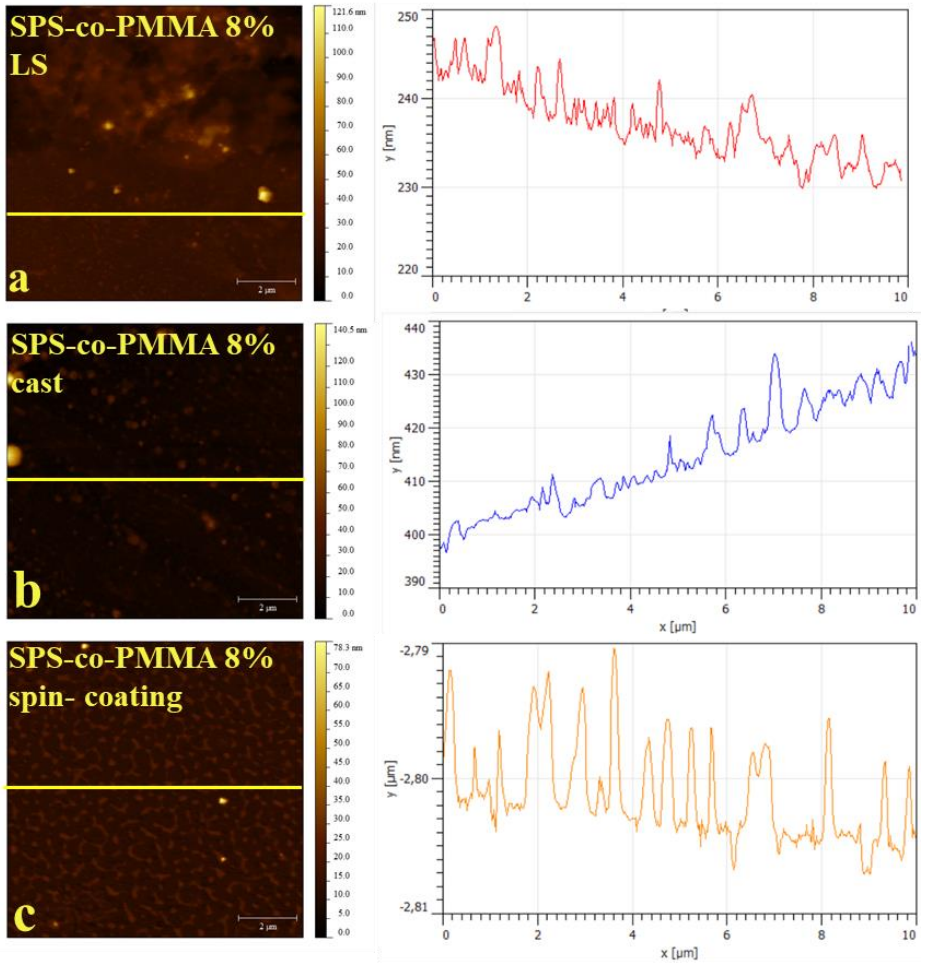

Figure 24- Topographic AFM images of SPS-*co*-PMMA films with 8% ions deposited by the technique of: (a) LS; (b) drop-cast; and (c) spin-coating.

Table 3-Mean values of Rms roughness of material SPS-*co*-PMMA with different degrees of sulfonation for LS, cast and spin-coating techniques.

Rms (nm)			
SPS-co-PMMA	**3%**	**6%**	**8%**
LS	3,33	8,36	5,8
Cast	1,73	14,25	4,5
Spin- coating	10,04	5,46	3,61

Figure 25(a) shows the images of the films manufactured from the Langmuir-Schaefer technique, where it is possible to observe that the region has an irregular roughness, and a Rms value of 34.05 nm, which much higher compared to the other techniques, as shown in Table 4.

The spin-coating technique presented the best result in relation to morphology with Rms roughness of 8.9 nm, when compared to the other techniques, LS and cast, with Rms values of 34.05 nm and 13.95 nm, respectively.

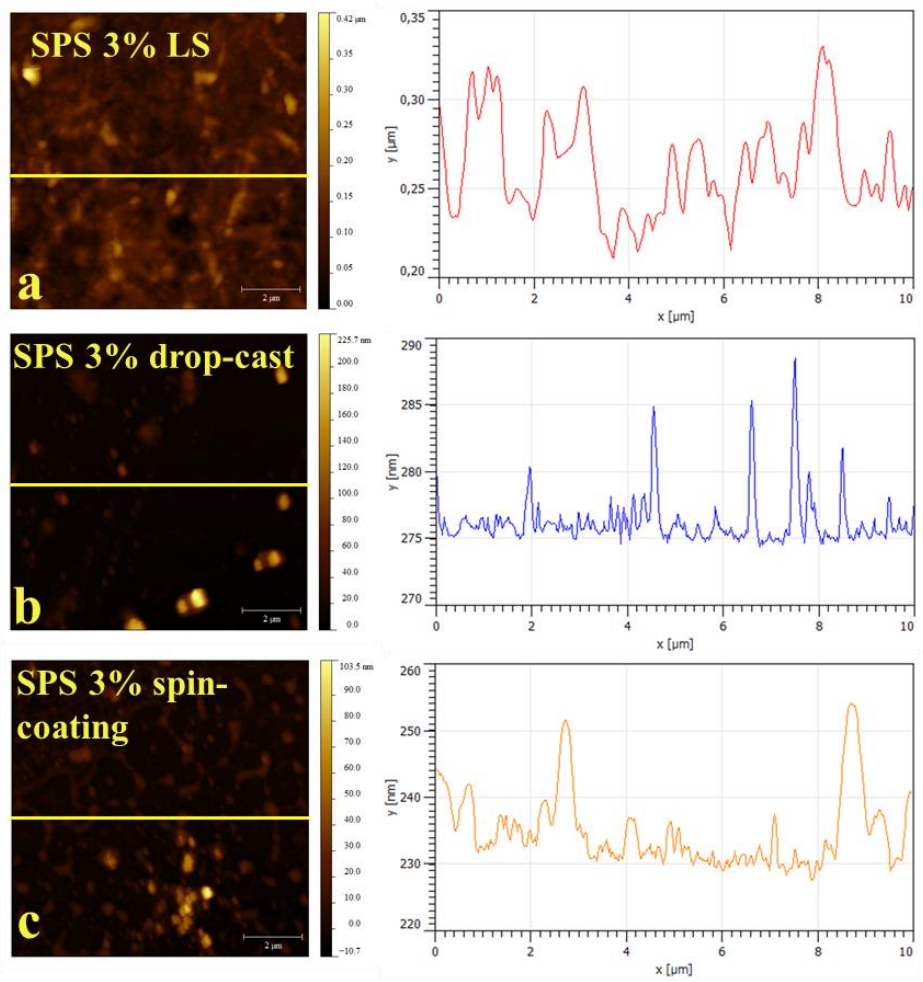

Figure 25-Topographic images of AFM of SPS films with 3% ions deposited by the technique of: (a) LS; (b) drop-cast; and (c) spin-coating.

Figure 26 shows the images obtained by AFM of the 6% SPS samples. The samples followed the same behavior for the sample with 3 % sulfonation, that is, the spin-coating technique showed greater regularity in morphology with an Rms value of 7.98 nm, being 9.7 nm and 54.35 nm, for drop-cast and LS films, respectively.

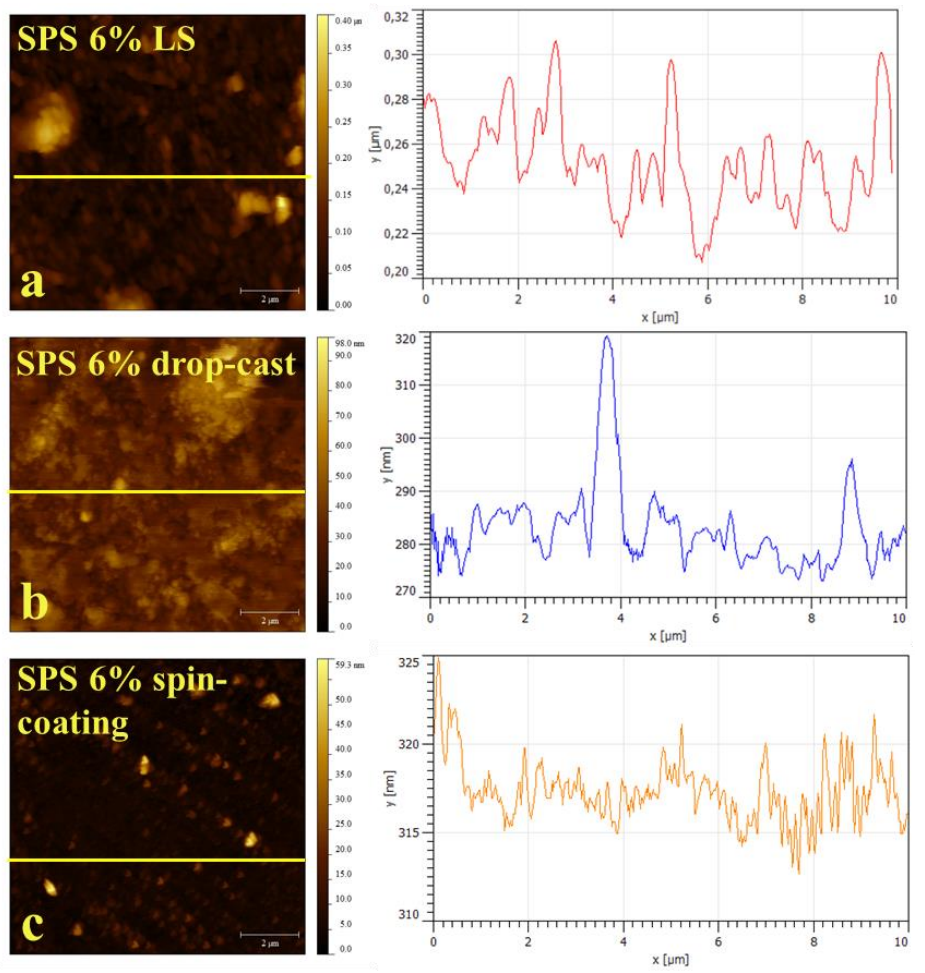

Figure 26- AFM topographic images of SPS films with 6% ions deposited by the technique of (a) LS, (b)drop-cast; and (c) spin-coating.

Finally, we have the images obtained by AFM of the SPS 20% material, in Figure 27 techniques, show rough and irregular regions, but despite the similarity the Langmuir Schaefer technique has a much higher roughness compared to the spin-coating technique, as shown in Table 4 film passes a just over 6 nm.

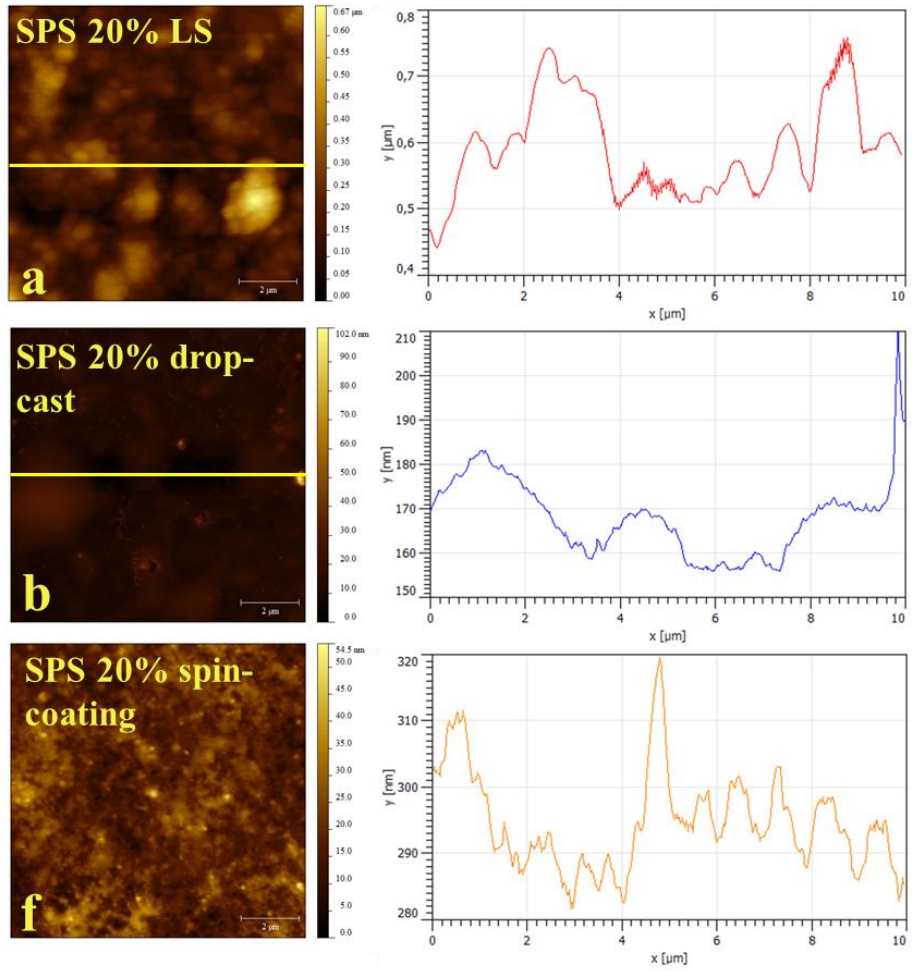

Figure 27- Topographic images of AFM of SPS films with 20% of ions deposited by the technique of: (a) LS, (b) drop-cast and (c) spin-coating.

On the other hand, the films using the cast technique present a low roughness and little variation in the peaks, and their Rms value is the lowest compared to the other techniques of thin film preparation.

Table 4- Mean values of Rms roughness of the material SPS with different degrees of sulfonation for the techniques of LS, drop-cast and spin-coating**.**

Rms (nm)			
SPS	**3%**	**6%**	**20%**
LS	34,05	54,35	87,8
Cast	13,95	9,7	5,58
Spin- coating	8,9	7,98	6,08

Processing by spin-coating presented the lowest values for the roughness and this suggest that there is a better organization of the obtained films. This is associated with the way the solvent evaporates more quickly during the film formation, differentiating it from other techniques. In the Langmuir and drop-cast techniques, the solvent evaporates slowly, allowing the formation of ionic aggregates, as proposed by Yu [82**Erro! Indicador não**

definido.]. In the spin-coating technique a centripetal force acts at the moment of the formation of the film, influencing its
final morphological characteristics. According to Müller-Buschbaum [118], the solution behaves like a Newtonian liquid, and possible irregularities of the surface contour are smoothed by the centrifugation process that occurs in the spin-coating technique.

2.3.3 - Electrical Characterization with Direct Current (DC)

In Figure 28 we can see the results obtained for SPS-*co*-PMMA with respect to current versus tension curves (i.e., *I versus V*). We can see that the samples presentedthe same order of magnitude in terms of electrical current, despite the different degrees of sulfonation, between applied tensions of -10 and 10 V. It is noteworthy that all had a linear behavior in the voltage range analyzed, which may be related to the neutral contacts in the Au/SPS-*co*-PMMA interfaces.

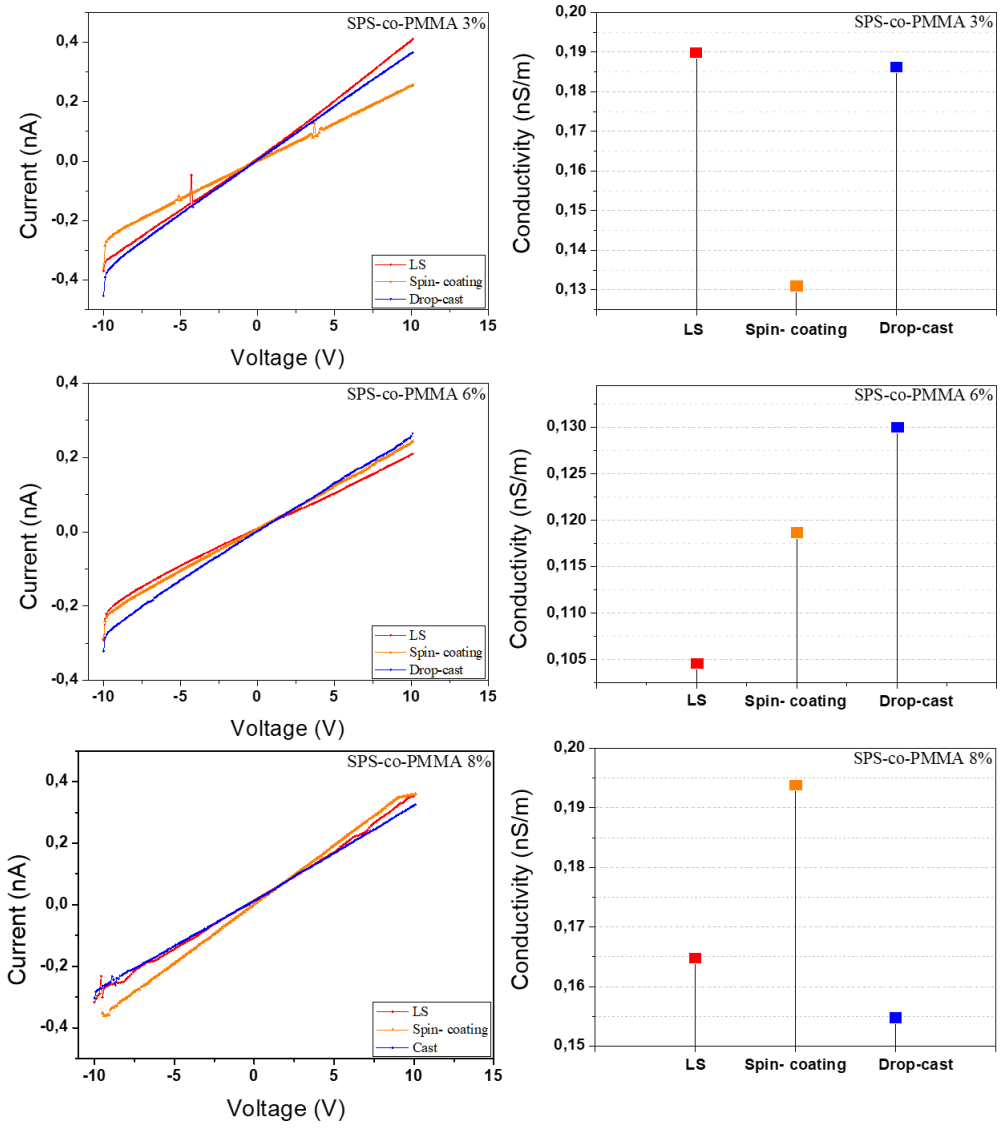

Figure 28-I *versus* V graph and DC electrical conductivity of LS films, spin-coating and drop-cast of SPS-co-PMMA 3, 6 and 8% ionomers.

However, in Figure 29 *I versus V* (left column) and DC conductivity (right column), the SPS samples have nonlinear responses when from the spin-coating and drop-cast films, with a degree of sulfonation at 6 and 20%, respectively. That is to say, the conduction in these cases is not ohmic and this behavior may be related to the conduction of current-limited charge carriers; this behavior is called SCLC (Space Charge Limited Current) arising due to the presence of traps [119,120]. This fact may also be associated with a strong tendency to form aggregates or clusters through their ionic groups being evident in SPS and not identified in SPS-*co*-PMMA due to the spacing of sulfonic groups present in SPS and absent in PMMA and PS, which hinders aggregation by steric impediment. These effects altered the conductivity of the SPS, but the current remained in the order of nA.

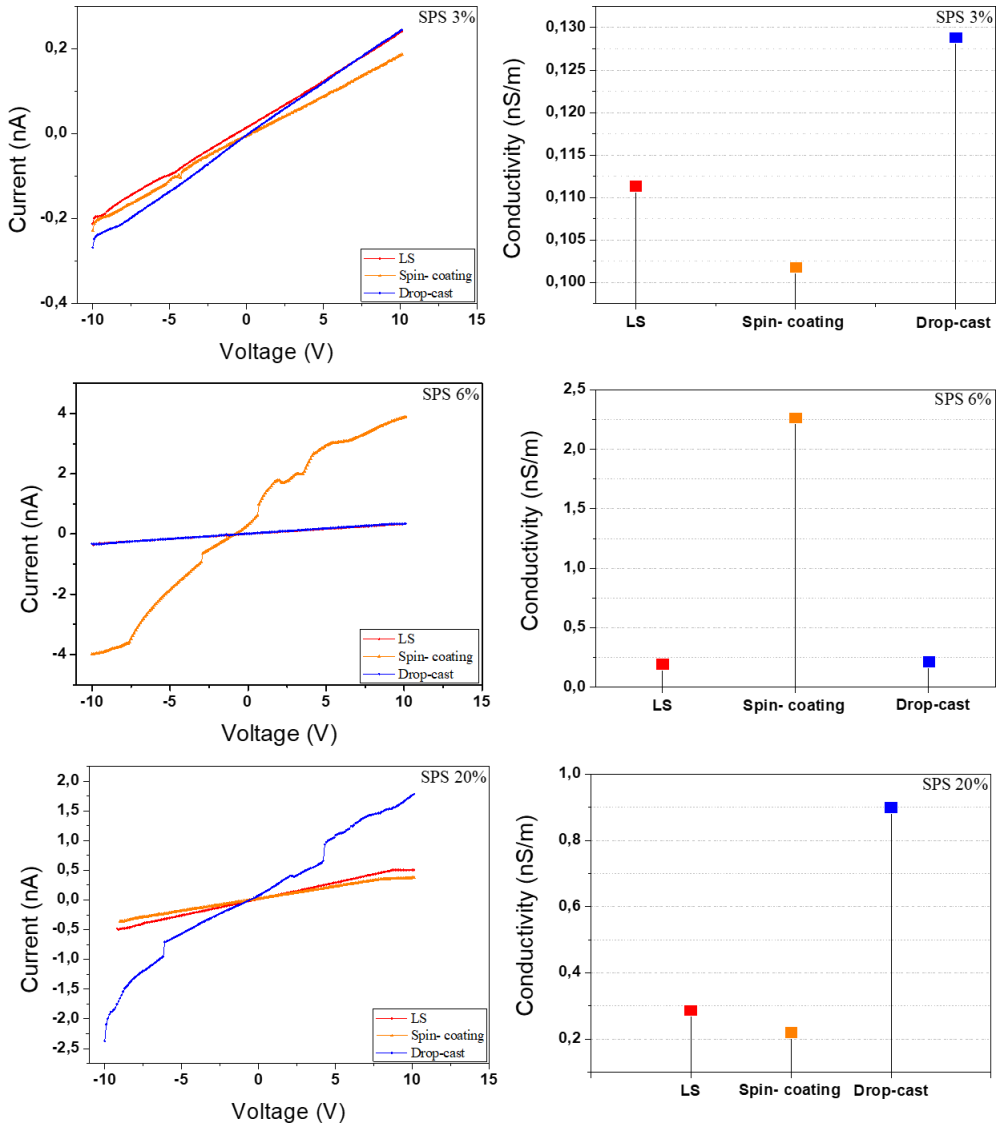

Figure 29-Graph IxV and DC electrical conductivity of LS films, spin-coating and drop-cast of SPS 3, 6 and 20% ionomers.

2.6.4 - Gas Sensors

The electrical behavior of the thin films of the SPS-*co*-PMMA and SPS ionomers was verified with the different degrees of sulfonation in the presence of ammonia gas (NH_3). The electric current was monitored in relation to the time during the nitrogen flow and ammonia gas flow, alternately, and the difference of acting potential in the films was in 5 V. The gas flows were interspersed in intervals of 1 minute of N_2 and 2 minutes of NH_3 totaling 10 cycles, as shown in

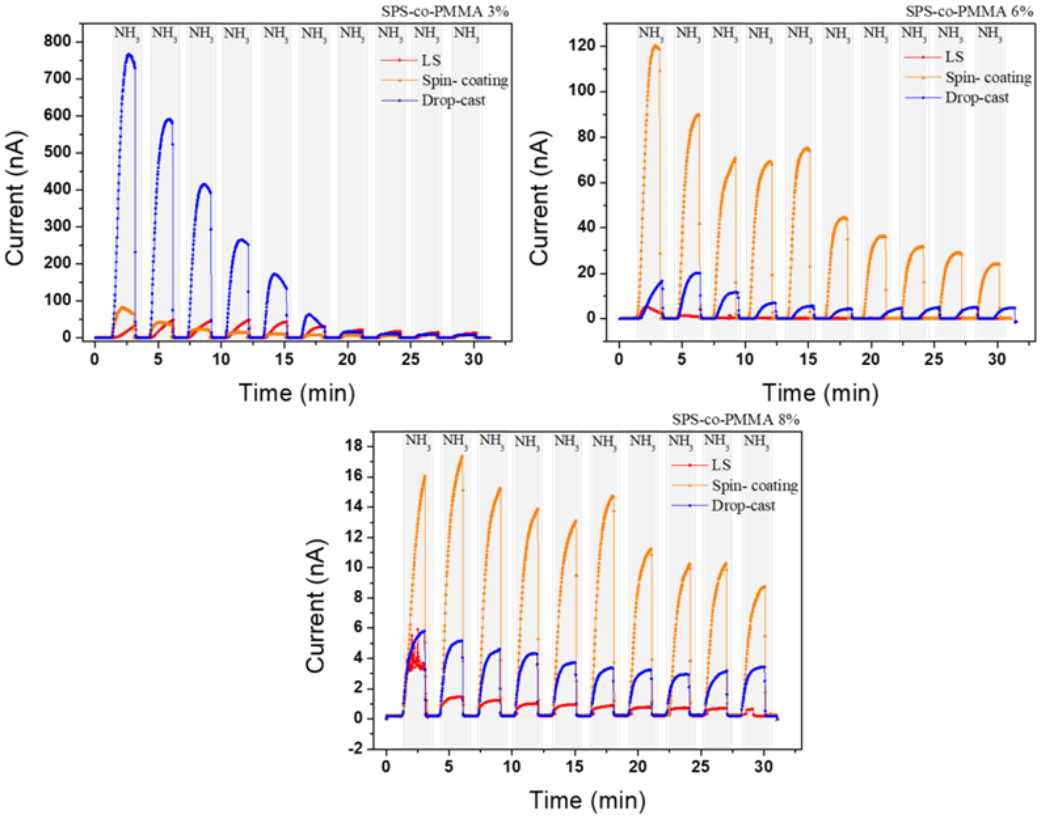

Figure 30 and Figure 32

Analyzing

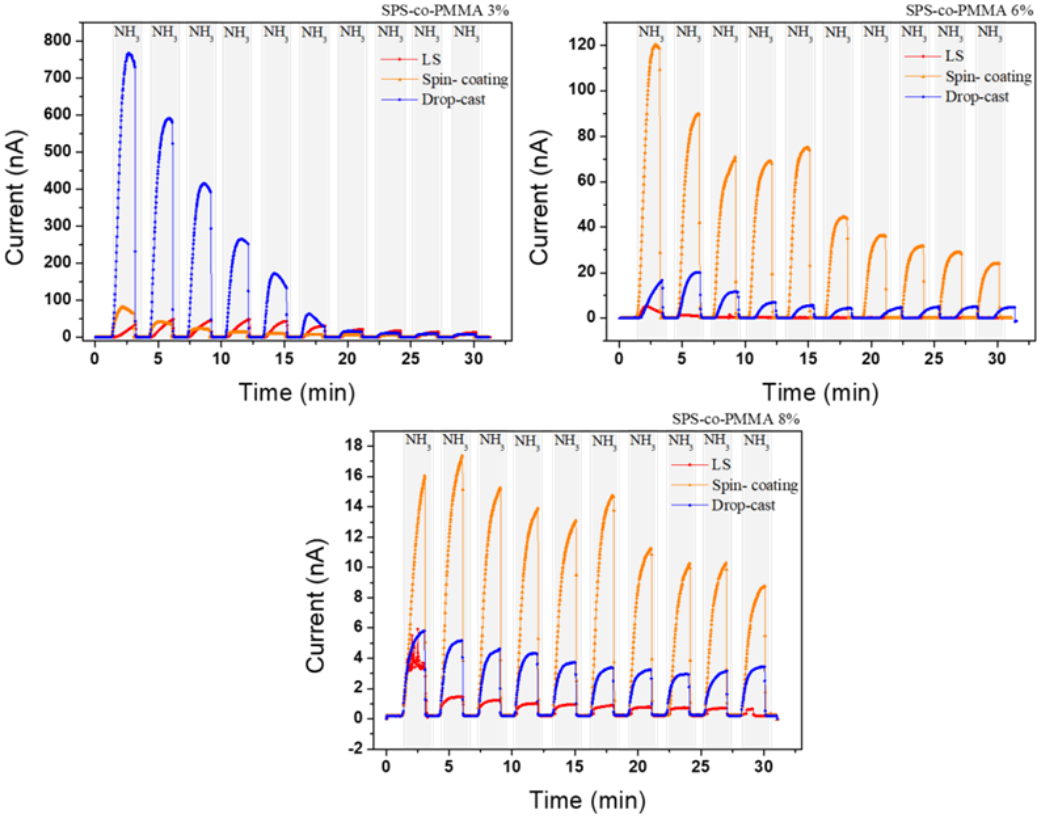

Figure 30 can observe that all SPS-*co*-PMMA ionomers presented a response to the presence of NH3 gas, but for a better understanding of theresults we will discuss each graph individually. With the SPS-*co*-PMMA 3% films

for the LS, spin-coating and drop-cast techniques, as it is possible to observe the film that stood out in the presence of ammonia gas, despite not maintaining the response with the passing of the cycles, was the drop-cast film, presenting an electric current in the range of 200 to 800 nA in the first four cycles.

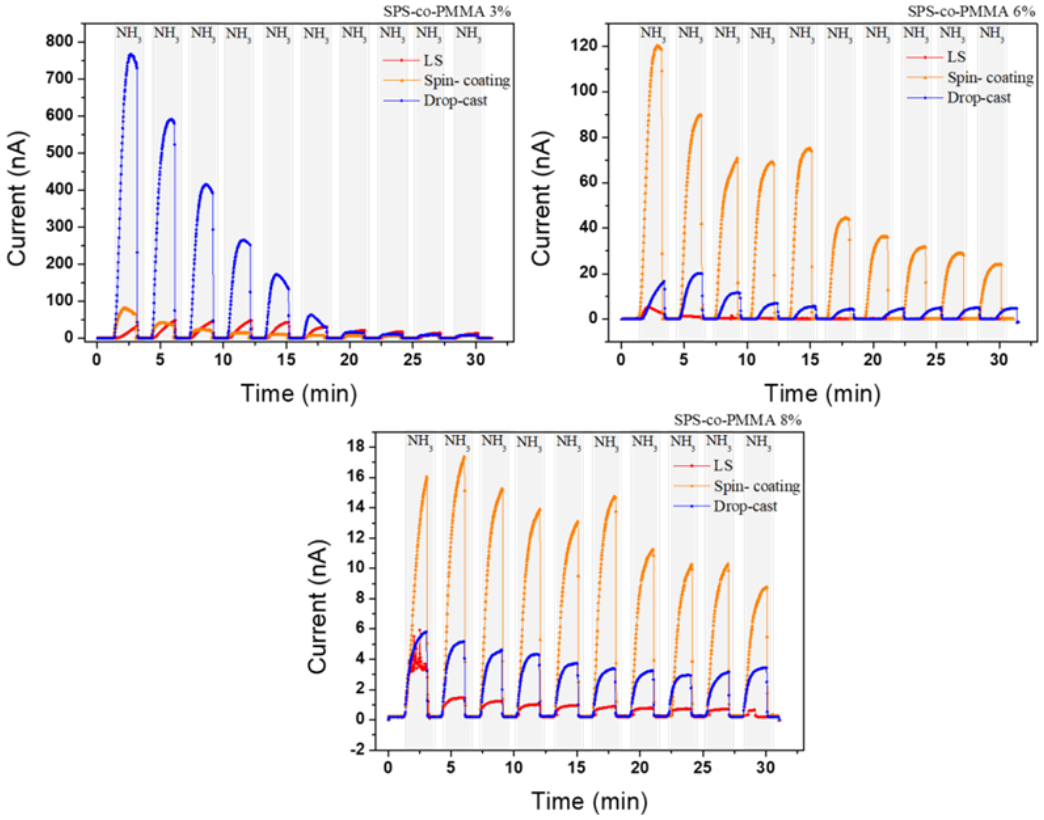

Figure 30-Measurements of gas sensors of LS films, spin-coating and drop-cast of SPS-co- PMMA 3, 6 and 8% ionomers.

The film produced by LS and spin-coating showed higher reproducibility between cycles when compared to drop-cast film, but the electric current of both films was below 80 nA.

The SPS-*co*-PMMA 6% film produced by spin-coating presented a higher conductivity in relation to the films produced by the other techniques, maintaining a good reproducibility throughout the cycles with an electric current that ranged from 120 to 50 nA, and in the LS and drop-cast films the current exceeded the value of 20 nA.

The 8% SPS-*co*-PMMA films followed a pattern, similar to the 6% sample, in which the best response was for the spin-coating film, but a lower electric current, when compared to the other samples in different degrees of sulfonation, not exceeding 18 nA, despite maintaining a good reproducibility for the 10 cycles.

Figure 31 shows the mean for the values of the electric current observed at

each peak, with its standard deviation, in which we can observe that the sample with electric current of response has the highest associated error in the measurement, that is to say, low reliability.

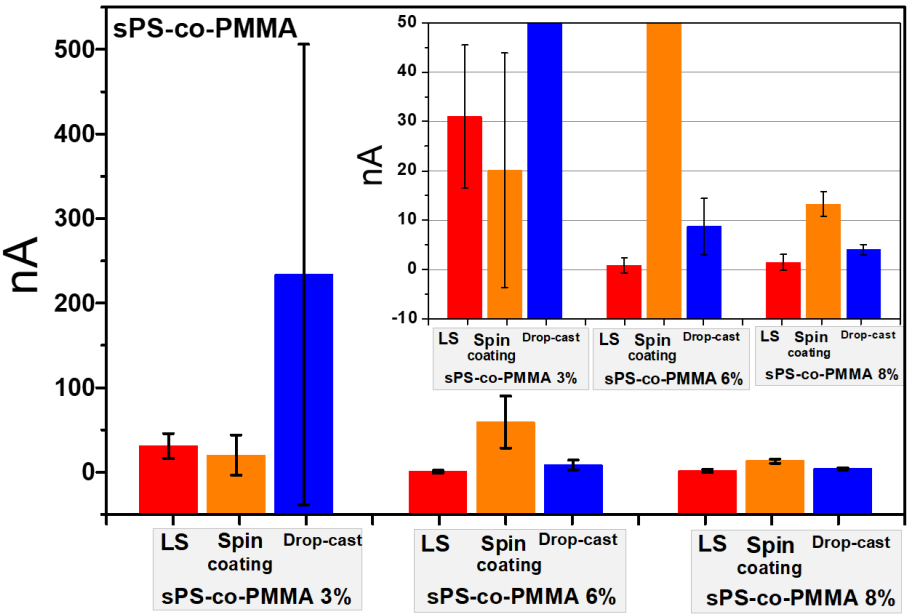

Figure 31-Graph in bar format for the material SPS-co-PMMA 3, 6 and 8% with the techniques of thin films LS, spin-coating and drop-cast.

Analyzing the morphology of these materials we can relate the best responseto the roughness value. Those three films had the lowest roughness value, as shown

in Table 3, and the best homogeneity of the films, as presented in Figure 22(b)Figure 23 (c)e Figure **24** (c) respectively.

Figure 32 shows the results obtained for the ammonia gas sensor of the SPS,in different degrees of sulfonation, in which it is observed that the materials had theirelectric current altered upon contact with the gas. For SPS 3% we can see that the best performance was for the film using the spin-coating technique, which maintainedthe electrical response throughout the cycles, with an electric current that superior tothe other samples, with the same degree of sulfonation and produced by different techniques.

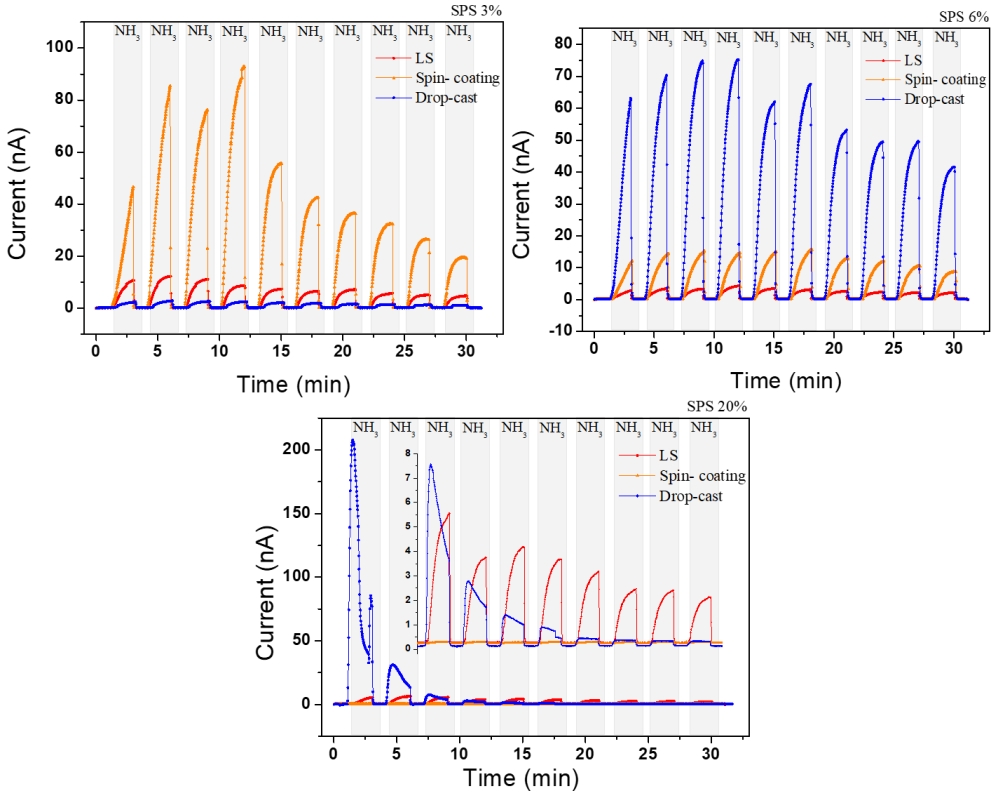

Figure 32-Measurements of gas sensors of LS films, spin-coating and cast of SPS 3, 6 and 20% sulfonation ionomers**.**

For the samples of the SPS 6% samples, the technique that stood out was the drop-cast film, which despite the electric current not exceeding 80 nA continued to respond in the presence of the gas in the other cycles. For the 20% SPS sample, the film produced by drop-casting presented an initially better response with its first cyclewith a current of 200 nA, but this current drops abruptly over the other cycles reachingclose to 0 (zero), after the sixth cycle, as it is possible to see in the magnification of the inset graph.

SPS had a behavior similar to that of the SPS-*co*-PMMA, as can be seen in Figure 33, in which the samples that presented the highest mean value of the electric current response, also presented a higher standard deviation, that is, greater variability during the measurements.

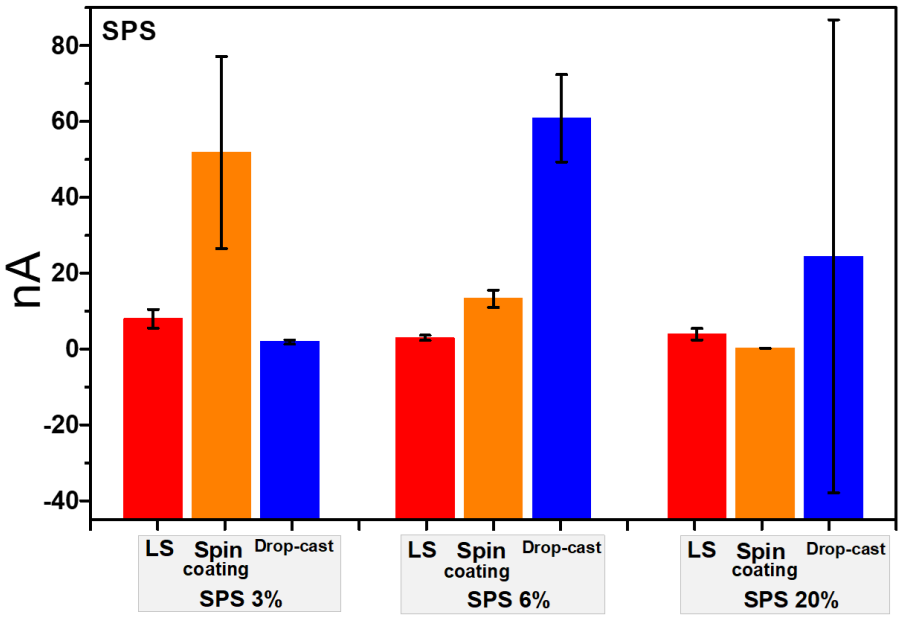

Figure 33-Graphic in bar format for SPS 3, 6 and 20% material with the techniques of thin films LS, spin-coating and drop-cast.

The techniques that stood out as a gas sensor, although they also presented greater variation in the results, compared to the other techniques of the same material, were the films of SPS 3% spin-coating, SPS 6% drop-cast and SPS 20% drop-cast, as shown in Figure 32.

The three best results, obtained as a gas sensor, had an Rms value lower than 10 nm, as shown in the Table 4.

For the SPS 3% spin-coating and SPS 6% drop-cast films, we have strong evidence that the response of the materials produced by the different techniques is associated with the homogeneity of the surface of the films. For the 20% SPS film, Figure 27(b) shows a non-linear region, which may have contributed to the drop in the sensor's electric current in the other cycles.

However, the LS films showed a higher stability when compared to the other thin film techniques. It can be a more reliable technique even with the lower current.

We can conclude that the ionomers of SPS-*co*-PMMA and SPS work as an ammonia gas sensor, having a fast detection when coming into contact with the analyte, ammonia gas, but studies to verify the reproducibility, durability and selectivity of these devices will be necessary, especially in relation to the understanding of the electronic and ionic conductivity of these materials, because a literature on the use of these ionomers as a gas sensor is scarce.

2.6.4- Principal Component Analysis

Seeking a better understanding of the measurements of current by time (*I versus t*) collected during the gas flow and to compare the different variations in the methods and materials, in each sensory unit, the Principal Component Analysis (PCA) method was used. The Figures 34-39 presented will illustrate the analysis of the capacity of each sensory unit produced and tested [121,122]. Aiming to explore the potential that each manufacturing technique studied here has to detect the gas used as an analyte (ammonia gas).

The Figures 34-36 show the PCA results for 3, 6 and 8% SPS-co-PMMA samples. In a general analysis of the response pattern, it can be seen that it is possible to separate the techniques in detecting the analyte. It is also noted that for the different materials used as active layer, the response is repeated. From the point of view of the stability of the sensor response, it can be inferred that the device that presents the greatest reproducibility is the one manufactured using the LS technique. The molecular organization that comes from this technique and the reproducibility of the films manufactured can justify this stable response.

Among the LS films, SPS-co-PMMA 6% stands out with excellent grouping, which may be related to the combination between the molecular organization and the low roughness of these films. In addition to the graphs presented, it is also possible to analyze the data in a more detailed way. quantitative through the Silhouette Coefficient and Variance values. According to the data presented in Table 5, it can be observed that the three materials presented a

Silhouette Coefficient value very close to 1, which suggests that this material was able to accurately identify the gas highlighted for SPS-*co*-PMMA 6 and 8%. This result can be attributed to the good grouping of the LS technique, which favors the sensor's accuracy.

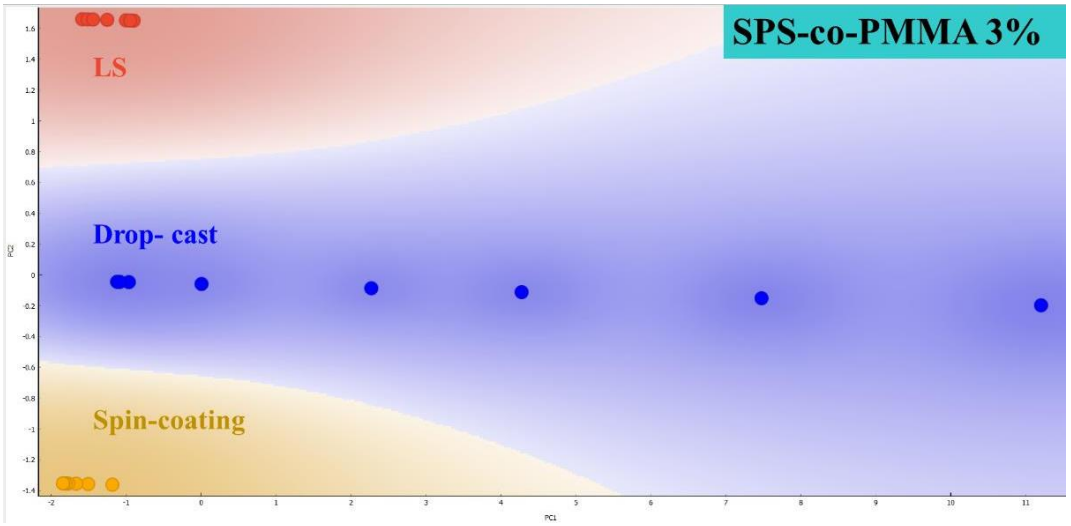

Figure 34-PCA analysis diagram for SPS-co-PMMA 3% films.

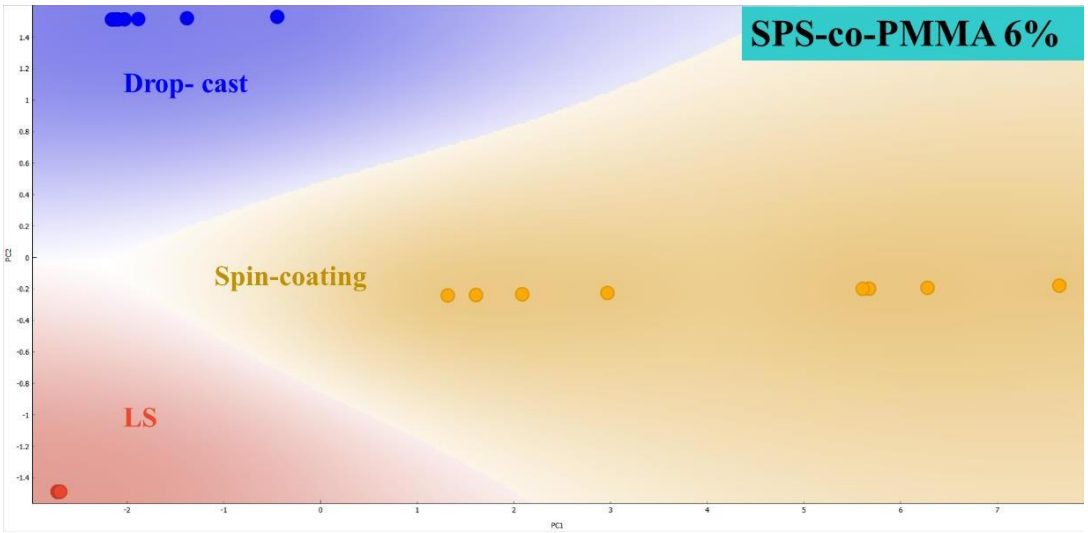

Figure 35-PCA analysis diagram for SPS-co-PMMA 6% films.

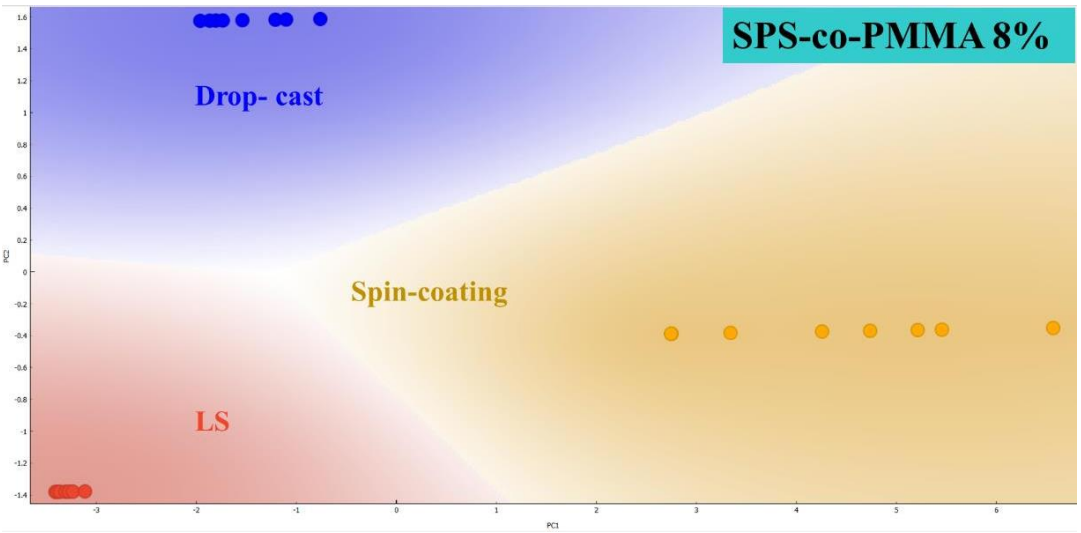

Figure 36-PCA analysis diagram for SPS-co-PMMA 8% films.

Table 5- Silhouette Coefficient and Variance Values for SPS-co-PMMA 3.6 and 8%.

SPS-*co*-PMMA	Silhouette Coefficient	Variance
3%	0,683	0,076
6%	0,690	0,022
8%	0,782	0,007

We now continue with the analysis of the PCAs of the SPS 3, 6 and 20% sulfonation samples. Contrary to what was obtained for SPS-*co*-PMMA, where the LS film stood out, in this case there was no reproducible behavior when using this technique. However, some behaviors can be noticed: there is less grouping of points in the PCA of spin-coating SPS 3% and drop-cast films (SPS 6 and 20%). We also note that the technique with the highest clustering is the 3% SPS drop-cast film and this may be related to the greater roughness observed in the AFM measurements. For the 20% SPS spin-coating film, an excellent grouping of the points was obtained, which is at odds with the roughness of the film, as this film has low roughness. Regarding the 20% SPS, it is important to say that it was the material with the furthest value from 1 of the silhouette coefficient as shown in Table 6, this means that it is the material with the lowest accuracy compared to the others, for gas detection. It is worth mentioning that for these materials, although the prepared devices have potential for application in ammonia sensors, it was not possible to relate the type of technique used with the reproducibility of the sensors.

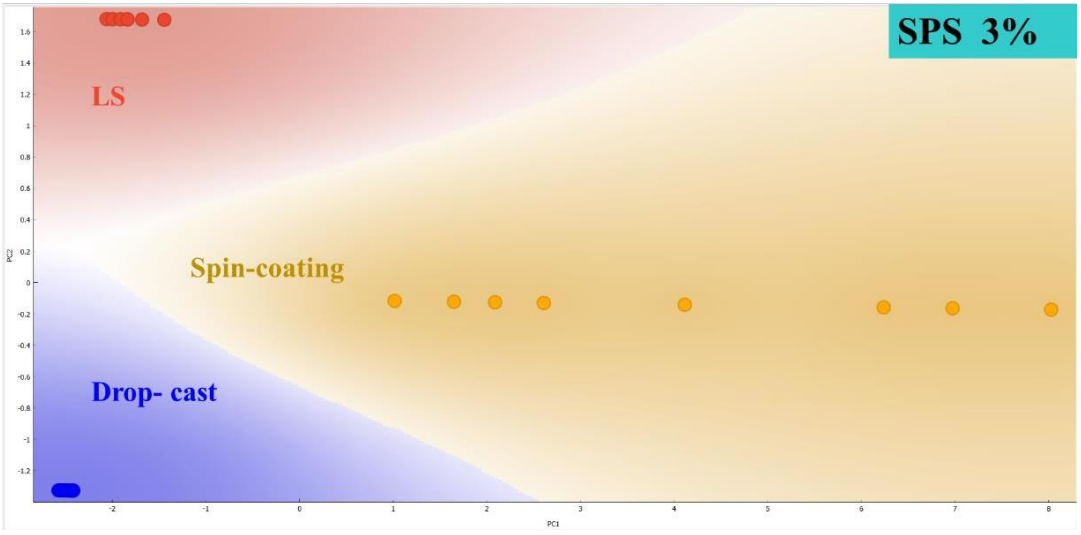

Figure 37-PCA analysis diagram for SPS 3% films.

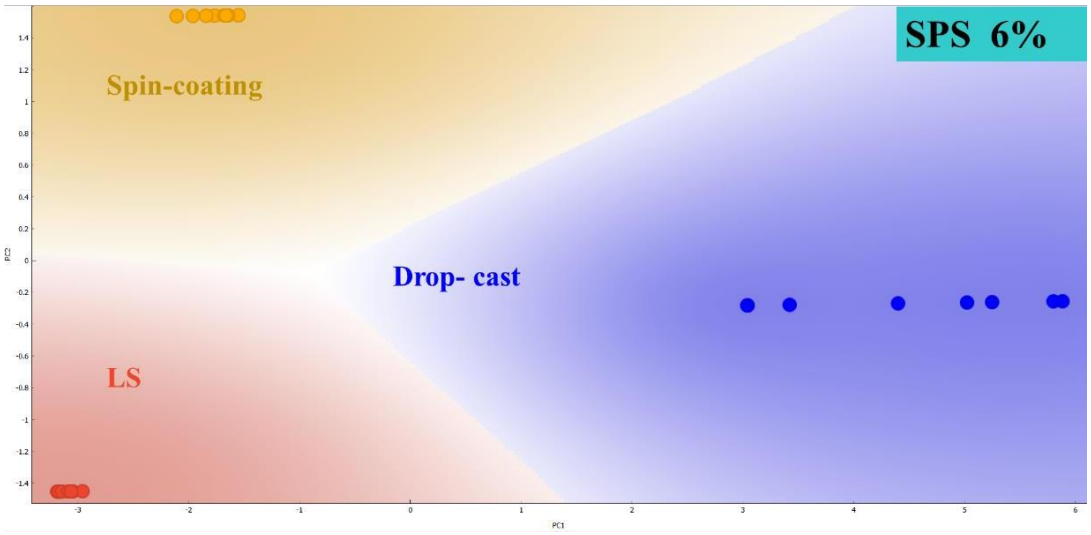

Figure 38-PCA analysis diagram for SPS 6% films.

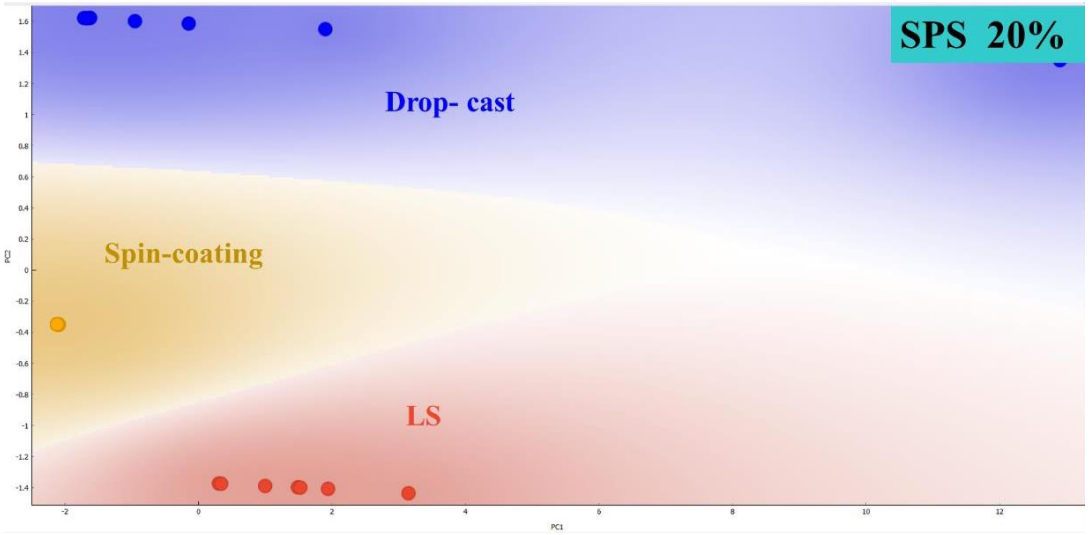

Figure 39- PCA analysis diagram for SPS 20% films.

Table 6- Silhouette Coefficient and Variance Values for SPS 3.6 and 20%.

SPS	Silhouette Coefficient	Variance
3%	0,794	0,026
6%	0,846	0,005
20%	0,626	0,092

In general, the LS films showed very similar behavior in the three materials tested, this may be related to the high roughness of the films, which, unlike the previous material, helped with the stability and constancy of the sensor.

Conclusion

The ionomers SPS-*co*-PMMA 3, 6 and 8% of sulfonation and SPS 3.6 and 20% of sulfonation, can be used as ammonia gas sensor in the different techniques of thin films tested LS, drop-cast and spin-coating, and the ionomers SPS-*co*-PMMA 3% drop-cast, SPS-*co*-PMMA 6 and 8% spin-coating presented a higher electric current when it comes into contact with the NH_3 gas, however, when the issue is stability and reproducibility, we can say that the LS films had the best behavior, which is shown in Figure 24, A, B and C. This fact may be related to the low values in roughness.

For SPS films, the best results were obtained with the spin-coated SPS 3 %, and SPS 6 and 20% for cast films, and these samples had an Rms value of less than 10 nm. For SPS 3% spin-coating and SPS 6% cast films, we have strong evidence that the response of the materials produced by the different techniques is associated with the homogeneity of the film surface.

CHAPTER 3 - Synthesis and Characterization of Block copolymer poly[fullerene-*alt*-(2,5-bisdocyloxy-1,4- terephthaldehyde)]-*block*-poly(ethylene oxide) (JC10) Thin.

3.1-Introduction

Copolymers are polymeric materials formed by two or more different types of monomers in their structure. An interesting example of a copolymer is the one formed by the combination of C60 fullerene (also known as buckminsterfullerene) with polyethylene glycol (PEO), a long-chain polymer composed of repeating ethylene glycol units.The incorporation of C60 fullerene into copolymers with PEO is an exciting area of research, as it combines the unique properties of fullerene with the flexibility and biocompatibility of PEO. C60 is a carbon molecule that forms a hollow spherical structure, composed of 60 carbon atoms arranged in hexagons and pentagons. This molecule is known for its unique electronic, optical and structural properties.

By combining C60 with PEO in a copolymer, researchers aim to obtain a material that can take advantage of the specific characteristics of both components. PEO provides flexibility, thermal stability and biocompatibility, while C60 can contribute unique electronic and photophysical properties. This combination makes these copolymers potentially useful in a variety of applications, such as electronic devices, sensors, and even biomedical systems for controlled drug delivery.

Furthermore, C60's ability to absorb light over a wide spectral range can be exploited in photovoltaic applications, making these copolymers interesting candidates for the development of new materials in organic solar cells.

However, it is important to note that the synthesis and characterization of these copolymers can present challenges, and understanding the properties resulting from the interaction between C60 and PEO is crucial to optimizing their practical applications. Thus, the study of these copolymers represents a promising area of research that aims to explore synergies between different structural units to create materials with specific properties and innovative applications.

3.2- Synthesis

3.2.1-Synthesis of the block copolymer poly[fullerene-*alt*-(2,5-bisdocyloxy-1,4-terephthaldehyde)]-*block*-poly(ethylene oxide) (JC10)

This work targeted the first example of an amphiphilic block copolymer containing a SACAP poly(fullerene). To synthesize the block copolymer **JC10** we made the poly(fullerene) block first and then reacted this with the chain-ends of poly(ethylene oxide) to give **JC10** show in Figure 40. The poly(fullerene), called **JC9**, was made by reacting fullerene with a comonomer **JC8** that we made in the lab.

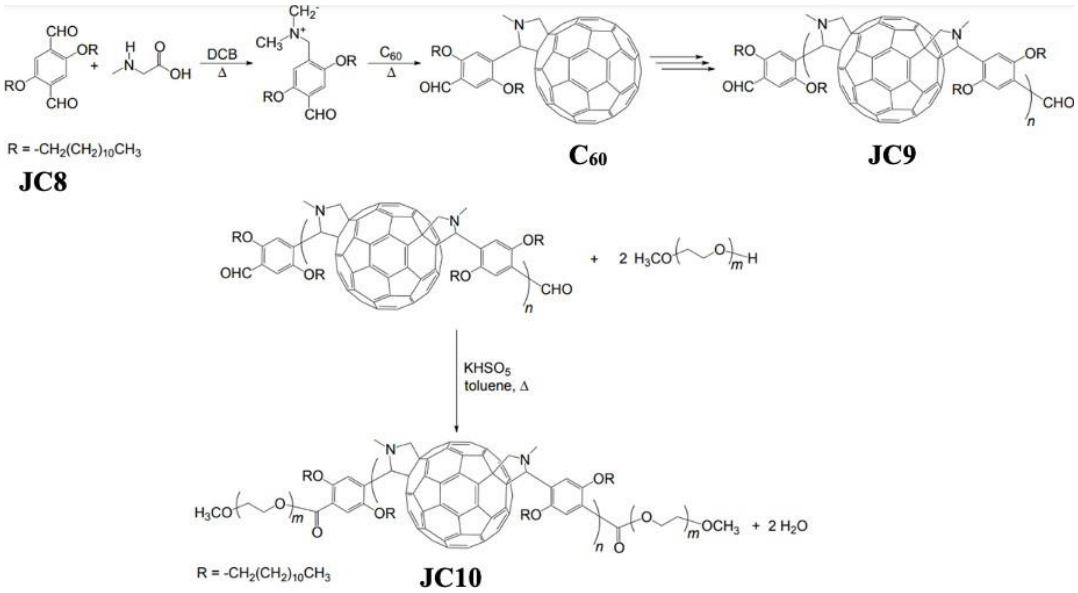

Figure 40-Chemical structure of block copolymer poly[fullerene-alt-(2,5-bisdocyloxy-1,4-terephthaldehyde)]-block-poly(ethylene oxide) (JC10)

3.2.2-Synthesis of the Comonomer JC8

To prepare JC8 we first started from the organic compound hydroquinone (molar mass = 110.11 g/mol) supplied by Sigma-Aldrich and shown in Figure 41. It was reacted with a bromoalkane in the Williamson condensation reaction shown in Figure 42 and then bromomethylated as shown in Figure 43

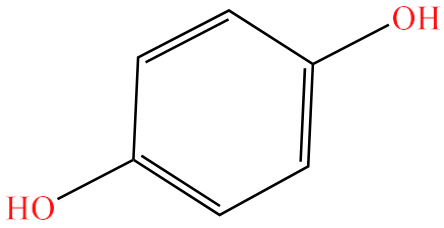

Figure 41-Chemical structure of hydroquinone.

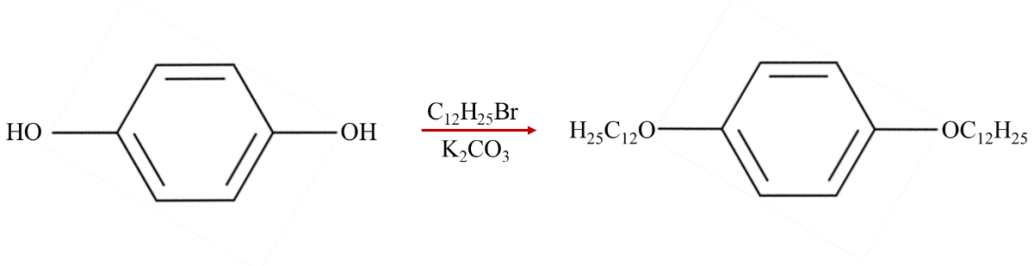

Figure 42-Preparation of JC6 from hydroquinone.

After obtaining the first monomer (JC6), as mentioned above, a bromomethylation was required, to be followed by a conversion to a bis-aldehyde, as shown in Figure 29.

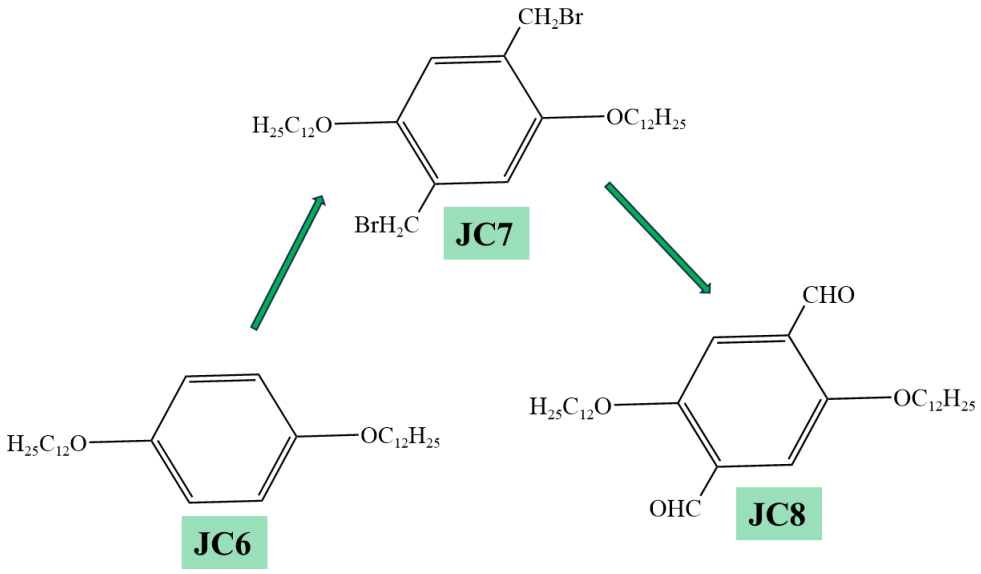

Figure 43-Synthetic steps to prepare, 1,4-bis(dodecyloxy)benzene (JC6), 1,4-bis(bromomethyl)-2,5-bis(dodecyloxy)benzene (JC7) and 2,5-bis(dodecyloxy) terephthaldehyde (JC8).

3.2.2-1,4 bisdodecyloxybenzene (JC6)

In a quite large reaction for our laboratory, hydroquinone (42 g, 38.14 mmol), anhydrous K_2CO_3 (159.6 g, 115.48 mmol), and n-dodecylbromide (238 g, 95.49 mmol) were stirred rapidly in acetone (1400 mL). The mixture was heated to 70 ºC for 48 h, without excluding air. After this time, the reaction was interrupted by pouring it onto cold water (3 L). The product was recovered by filtration. Finally, it was purified by dissolving it into a minimum of hot chloroform (approximately 60 °C) and precipitated into cold methanol (around 5 °C). The product, labelled **JC6**, was dried under reduced pressure to give 80.65 g, or 47.4 % yield. The details of its characterisation are given in the appendix.

3.2.3-2,5-dibromomethyl-1,4-bisdodecyloxybenzene (JC7)

HBr (30 mL, 31% by mass acetic acid) was added in one shot to a suspension of **JC6** (5 g, 11.2 mmol) along with paraformaldehyde (2 g, 67.2 mmol) in acetic acid (30 mL). The mixture was stirred at 70 °C for 2 h in a closed vessel so that the hydrogen bromide did not escape, as shown in Figure 44. Caution: the vessel was only closed when the reaction temperature of 70 ˚C was reached so that a build-up of pressure was avoided.

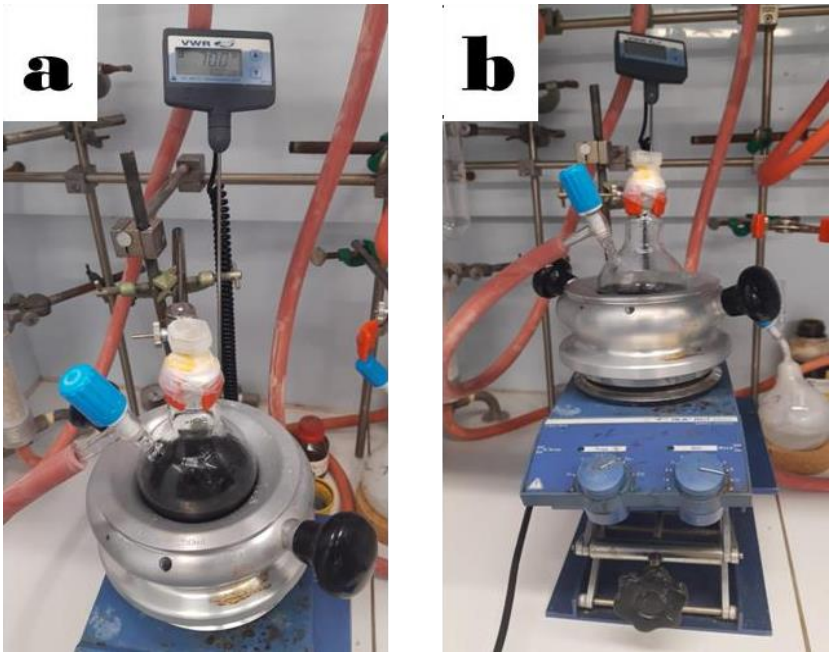

Figure 44-Images (a) and (b) show the beginning of the reaction to obtain the compound

Once cooled to room temperature (around 20 °C), the solution was added dropwise to ultrapure water (300 mL) to produce a white precipitate as shown in Figure 45. The brut product was recovered by filtration, and three times purified by dissolving in the minimum of hot chloroform (60 °C) and precipitating in chilled methanol (5 °C). After drying for 24 h under reduced pressure, we obtained a white, granulated solid, 8.51 g, with a yield of 73%.

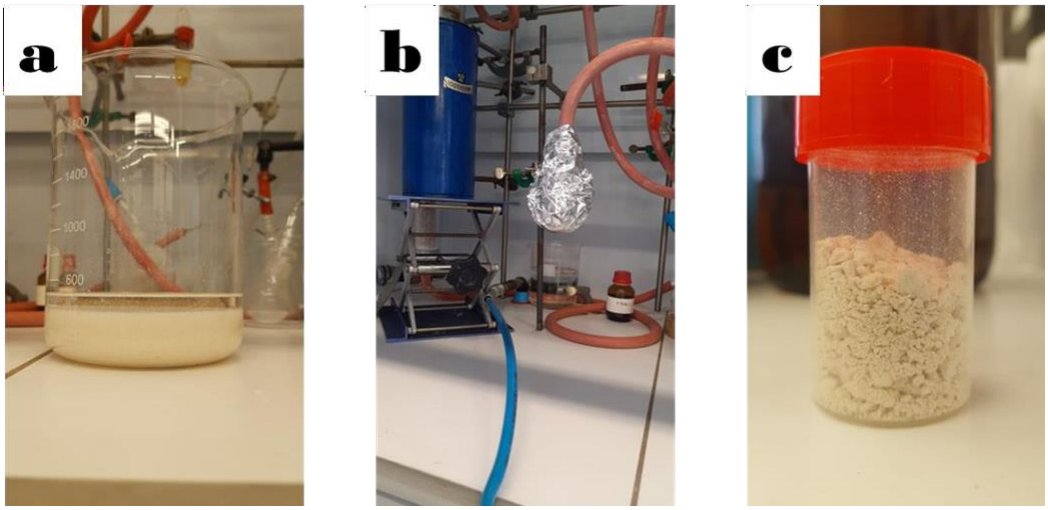

Figure 45-Obtaining the compound JC7: (a) washing and precipitation in water; (b) dried under reduced pressure with exclusion of light; and (c) the finished material.

3.2.4-1,4-bisdodecyloxy-2,5-terephthaldehyde (JC8)

A mixture of **JC7** (1.07 g, 3.8 mmol), $NaHCO_3$ (2.13 g, 90 mmol) and DMSO (44.5 mL) was stirred at 115 °C for 3 h under dry nitrogen. The reaction was then dropped into water (450 mL) at room temperature. After filtration and drying under air, the product was purified by chromatography in silica gel column using pentane/chloroform $CHCl_3$ (1/2, V/V) as eluent. Figure 46 shows the process of chromatographic separation of JC8 from impurities.

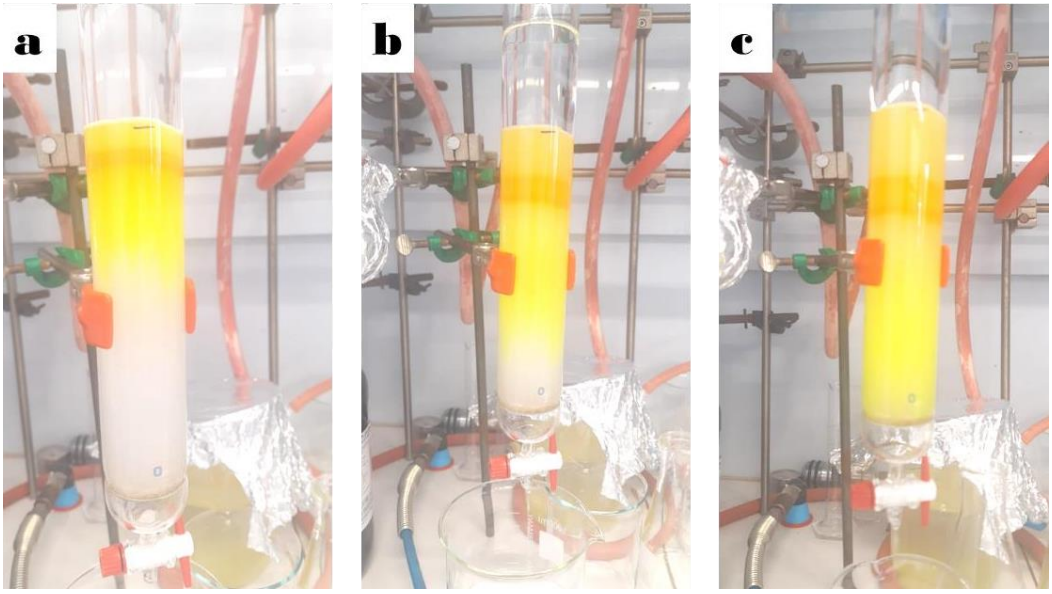

Figure 46-Purification of JC8 comonomer by using the silica gel column chromatography technique.

The process gave 6 solutions as shown in Figure 47. From each a small sample was taken to perform thin-film chromatography, as shown in Figure 47. This, with UV light, made it possible to determine which solutions had the same compounds. We could then join the solutions that contained the same compounds together, rota-evaporate the solvents, and then recover the separated products.

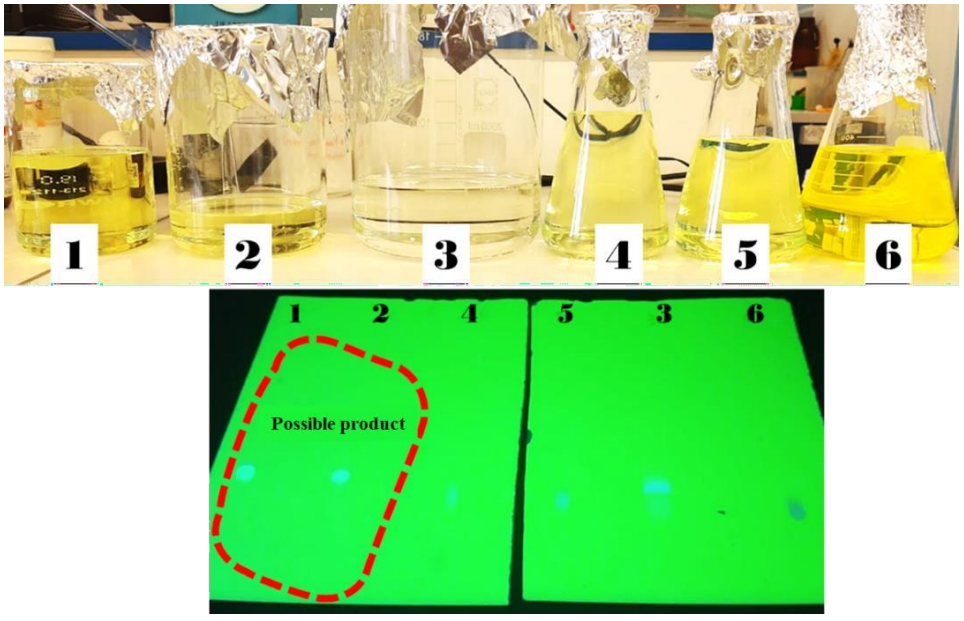

Figure 47-(Above) solutions obtained after performing the column, and (below) the characterisation of the solutions using thin-film chromatography to find out which solvents had common materials.

After the thin-film chromatography test, it was evidenced that the solutions of interest would be solutions 1 and 2. The evaporation of the solvent under reduced pressure resulted in 0.26 g of a bright yellow solid material as shown in Figure 48 presenting a 30.6 % yield.

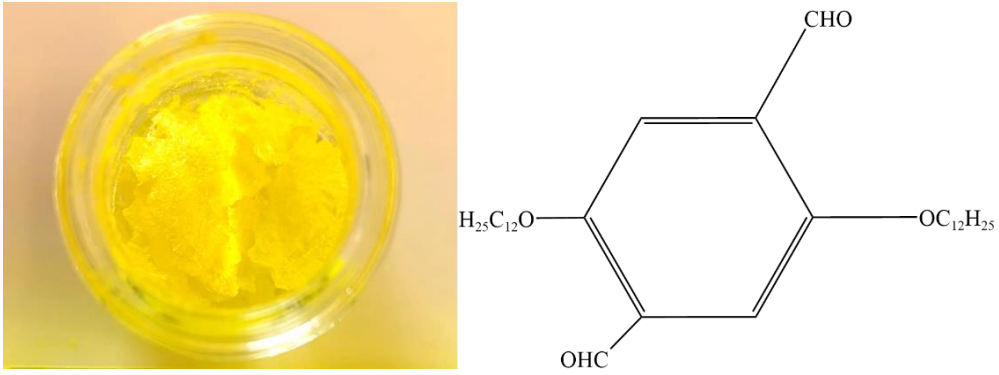

Figure 48-Image of JC8 and its molecular structure.

3.2.5-Synthesis of poly[fullerene-*alt*-(1,4-bisdodecyloxy-2,5-terephthaldehyde)] (JC9)

To prepare **JC9**, the yellow compound **JC8** (0.160 g, 0.0316 mmol), C_{60} (0.228 g 0.0316 mmol) and sarcosine (0.056 g, 0.0632 mmol), were placed in a 50 mL round bottom flask flushed with dry nitrogen. The products were then dissolved in degassed dichlorobenzene (9.2 mL) and stirred at 140 °C.

So that we could find the ideal length of time for this reaction, we performed a kinetic study. Aliquots of solution (0.5 mL) were removed and characterized by UV-visible spectroscopy. As shown in Figure 49, fullerene and JC8 have peaks at 335 and 395 nm, respectively.

We can see that the absorption of JC8 disappears very quickly, within 30 minutes, but that the curve for the C_{60} changes quite slowly. This means that the comonomer JC8 underwent a fast reaction with the sarcosine before reacting with C_{60}. The first reaction is much faster than the second, because we can see that the curve for JC8 changes completely after 30 minutes. This means that we can suggest the reaction mechanism shown in Figure 50 below, where the azomethine ylide is formed first, before reacting with the C_{60} to give the polymer.

This information is important because it means that we have to be careful that reactive aldehyde chain-ends are still available when we wish to make the block copolymer (**JC10**).

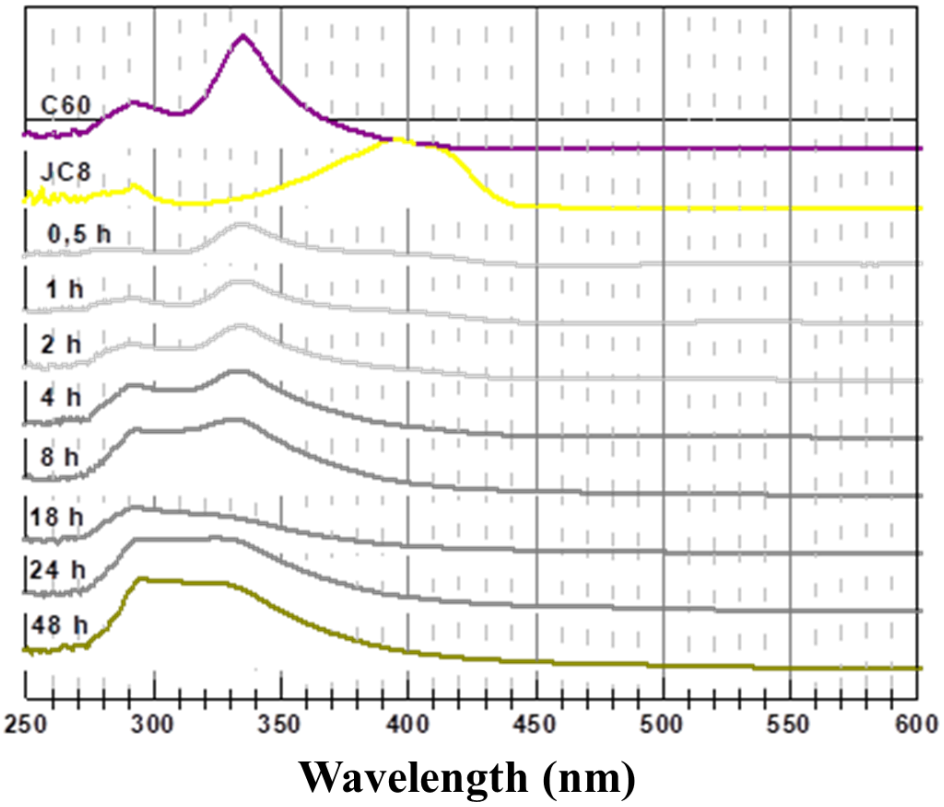

Figure 49-Kinetic study using UV-visible spectra to monitor the synthesis of polyC60.

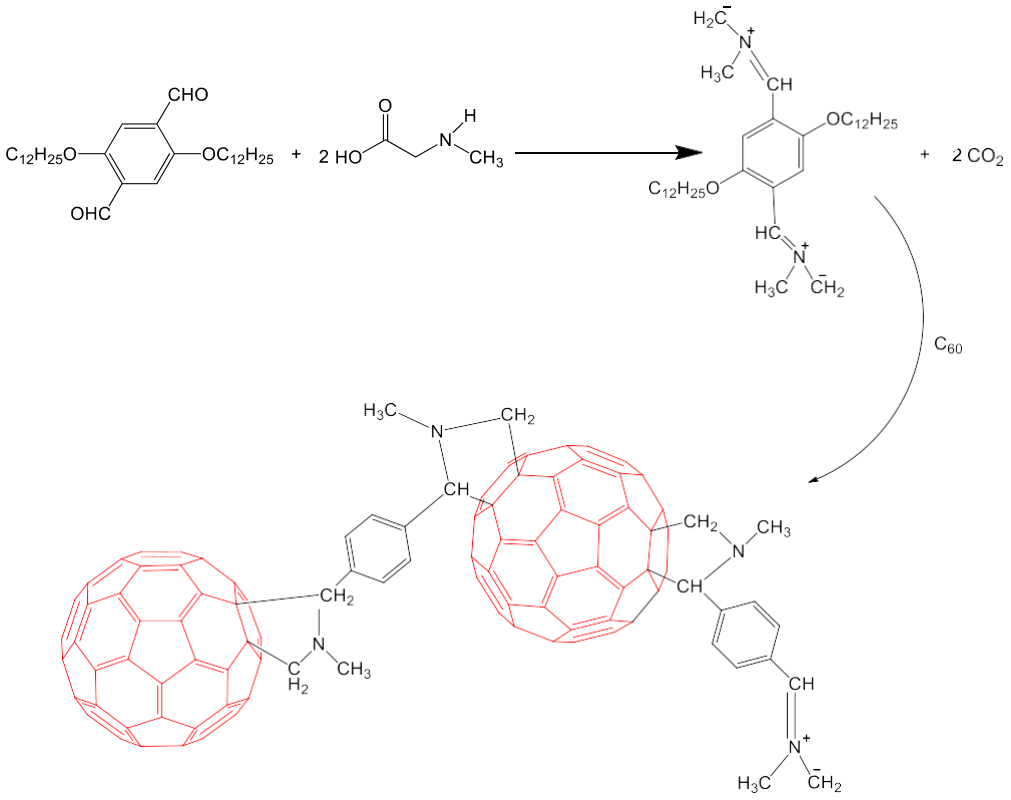

Figure 50-Aproposed mechanism for the synthesis of JC9, where the azomethine ylide is formed before the reaction with the C60.

With this information in hand, a new synthesis was started for 18 h, then added in methanol (110 mL) for precipitation. The precipitated material was recovered by filtration in a Soxhlet filter. The purification process was purified through the process of Soxhlet with acetone as shown in Figure 37 for 3 days and finally recovered the material of interest a glossy black powder (0.173 g, 30.7% yield).

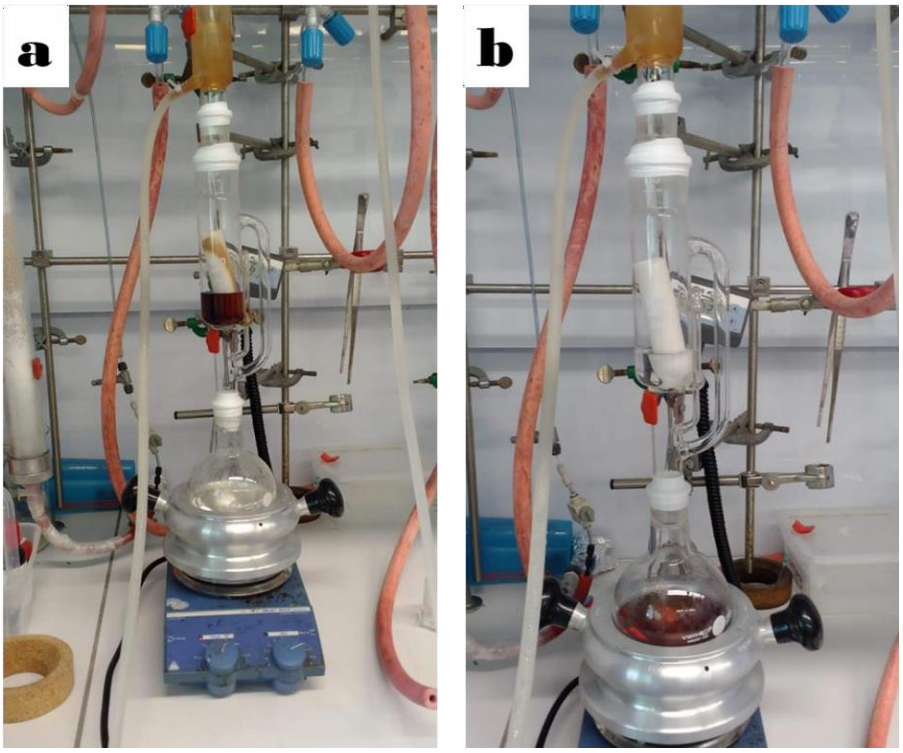

Figure 37- PolyC_{60} purification process using a Soxhlet in which the red color comes from low molecular weight oligomers.

3.2.6-Synthesis of poly[fullerene-*alt*-(1,4-bisdodecyloxy-2,5-terephthaldehyde)]-*block*-poly(ethylene oxide) (JC10)

The synthesis of the copolymer was divided into two stages. In the first, a large excess of poly(ethylene oxide) (0.200 g, 0.0693 mmol) was added to a 10 mL flask in 5 mL of toluene, and this solution was heated to 50 °C for approximately 40 min until complete dissolution of the polymer. After that, the heating was turned off and waited until the solution reached room temperature. Then, we started the second step where **JC9** (0.020 g, 0.00112 mmol) and oxone (1 g, 0.325 mmol) were added to the initial solution, under agitation at room temperature for 6 days, to give the copolymer **JC10**

with the structure shown in Figure 40. Finally, the material was placed in chloroform, filtered and taken to roto-evaporator for the recovery of the material of interest.

The curve resulting from the gel permeation chromatograph (GPC) is shown in Figure 51.The retention volume is inversely proportional to the molecular weight of the polymer. In the graph we can see the peaks due to the low molar mass poly(fullerene) in purple, and the orange peak due to PEO. In the former, there are multiple peaks because it is an oligomer, and each additional unit of fullerene in the main chain creates another peak. At the higher molar masses, the peaks blend and smooth out. The PEO, a commercial sample has two peaks. One is the main material:

CH_3-(-O-CH_2CH_2)-OH

which has one reactive chain-end. The other, small peak, is most-likely a by-product of the manufacture of this material:

CH_3-(-O-CH_2CH_2)-O-(CH_2CH_2-O-)-CH_3

This macromolecule arises from the polycondensation of two polymers during the production and has twice the weight of the main PEO. Obviously it cannot react with the poly(fullerene).

When fullerene goes through the GPC column, it is held back because it has the same size as the pores in the column (approximately 1 nm diameter). It actually comes out *after* the marker, toluene. This means that it is difficult to calibrate against and also gives very erroneous results. Similarly, the poly(fullerene) also gives values which are about 1/5 of its actually molar mass [55]. In this case though we can see a very slight increase in the peak of the molar mass of the copolymer with respect to the PEO. This would tend to confirm that the copolymer has been made. This said, further work needs to be done, to deconvolute the curves, but they prove the formation of block copolymer using this route.

The proton nuclear magnetic resonance spectrum (^{1}H NMR), however, showed only a simple peak of PEO. This was to be expected as similar block copolymers have given similar results, and the poly(fullerene) was carrying few protons that would not have easily relaxed their being in micelles.

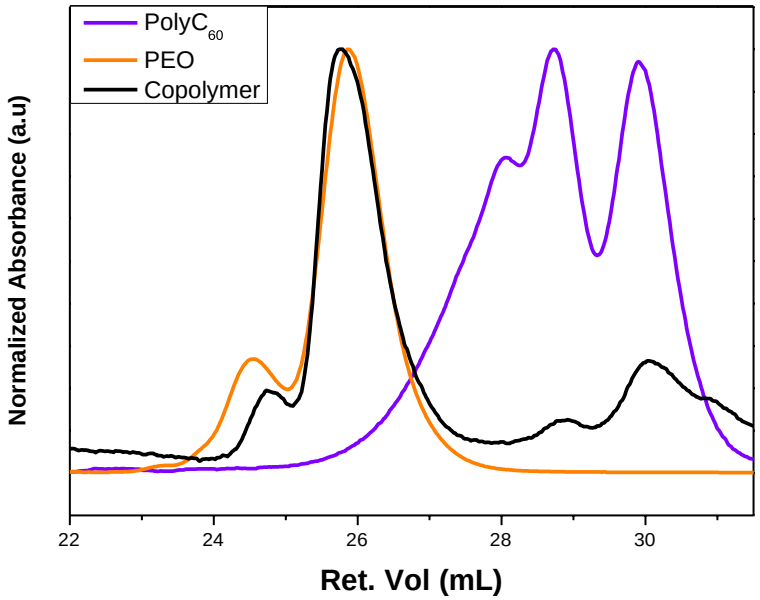

Figure 51-GPCs of JC10, PEO and the poly(fullerene) called JC9.

The UV-visible spectra of the copolymer JC10 is shown in Figure 52. We can see peaks at 240 nm and 605 nm. The former peak arises from a combination of the PEO [118] and the latter from the JC9 segments in the material. While a peak normally arises around this region for modified C_{60}, this one is quite high and might be due to doping with oxone, or aggregation effects. There is also a shoulder in the absorption spectrum at 300 to 350 nm which is typical for modified C_{60}.

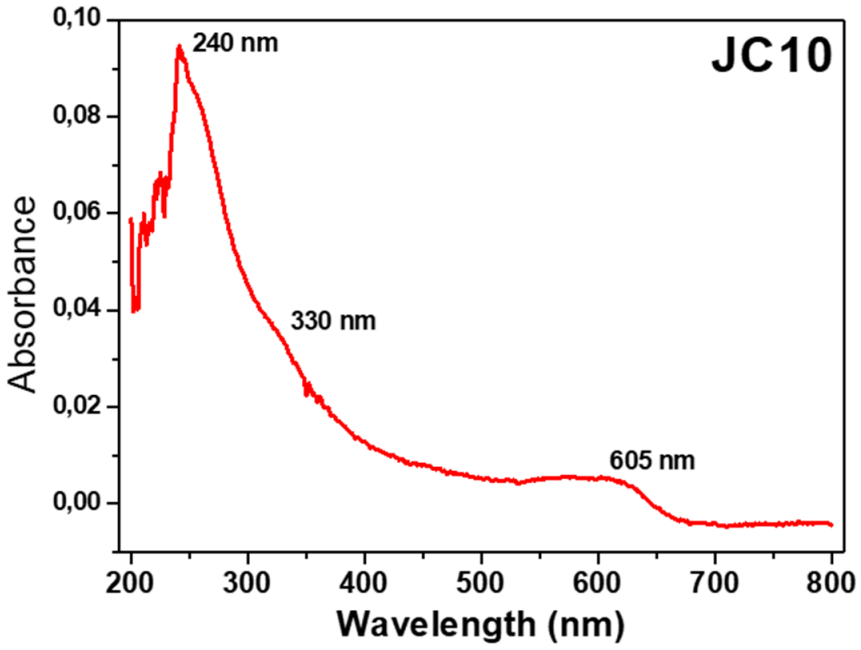

Figure 52-- UV-visible spectrum of the amphiphilic copolymer poly[fullerene-alt-(1,4-bisdodecyloxy-2,5-terephthaldehyde)]-block-poly(ethylene oxide) (JC10).

In this chapter will be presented the results with respect to the preparation of Langmuir-Schaefer and cast films of the JC10 copolymer, and the electrical characterization and its performance as a gas sensor.

3.3- Langmuir Films

The study of the surface pressure isotherm of the Langmuir copolymer film (JC10) was carried out in order to study the molecular organization of the thin films in the aqueous subphase. Through the obtained result it was possible to estimate at which surface pressure the Langmuir film has a higher ordering for the transfer to the solid substrate and consequently better morphology.

Figure 53 shows results obtained from the surface pressure isotherm per area (π-A) for the Langmuir film of the copolymer (JC10) with the solution at a concentration of 0.2mg/mL with the barrier velocity at 10 mm/min. It is possible to observe the condensed phase of the Langmuir film at a pressure around 20 mN/m, being the ideal surface pressure for deposition of the material and another data observed is that the Langmuir film of the studied material has the melting point between 30 mN/m.was above 30 mN/m.

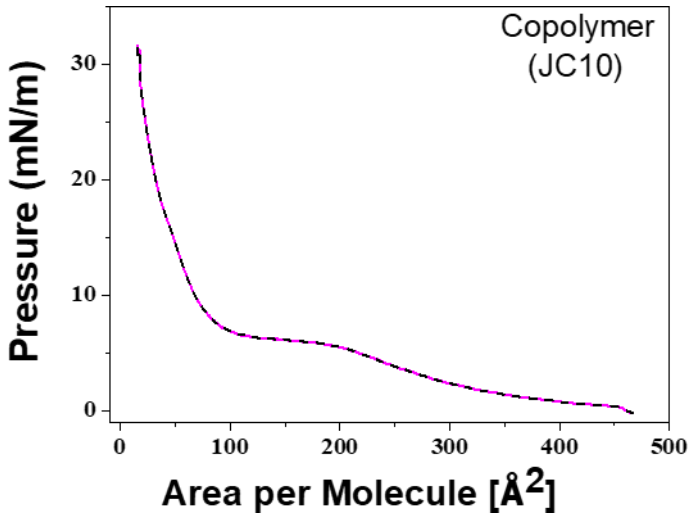

Figure 53- Surface Pressure Isotherm per molecular area of the JC10 copolymer.

From the graph we can extrapolate the curve in the condensed phase of the pressure isotherm of a Langmuir film, making it possible to estimate the average molecular area of the material, being 64.16 Å².

The JC10 copolymer has sites that interact in different ways with the water present in the Langmuir trough, where the PEO chains are hydrophilic, and this will impact the surface activation, while in the polyC_{60} sites, these large macromolecules would be expected to float on the surface of the water due to the hydrophobicity of C_{60}.

3.4- Electrical Characterisations - Direct Current (DC)

Figure 54 presents the same order of magnitude in the electric current response. It is possible to observe that both films had a linear behavior in the voltage range analyzed with a slightly higher slope of the line one for the cast films. In Figure 54, on the right, we have the conductivity of the films studied in which it shows that the cast film presented a higher conductivity, which passed 0.26 nS/m. This better result of the cast films may be related to the amount of material deposited on the substrate.

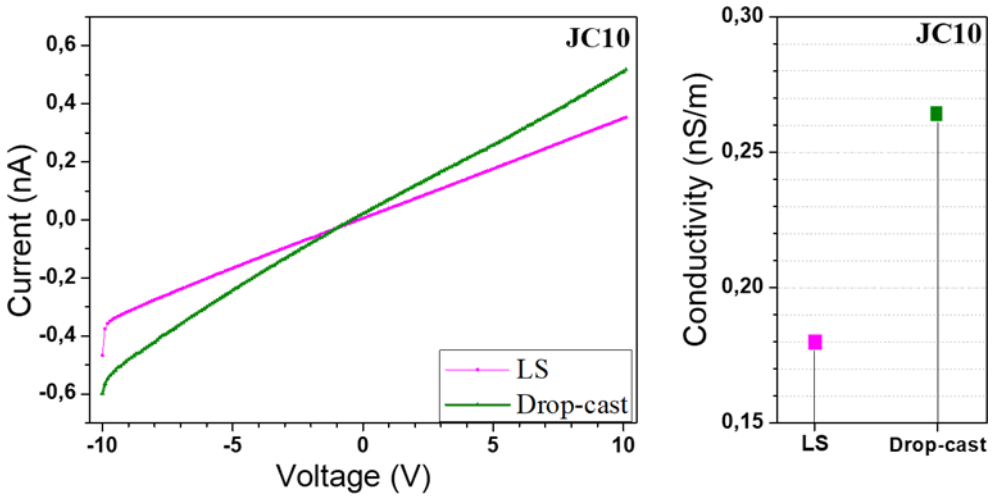

Figure 54-I vs. V electrical measurements in direct current (a) and conductivity (b) of the LS and drop-cast films of the JC10 copolymer films.

3.5- Gas sensors: using JC10 to sense ammonia

In this section, the electrical behavior of the thin films with the JC10 copolymer in the presence of ammonia gas (NH_3) was verified. The electric current was monitored in relation to the time during the passage of nitrogen flow and ammonia gas flow, and the difference of acting potential in the films was adjusted to 5 V. The gas flows were interspersed in intervals of 1 minute of N_2 and 2 minutes of NH_3 totaling 10 cycles.

As shown in Figure 55 we can observe that the material presented response in the presence of NH3 gas, both by cast and for LS, however the best response, in

terms of the intensity of the electric current, was that of the cast film however, the LS film maintained an electric current with the same intensity throughout the cycles of NH_3 injected, value of approximately 10 nA, while the sensor with the cast film detected an electric current around 110 nA initially, reducing this value over the injection cycles of NH_3, with the value of 20 nA for the last 3 cycles.

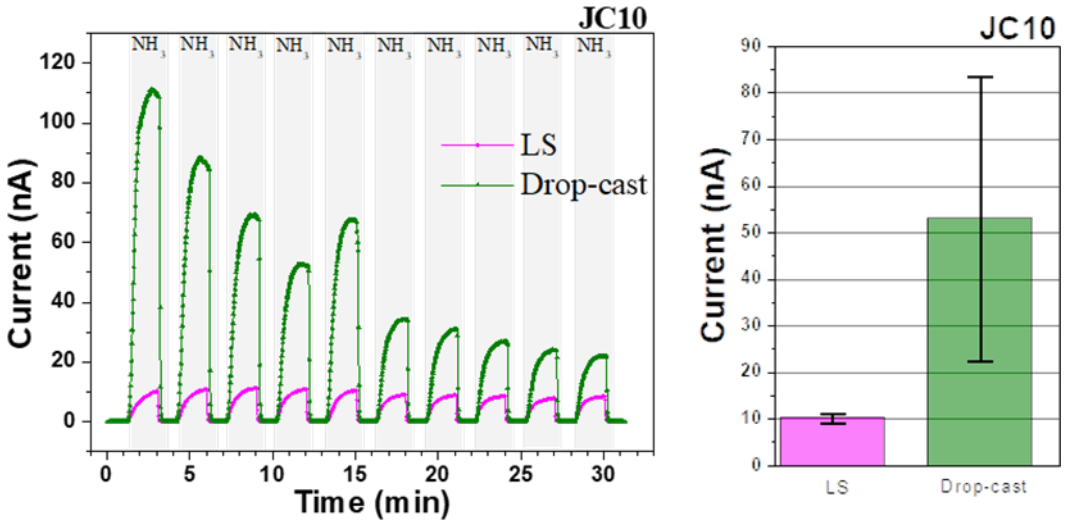

Figure 55-Gas sensor measurements of the LS and cast films of the JC10 copolymer, on the left and, on the right, the mean conductivity with the standard deviation for the measurements performed.

The film obtained by processing through the Langmuir Schaefer technique showed lower conductivity in relation to the film produced by drop-cast, but in the same order of magnitude and with less deviation from the measurements in each cycle.

3.6 - Conclusion

The JC10 copolymer, synthesized in France, also worked as a gas sensor inthe two tested techniques LS and cast, in which, in both cases, we had goodreproducibility in all cycles, but the cast film had a higher electrical response, in relation to the electric current, than for the LS film. This better cast result may be related to the amount of material that is larger than that of the LS film.

CHAPTER 4 - THE PREPARATION OF THIN FILMS USING THE NOVEL2-DIMENSIONAL POLYMER (JB17)

4.1 - Intruduction

In organic electronics there is a need for materials that make an interface between organic materials which are very hydrophobic, and inorganic materials which are very hydrophilic. A good example of this is in organic photovoltaic devices where the active layer, made from Y6 and PM6 for example, does not like water, whereas the electrode which is made from titanium oxide or a similar material does.

This means that the materials often come apart.

In this work we decided to use LB techniques to try and generate a new type of materials that is very thin, to let charge through, but has hydrophobic and hydrophilic sides to help with adhesion.

We could not find similar films that are one side hydrophobic and the other hydrophilic. However, we are aware in the literature that there are examples of very thin (atom and molecule) films. Mostly they seem only to be limited to very very small items, just several μm^2 wide, although some using rather more complex systems (rare earth catalysts) can reach larger cm^2 sizes. For example, amphiphilic films made of around 3 mm^2 using anthracene-based materials which are relatively unstable have been made[123], as have cm^2 polymeric film based on complex anthracene system carrying an amphiphilic tail [124] .Also toxic amines have been used in a porphyrin Schiff-based polycondensation [125] to give films about 1 mm^2. Some covalent organic framework (COF) thin films [126] have been made but they took 72 hours to form and did not give a single layer. A system based on anthracene was of great interest with a very regular structure made with light reaction [127]. However, is also very small films (μm^2 size at most).Also very regular 2D polyimides have been made on a water surface however they are only several μm^2 large, do not have one side hydrophobic and the other hydrophilic [128] A good general review can be found at reference [129]. Of course, there are modified films of graphenes, but these materials can only be produced fold-free and at large sizes by using extremely high temperatures near 1000 K (see for example [130])

In this work we show a way to make a thin film that is hydrophobic on one side and hydrophilic on the other, using room temperature and UV-light in a non-toxic process.

3.2-Synthesis of a novel 2-dimensional polymer

In this section we detail the methods used to prepare a novel 2-dimensional polymer.

Materials

In preparation for this synthesis, heptane (200 mL) was rigorously dried from over CaH_2, flushed with nitrogen, and then subjected to three freeze-thaw cycles with liquid nitrogen and under vacuum in a 500 mL round-bottom flask to remove oxygen.

4.2.1-1,2,3,4,5,6-Hexaethylbenzene (JC15)

Into a 500 mL Schlenk was injected heptane (70 mL), $TiCl_4$ (0.003 mol, 0.60 g, 0.347mL) and trioctyl aluminium (0.003 mol, 10 mL of a 25% solution in hexanes. The solution was gently stirred and left to 'age' for 30 min, and then to it was added more heptane (130 mL). 3-Hexyne (0.097 mol, 8 g, 11.34 mL) was added dropwise. The solution was then left stirring at 43 ˚C for 48 h. Once complete, the solution was evaporated to near dryness, to leave a thick, golden syrup. A small amount of ethanolwas added to drive the crystallisation, and the material left in the fridge for two daysto give the brut sample shown in Figure 56. Filtering was used to remove the excess ethanol and then left to dry. Recovery by filtration and drying at reduced pressure gave **JC15** (6.55 g, 80.6% yield) as clear needle-like crystals.

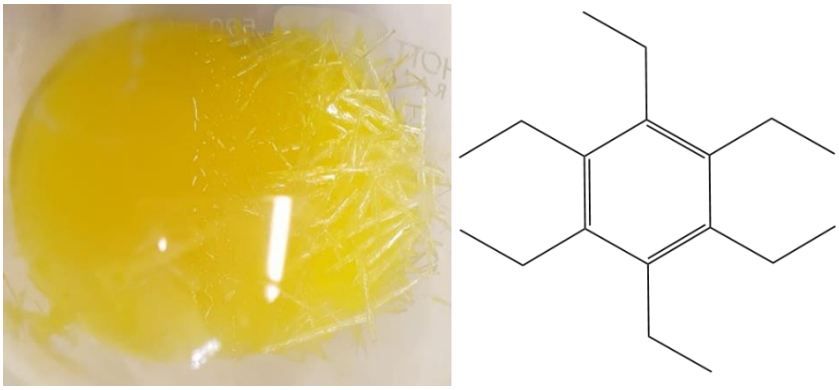

Figure 56-Yellow, needle like crystals appearing during the purification of JC15.

4.2.2-1,2,3,4,5,6-hexakis(1-bromoethyl)benzene (JC16)

In a 100 mL round-bottom flask were placed **JC15** (0.73 g, 0.00296 mol) and dichloromethane (36.5 mL). To this solution was injected bromine (2.88 g, 0.018 mol). The flask was fitted with a reflux condenser and was stirred magnetically whileunder strong illumination from a 400 W tungsten-filament lamp, used to generate bromine radicals. After about 15 min the solution had heated to reflux and hydrogenbromide was evolved. After another 15 min of illumination, a white precipitate beganto form, as can be seen in Figure 57. After a total illumination time of 2 h, the solutionwas cooled to room temperature, and rota-evaporation with drying gave **JC16** (1.867g, 80% yield) as a grey-white powder.

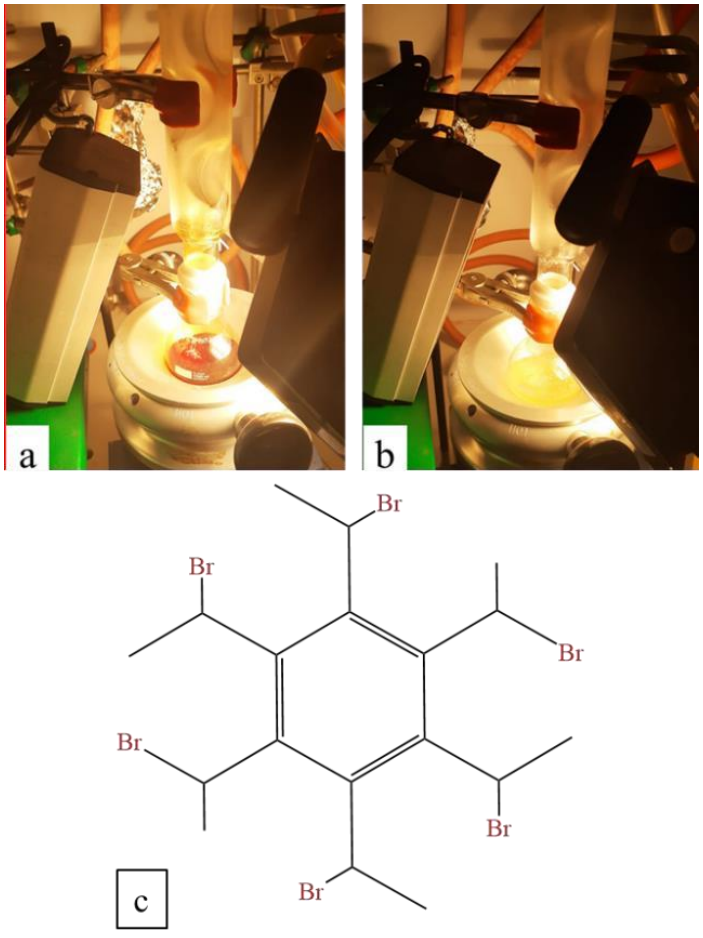

Figure 57-Preparation of JC16 with bromine and UV-illumination: (a) start of reaction showing the presence of bromine; and (b) near the end of the reaction with the white product precipitating and (c) JC16 structure.

4.2.3-1,2,3,4,5,6- Hexavinylbenzene (JB17)

In a 100 mL round-bottom flask was added heptane (7 mL), **JC16** (0.25 g, 0.00032 mol), potassium tert-butoxide (0.25 g, 0.00223 mol) and 18-crown-6 (0.030 g,0.000113 mol). A condenser was connected and the solution stirred for 3 h at a temperature of 110 °C. To wash the product, the reaction was precipitated in ice waterand add one drop of sulfuric acid was added to balance the pH. Extraction was performed three times with dichloromethane, and the brut product recovered by roto- evaporation. For the crystallization process, a minimum of ethanol was added, gentlyheated in a water bath and left in the refrigerator for at least 5 days. At the end of thisprocess, ethanol was carefully removed to leave **JB17** (21 mg, 27.8% yield) as yellowcrystals shown in Figure 58.

Figure 58-Small crystals formed at the end of JB17 purification.

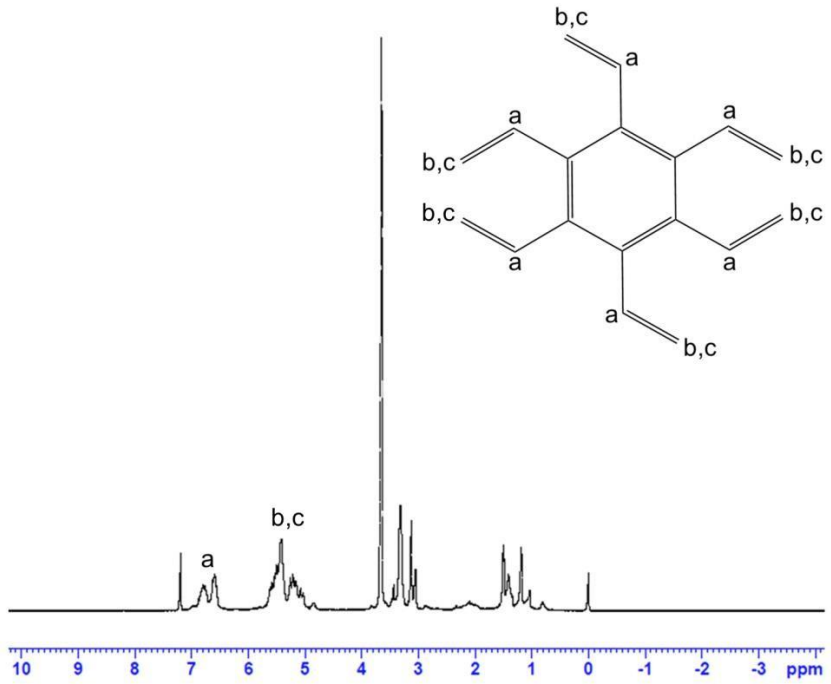

Figure 59-1H NMR (400 MHz) in CDCl3 of hexavinylbenzene (JB17). Note the peaks between 4 and 0 ppm arising from methanol and ethanol. These were not removed due to time constraints and the risk of possible sublimation of JB17 under reduced pressure.

In this chapter will be presented the results with respect to the preparation of Langmuir-Schaefer films of the JB17, and the electrical characterization and its performance as a gas sensor.

As far as we are aware, there has not yet been the preparation of extremely thin films that show one side hydrophilic and the other side hydrophobic. This wouldbe a major step for organic electronic devices.

Many small films have been made. For the most part though, they are only several μm^2 wide, although some more complex systems using rare earth catalysts can reach larger cm^2 sizes. The main items are these cited here. Amphiphilic films around 3 mm^2 have been made using anthracene-based materials which are relativelyunstable [127]. Also, anthracene has been used to make large cm^2 polymeric film based on complex anthracene system carrying amphiphilic tails which give good films [128]. Other films often require very long times to be made, for example, cm^2 films can be made in 72 h or so [129] or require expensive and toxic rare earth catalysts to make reaction much faster.

As shown in earlier chapters, we performed the reactions shown below in Figure 60 The chemistry is well known.

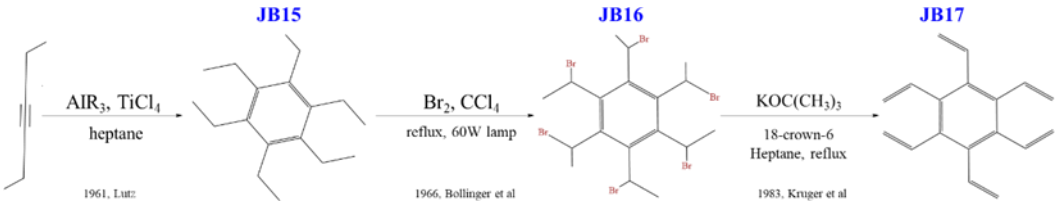

Figure 60-Synthesis of the molecule JB17 via known steps [131,132].

4.3- Langmuir Films of the JB17 without Additions

To perform the isotherm of the study material, we made a solution of JB17 in 0.12mg/ml xylene. Of this same solution, 500 µl were spread in the Langmuir troughto each isotherm. In this stage we perform two tests, the first a normal isotherm withthe speed of the barriers at 20 ml/min and without UV light, in the second isotherm we follow the same parameters but we add UV light at the beginning of the isothermwith the intention of carrying out the chemistry shown in Figure 63.

Note that Figure 61 presents the results of the isotherms without UV lightand with UV light, in which we can observe that the behavior of the curve changesin the gas phase, which shows a decrease in the area per cell when UV light is applied.

We did this by repeating the experiment with the light on at the first point of the compression curve to see if the curve would change. It did not (as shown in Figure 62), indicating that there was no reaction. This meant that the molecule **JB17**would not undergo a 2+2 cycloaddition in the conditions we used.

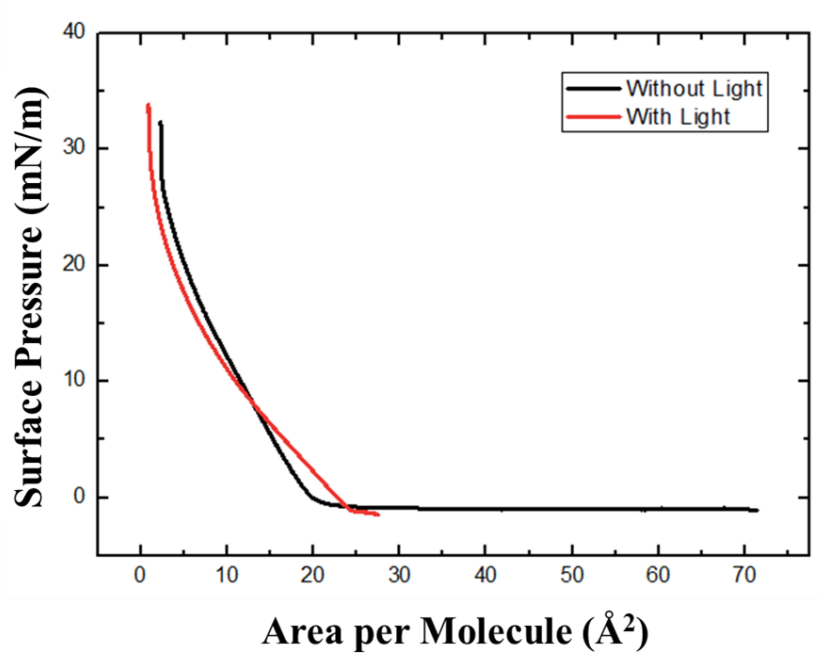

Figure 61-Pressure area isotherms curves of the molecule 4 (black) without and (red) with light showing no change beyond that of experimental error and indicating that no reaction had occurred when light had been put on the molecule JB1

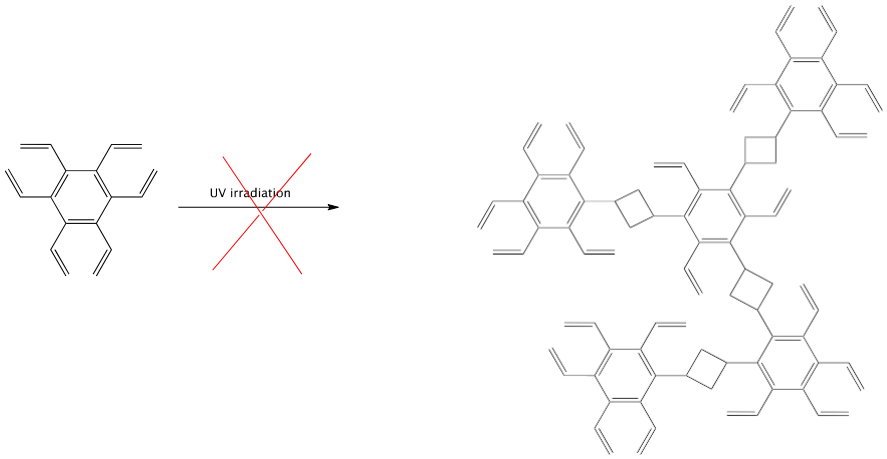

Figure 62-A possible but unsuccessful route to react JB17 to give a flat, 2D network polymer.

This does not mean it cannot happen, but rather, in the time available we could notfind the right conditions.

4.4- Langmuir Films of JB17 with a Light-responsive Initiator

We chose a new method, which was based on the use of a light-responsive molecule.In this case, we chose 2-hydroxy-4′-(2-hydroxyethoxy)-2-methylpropiophenone (HHMP), which is also known as irgacure-2959, which undergoes a reaction in the presence of UV-light to form radicals, as shown in Figure 70. Its absorption maximumis at 273 nm. [133]

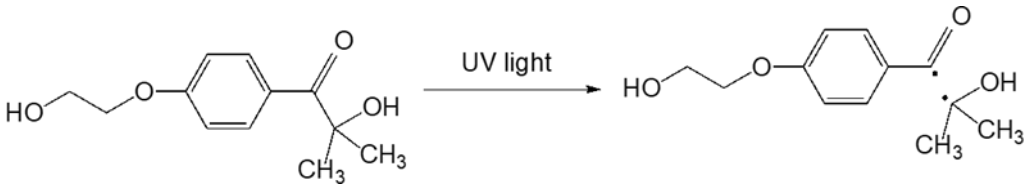

Figure 63-The process of radical formation by 2-hydroxy-4′-(2-hydroxyethoxy)-2-methylpropiophenone (HHMP) on exposure to UV-light**.**

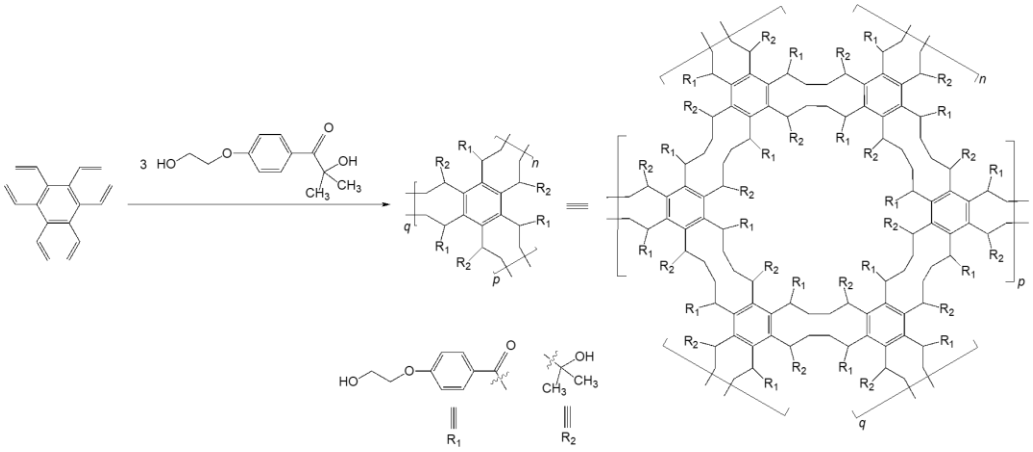

Figure 64-Route to planar molecule, which we believe will give a hydrophobic surface on one side and hydrophilic on the other.

A new solution was made with HHMP, and it contained so that it hadan approximate ratio of 1 part JB17 to 9 parts HHMP. We used this high ratio of HHMP to JB17 to ensure that there would be enough water dispersed HHMP at thesurface, showed in Figure 64. Approximately 0.5 mL was spread over the Langmuirtrough and then compressed at 20 mL/min. In this isotherm we turn on the light (UV light from an Osram 300 W ultra vitalux) in the transition from the gas phaseto the liquid phase, for ten minutes, while we let the system work. This showed a definite difference in the curves, indicating that a reaction had occurred, as shownin Figure 65.

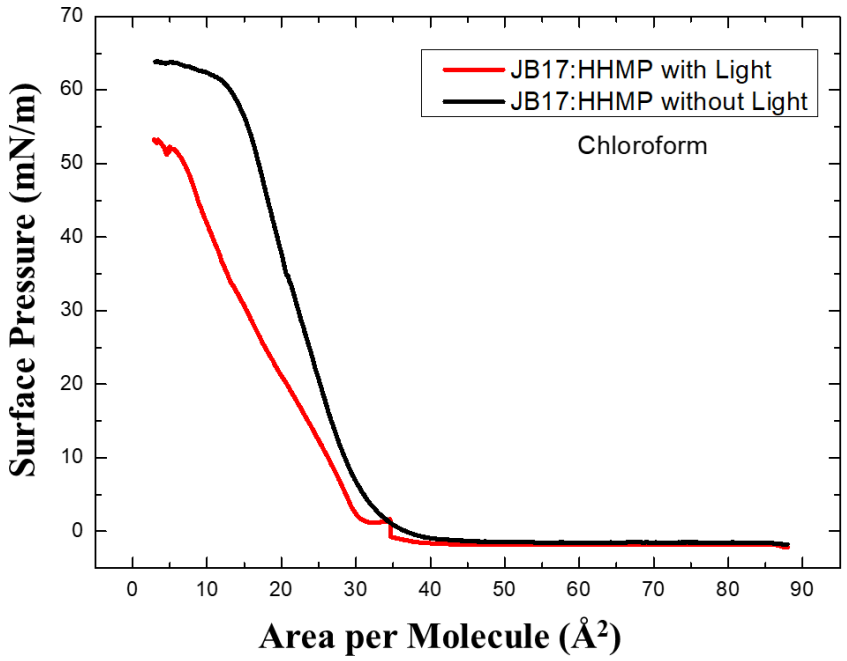

Figure 65- Isotherms of JB17 with HHMP solution (black without light, red with light) change in mean molecular area resulting from the impact of light starting a reaction in the system (black without light, red with light). Note the small jump from when the light

The work was repeated, this time in xylene. However, this time, we used a much lower amount of HHMP with respect to JB17 (i.e., 25%) ratio. The reason was to tryand extend polymerizations over a much longer distance between various structures. As shown in Figure 71 in the introduction, a low amount of initiator can prepare verylong chains.

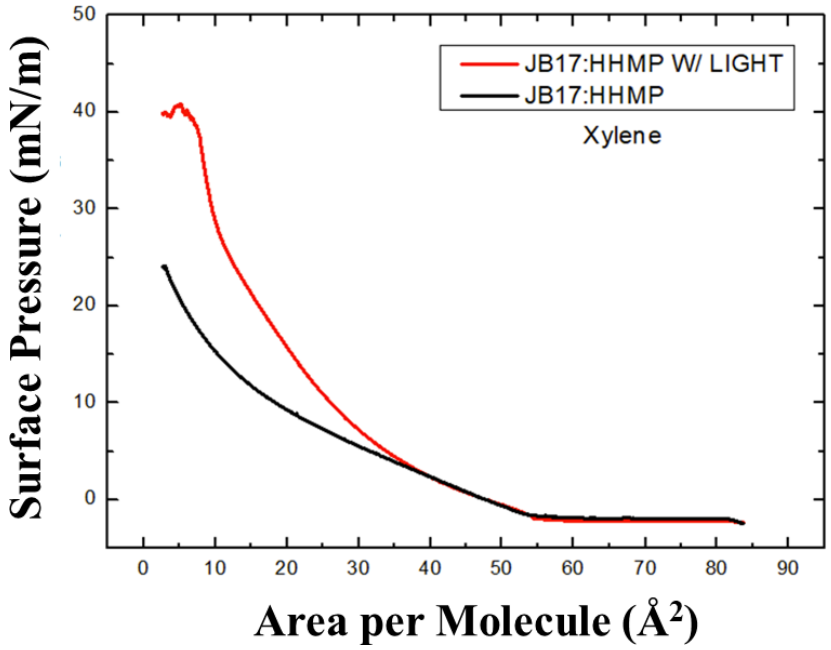

Figure 66-Pressure-surface area isotherms for xylene-based products. Black without light, red, with light confirming the reaction by way of the change in position.

Comparing Figure 65 Figure 66, we can see that when we use chloroform (with more HHMP) the isotherm with light has a smaller average molecular area compared to that without light. While in the isotherms with xylene (less HHMP) the curve that was used with light presented a greater average molecular area in relation to the curve without light. This result may be due to the impact of using less HHMP, which allowed long-range polymerizations, creating a more stable structure. This will be studied in future work.

4.5– AFM Results

The films were deposited on a silicon substrate for AFM measurements. The filmswere made as shown in Figure 67 using the Langmuir Schaeffer technique (a) andanother method we are calling (AM-H) (b) which deposits the films from bottom to top.

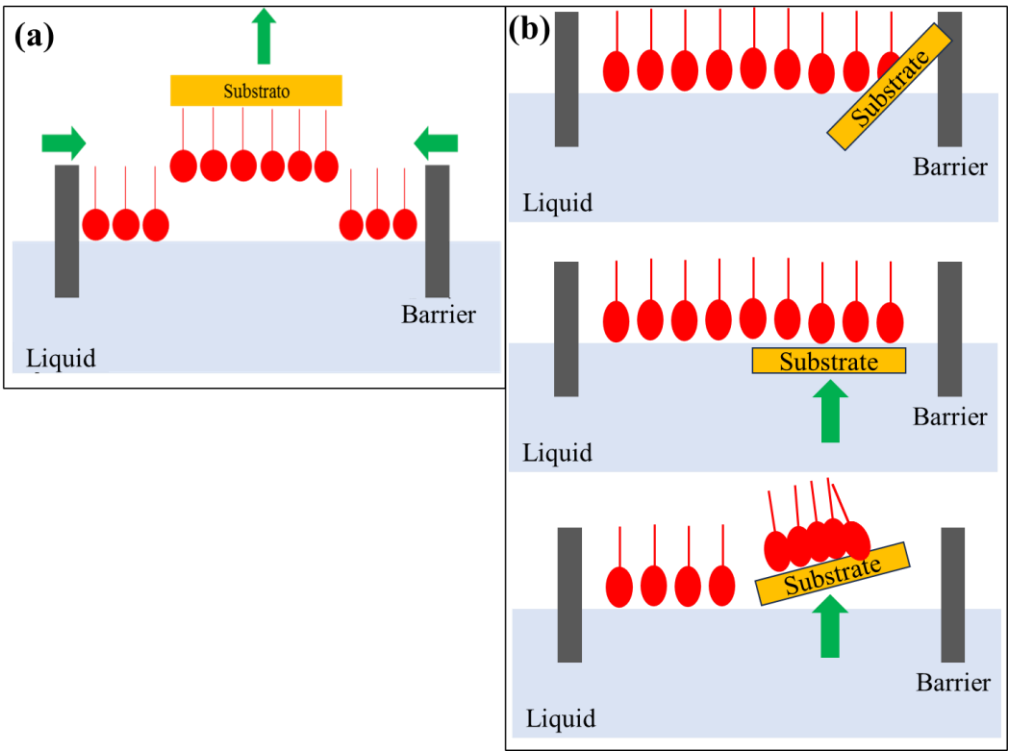

Figure 67-Langmuir Schaeffer technique (a) and another method (AM-H) (b) which deposits the films from bottom to top.

The following figures show the films we created. In the first cases, we cansee what is done when there is no light Figure 68, and we end up with oily, disorganized blobs of unreacted materials.

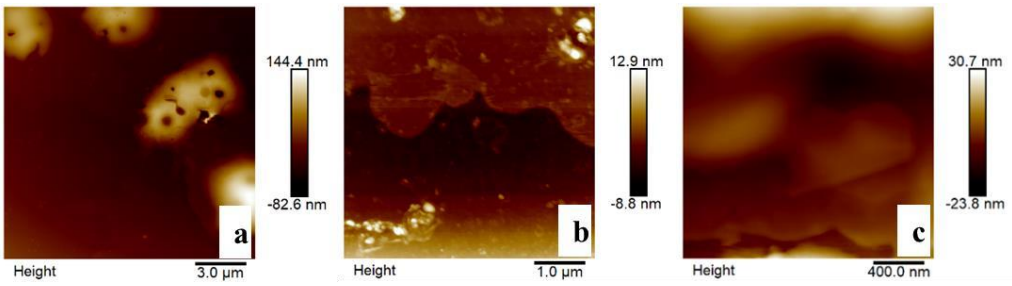

Figure 68-Increasing small scale images of AFMs of JB17 that has not been exposed to light (collected using what we have named the (AM-H) in which the film is scraped off the surface of the water with a continuous movement in one direction). (a) At 3.0 µm; (b) at1.0 µm; and (c) at 400 nm scales as indicated bythe bars.

In the last cases where we exposed the samples to light (Figure 69 and **Figure 70**), we could observe fibers, which clearly indicates the formation of polymers. In the first case (Figure 76) the Langmuir-Schaeffer technique was used.

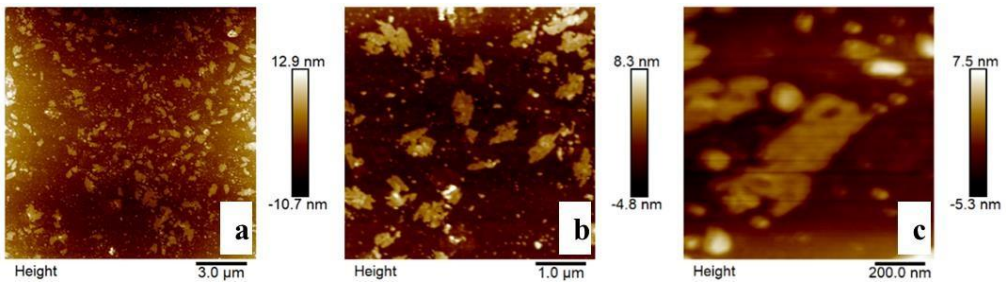

Figure 69-Small-scale AFM crescent images of JB17 that were exposed to light collected by the Langmuir-Schaeffer technique. (a) Up to 3.0 µm; (b) up to 1.0 µm and (c) scales up to 200 nm as indicated by bars.

In Figure 77, the collection method, (AM-H), means that the materials havebeen scraped up together, forming fibers from over the surface. This clearly indicatesthat we have an extended polymer formation at the air/water interface.

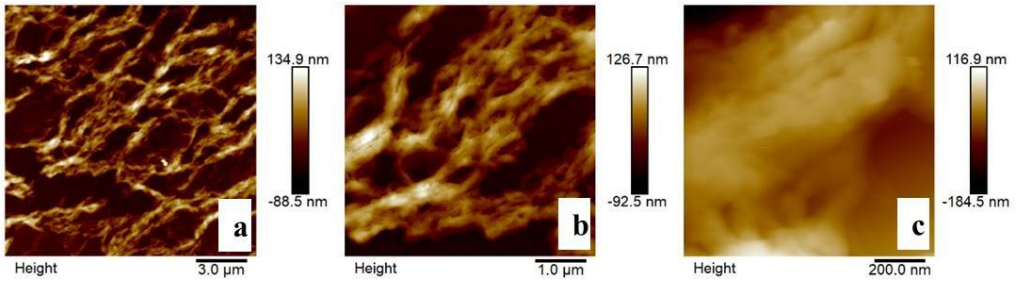

Figure 70-Remarkable formation of polymers from JB17 exposed to light with HHMP. Increasing small scale images of AFMs of JB17 that has been exposed to light collected using the so-called (AM-H) over a large area of several tens of cm. (a) At 3.0 µm; (b) µm; and (c) at 200 nm scales as indicated by the bars.

Figure 70 shows the extraordinary formation of fibers, clearly indicating thepresence of polymeric materials formed following exposure of JB17 to light. Figure 71 shows the results of the repeated experiment, with an exceptional fiber formationover large distance.

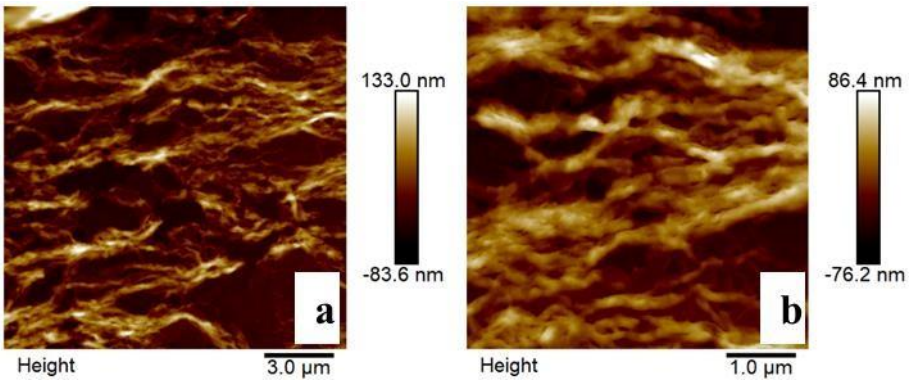

Figure 71- Fibrous formation of polymers from JB17 exposed to light with HHMP. Increasing small scale images of AFMs of JB17 that has been exposed to light collected using the so-called (AM-H) over a large area of several tens of cm. (a) At 3.0 µm; (b) at 1.0 µm; and (c) at 200 nm scales as indicated by the bars.

4.6 - Conclusion

The AM-H methods shows an extraordinary formation of fibers, clearly indicating the presence of polymeric materials formed following exposure of JB17 tolight.

NEXT STEPS AND PERSPECTIVES

In the Brazilian system, changing the PhD title is not a simple thing, but an official move will be made to change the title to better adapt it to the work. It is thus suggested that it becomes, ‘Synthesis and characterisation of polymeric materials for nanostructured organic devices’.

Beyond this will expect to prepare new samples of JB17 (it was all used in this study), and then make further studies to try and improve the formation of the film over large areas. Particularly, AFM, TEM and SEM studies will be carried out to understand its formation and spread of this exciting new material, which might find uses in organic electronics. We expect to prepare at least four papers from this work for high impact journals.

Further into the future, other students of Professor Olivati will be applying the JB17 to photovoltaic devices and sensors as an interlayer to resolve problems of adherence.

APPENDIX

Materials and Methods

Thin Film Preparation Techniques

In this section, methods of processing, spin-coating, drop-cast and Langmuir Schaefer(LS) of ionomers for the manufacture of sensors is presented. The films were fabricated onto different substrates (glass, interdigitated electrodes),depending on the characterization/application.

Drop-cast and Spin-coated Films

The drop cast films were processed by dripping the solution of the materials under ambient conditions (T= 23°C), with a microsyringe (spread volume-150 µL), with the following concentrations: for the ionomer films (0.2 mg/mL in xylol); and for the copolymer films (0.2 mg/mL in chloroform) onto the substrate on a level basis, forming the films with solvent evaporation, time of drying (30 minutes).

For the production of the spin-coating films, the VTC-Vacuum Spin Coaterequipment (MTI Corporation) was used, at the same concentration and conditions used for the cast films, in which these solutions were spread over the substrate and taken to a rotation of 2000 rpm for 60 s.

Langmuir and Langmuir-Schaeffer Films

Unlike the aforementioned techniques, for the manufacture of Langmuir thin films itis necessary to use equipment known as a Langmuir though as shown in Fig A1, which consists of a Teflon tank where a liquid is added, which is usually ultrapure water and on the surface of this liquid is spread the solution of interest. After doing this, the barriers begin the compression process of the material, making it possible toform a film with the molecularly organized material. Each chapter provides a detailed description of the parameters related to the concentration of the materials, spread volume, barrier compression, and the number of layers of the films fabricated and characterized.

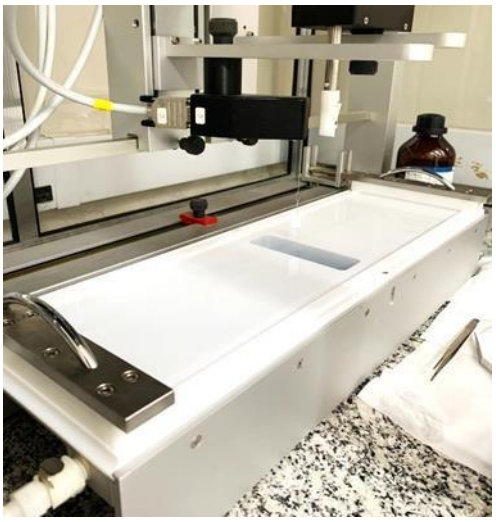

Fig-A1 - Langmuir device.

Substrates

For the DC electrical measurements and tests such as a gas sensor, interdigitated gold electrodes, IDEs (Interdigitated Electrodes), were used, as shown in Fig A2. The IDE-Au was fabricated using photolithography using glass as substrate as described elsewhere. The use of the IDE is important, because in each pair of digits of the electrode the total current is amplified, which makes it easier to characterize materials with low conductivity.

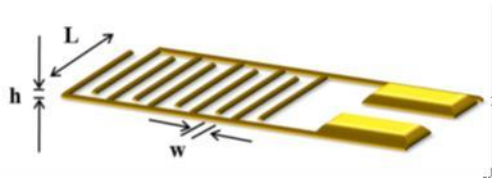

Fig A2 - IDE representation with N = 10 digits, h height, L length and w digit width, dimensions 110 nm high (h), 8 mm long (L) and 100 μm wide (w).

These substrates were produced at the Laboratory of Microfabrication and Thin Films (LMF) of the National Nanotechnology Laboratory (LNNano) at the National Center for Research in Energy and Materials (CNPEM) but before using them, they need to undergo a cleaning process which consists of immersion in isopropyl alcohol and acetone at a temperature close to 50 ºC.

Characterization Techniques

In this short section, the characterization techniques used for the films of ionomers

and copolymers are presented.

Atomic Force Microscopy (AFM)

AFM measurements were performed to verify the nanoscale morphology of the produced films. An area of 10×10 μm^2 was analyzed, using the Nanosurf microscope, EasyScan 2 model, silicon tip coupled to a cantilever and contact operation mode. The images were treated and analyzed using the Gwyddion 2.41 software, and the roughness was analyzed in terms of RMS - Root Mean Square roughness.

UV-Visible Characterisations

The thin films of the copolymer manufactured by the LS technique were characterized by visible ultraviolet (UV-Vis) spectroscopy, through a Cary 100 UV-Vis spectrometer shown in Fig A3, scanning between the deposited wavelengths of 300-900 nm on BK7 glass substrates.

Fig A3- Cary 100 UV-Vis Spectrometer

Electrical Characterization in Direct Current (DC)

I versus *V* measurements were performed to characterize the samples when direct current (DC) was applied, using a Keithley 238 Source (High Voltage SourceMeasure Unit), as shown in Fig A4 at voltages ranging from -10 to 10 V in 1V steps over a time interval of 100 ms.

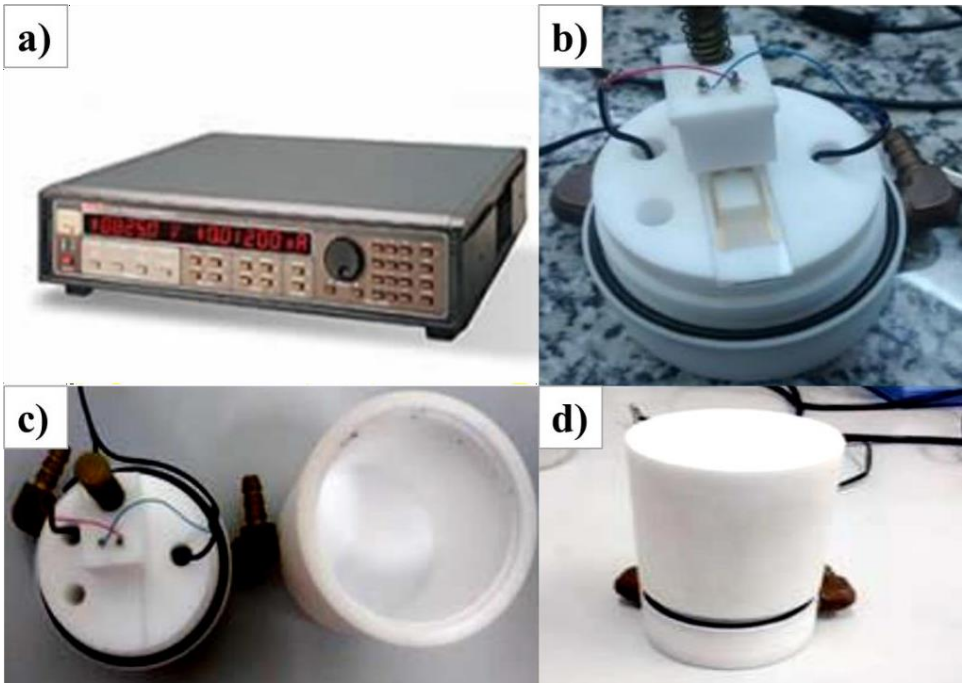

Fig A4 - Source Keithley 238 (a) and sample holder for electrical characterization measurements (b, c and d).

To calculate the conductivity (IDEs) it is necessary to adjust the graphs with a first-degree equation of the type (y = ax + b), where b = 0. Through Ohm's Law using equations (1) and (2), from *I versus V* curves it´s possible to estimate the conductivity for this type of electrodes configuration using the method developed by Olthuis *et al.*, where R is resistance and k_{cel} is the cell constant that is equal to $5.1 m^{-1}$ [108.] This value takes account the digit height, spacing, number and length of the IDE.

$$V = R.i \quad (1)$$

$$\sigma = \frac{1}{R}.k_{cel} \quad (2)$$

Characterization of the Gas Sensor Device

To analyze the performance of the materials used as active layer of sensors (ionomers and copolymers), the films deposited in the IDE's were inserted in the sample holder, as shown in Fig A5, then current measurements were performed as a function of time (*I versus t*), maintained an electrical voltage of 5 V, then a nitrogen flow is applied, which serves as a baseline, in which the sensor should not present any response, remaining relatively constant, being a flow of 60 NL/h (normal liter per hour), for a time of 1 minute. Given this time, the ammonium hydroxide vapor is released and carried by the nitrogen flow to the sample port, where the sensor is located, this process occurring for a time interval of 2 minutes.

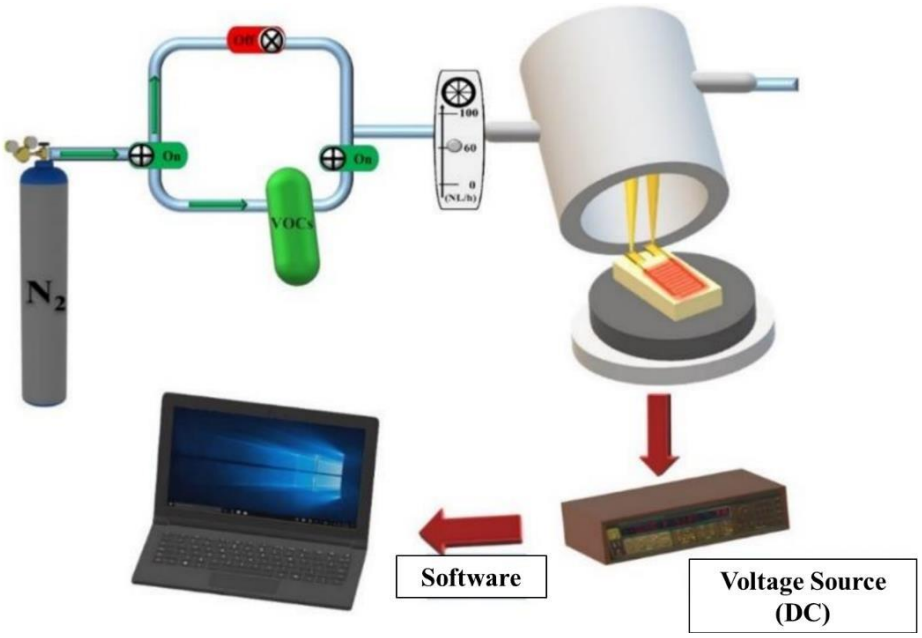

FigA5- Schematic structure of sensor measurement systems in a saturated atmosphere, connected to an electrical voltage source, with the sensor positioned inside the sample holder [109].

At the end of this interval, the ammonium hydroxide vapor is closed, returning only nitrogen to the sensor, and this procedure is repeated for 10 cycles.

Principal Component Analysis

In this work, a statistical method was used to analyse sensory response data. This method is a tool that can help deepen the understanding of the data obtained. There are several techniques and methods available to process and analyze results obtained in different studies. To obtain more precise conclusions, it is possible to apply a data analysis that can be adjusted to the variables presented in several contemporary research fields. These techniques are widely applicable in all areas of data science, especially in a "Big Data" context"[110].

One of the most widely used multivariate statistical techniques is PCA, which was originally proposed by Karl Pearson in the early 20th century [108]. PCA allows for understanding and conclusions about a large amount of varied information related to a problem, situation, or multiple correlated outcomes, which would otherwise require time-consuming manual analysis. Initially, it is possible to identify some variables that stand out or draw more attention during data analysis. From these variables, it is possible to reduce the size of the grouped linear information, resulting in combinations called principal components. The goal of this technique is to reduce

the number of variables present in the database, either by eliminating noise or less relevant factors, which can be identified in advance or through artificial intelligence algorithms, such as machine learning.

This widely used method is suitable for the analysis of random behavioral data, values, trends and also for the understanding of multiple electrical responses of sensors in different variables studied. The PCA were used, in this work, as an additional tool for a better understanding of the various and various sensory units produced here, with diverse variations among materials and techniques used for each type of sensor manufactured.

In the results will be displayed PCA comparisons between the techniques LS, drop-cast and spin-coated of the ionomers SPS and SPS-*co*-PMMA.

For the organization of results the Free Software "Orange Data Mining" was used, available for free (https://orangedatamining.com). The results used for analysis were obtained from the current curves per time (*I versus t*) of the measurements in the presence of the gases applied under the samples. For organization and insertion in the software, the sensory units of responses were organized according to the scheme below, thus using the separation capacity of the gas sensor measurements through the similar separations in the main component diagrams Fig A6.

	A	B	C	D
1	**Pontos 1 até 10**	**1 ... 10**	**1 ... 10**	**1 ... 10**
2	**PS3% (2° pico)**	PS3% LS	PS3% Spin	PS3% Casting
3	**PS3% (3° pico)**	PS3% LS	PS3% Spin	PS3% Casting
4	**PS3% (4° pico)**	PS3% LS	PS3% Spin	PS3% Casting
5	**PS3% (5° pico)**	PS3% LS	PS3% Spin	PS3% Casting
6	**PS3% (6° pico)**	PS3% LS	PS3% Spin	PS3% Casting
7	**PS3% (7° pico)**	PS3% LS	PS3% Spin	PS3% Casting
8	**PS3% (8° pico)**	PS3% LS	PS3% Spin	PS3% Casting
9	**PS3% (9° pico)**	PS3% LS	PS3% Spin	PS3% Casting
10	**PS6% (2° pico)**	PS6% LS	PS6% Spin	PS6% Casting
11	**PS6% (3° pico)**	PS6% LS	PS6% Spin	PS6% Casting
12	**PS6% (4° pico)**	PS6% LS	PS6% Spin	PS6% Casting
13	**PS6% (5° pico)**	PS6% LS	PS6% Spin	PS6% Casting
14	**PS6% (6° pico)**	PS6% LS	PS6% Spin	PS6% Casting
15	**PS6% (7° pico)**	PS6% LS	PS6% Spin	PS6% Casting
16	**PS6% (8° pico)**	PS6% LS	PS6% Spin	PS6% Casting
17	**PS6% (9° pico)**	PS6% LS	PS6% Spin	PS6% Casting
18	**PS20% (2° pico)**	PS20% LS	PS20% Spin	PS6% Casting
19	**PS20% (3° pico)**	PS20% LS	PS20% Spin	PS6% Casting
20	**PS20% (4° pico)**	PS20% LS	PS20% Spin	PS6% Casting
21	**PS20% (5° pico)**	PS20% LS	PS20% Spin	PS6% Casting
22	**PS20% (6° pico)**	PS20% LS	PS20% Spin	PS6% Casting
23	**PS20% (7° pico)**	PS20% LS	PS20% Spin	PS6% Casting
24	**PS20% (8° pico)**	PS20% LS	PS20% Spin	PS6% Casting
25	**PS20% (8° pico)**	PS20% LS	PS20% Spin	PS6% Casting

Fig A6- Organization of the points (1 to 10) within each cell for recognition of each sensory unit in its entirety.

The methodology used consisted of performing measurements (*I versus t*) with ten cycles between gas and nitrogen, where the 2nd to the 9th cycles inclusively of each measurement were chosen for analysis. Each cycle was initiated from the moment the gas came into contact with the sample, and from the increasing electrical response close to the maximum current peak displayed, 10 points corresponding to the electrical response attributed to the interaction between the sensor and the gas in flux were selected.

We chose not to use the first and last response cycles due to the abrupt variation of electric current that occurs in the first contact with the gas in some of the sensors, which could generate erroneous results compared to the other cycles more constant in their displayed responses. The data obtained were organized in cells in Excel and later transposed in the Orange Datamining software, where the cluster and dimensionality reduction analyses were performed using the principal component analysis (PCA) technique. This organization into cells allowed a clearer and more organized visualization of the data, facilitating the identification of patterns and clusters/clusters of electrical response of the sensors to the different gases tested.

Analysis of Statistical Components

In principal component analysis, principal components are the new variables that capture most of the variance of the original dataset. The first principal component (PC1) is the linear combination of the original variables with the greatestpossible variation, i.e. it captures the greatest amount of information contained in theoriginal data set. PC1 is the direction in the variable space with the greatest variationof the data. It represents the largest source of variation in the dataset and is the dimension that best explains the total variance.

The second principal component (PC2) is the linear combination of the original variables with the greatest possible variation, given the constraints of being orthogonal (perpendicular) to PC1. PC2 is the direction in the variable space with the second largest variation of the data and is orthogonal to PC1. It represents the second largest source of variation in the dataset and is the dimension that explains most of the variation that is not explained by PC1. Together, PC1 and PC2 allow you to visualize data in a two-dimensional plane. These new variables are called principal œmponents because they are the principal dimensions that capture most of the variance in the data. The combination of PC1 and 70 PC2 values for each sample allows you to visualize the relationship between the samples and how they group together in relation to the original variable.

In summary, PC1 and PC2 are the first two main components that capture most of the variation in the data. They are used to reduce the dimensionality of the dataset and visualize the relationships between samples in a two-dimensional space. PC1 represents the largest source of variation, while PC2 represents the second largest source of variation and is orthogonal to PC1.

Silhouette Coefficient and Variance

The Silhouette Coefficient in Principal Component Analysis (PCA) is an important factor for clustering/clustering analyses. This silhouette coefficient is a measure of assessing cluster quality, ranging from -1 to 1, where values closer to 1 indicate that the instance (point) is well associated with its group and distant from the other clusters, while values close to -1 indicate that the instance is closer to a neighboring cluster than to its own.

In principal component analysis, the goal is to find the linear combinations of variables that maximize the variance of the data. This is done without considering the grouping structure of the data, which is the focus of the silhouette coefficient. To aid in the quality of a PCA, the measures of proportion of variance allow us to evaluate the effectiveness of the PDA obtained.

Variance is a statistical measure that indicates the dispersion of values around the mean. It is calculated as the mean of the squares of the differences between each value and the corresponding mean. In principal component analysis (PCA), variance is used to identify the amount of variance in the data that is explained by each principal component. The principal components with greater variance explain more information in the data and are therefore extremely relevant for this type of statistical analysis.

REFERENCES

[1] NYLANDER, C.; ARMGARTH, M.; LUNDSTRÖM, I. An ammonia detector based on a conducting polymer. In: Anal. Chem. Symp. Ser. 1983. p. 203- 207.

[2] MAHESH, K.; KARPAGAM, Subramanian; PANDIAN, K. How to design donor–acceptor based heterocyclic conjugated polymers for applications from organic electronics to sensors. Topics in Current Chemistry, v. 377, p.1-39, 2019.

[3] LIU, Xianghong et al. Conducting polymer-based nanostructures for gas sensors. Coordination Chemistry Reviews, v. 462, p. 214517, 2022.

[4] SONG, Ruxin et al. Gas-sensing performance and operation mechanism oforganic π-conjugated materials. ChemPlusChem, v. 84, n. 9, p. 1222-1234, 2019.

[5] DE OLIVEIRA, Vinícius Jessé Rodrigues et al. Using Langmuir-Schaefer deposition technique to improve the gas sensing performance of regiorandom polythiophene films. Sensors and Actuators Reports, v. 4, p. 100094, 2022.

[6] LV, Dawu et al. Emerging poly (aniline co-pyrrole) nanocomposites by in-situ polymerized for high-performance flexible ammonia sensor. Sensors and Actuators A: Physical, v. 349, p. 114078, 2023.

[7] LAWANIYA, Shiv Dutta et al. Functional nanomaterials in flexible gas sensors: recent progress and future prospects. Materials Today Chemistry, v. 29, p. 101428, 2023.

[8] KOLTZENBURG, Sebastian; MASKOS, Michael; NUYKEN, Oskar. Polymer chemistry. Berlin, Germany: Springer, 2017.

[9] CARRAHER Jr., C.E. Polymer chemistry: an introduction, 4th ed., p.348, 1996.

[10] STEVENS, M. P. Basic principles. Polymer Chemistry: An Introduction. NewYork: Oxford University Press Inc, p. 3-34, 1999.

[11] CANEVAROLO JR, Sebastião V. Ciência dos polímeros. Artiliber editora, São Paulo, v. 24, 2002.

[12] HAGE JR, Elias. Aspectos Históricos sobre o Desenvolvimento da Ciência e da Tecnologia de Polímeros. Polímeros, v. 8, p. 6-9, 1998.

[13] MANO, E.B.; MENDES, L.C. Introdução a polímeros, Ed. Edgar Blücher, 2 ed.,Cap 1, 1999.

[14] YOUNG, Robert J.; LOVELL, Peter A. Introduction to polymers. CRC press, 2011

[15] LUNARDI, G.; BRETAS, R.E.S., Polímeros Intrinsecamente Condutores Elétricos. Revista Brasileira de Engenharia Quimica. Vol. 10, nº 3, p. 34-40,1987.

[16] YILMAZ, Faris (Ed.). Conducting polymers. BoD–Books on Demand, 2016.

[17] KARAN, Kunal. Interesting facets of surface, interfacial, and bulk characteristics of perfluorinated ionomer films. Langmuir, v. 35, n. 42, p. 13489-13520, 2019.

[18] ALLEN, R. D.; YILGOR, I.; MCGRATH, J. E. Coulombic Interactions in Macromolecular Systems. In: Eds. A. Eisenberg, F. E. Bailey, ACS Symp. Series. 1986. ch. 6, p. 7214

[19] SCHLICK, Shulamith. Ionomers: characterization, theory, and applications. CRC press, 1996.

[20] TANT, Martin R.; MAURITZ, Kenneth A.; WILKES, Garth L. (Ed.). Ionomers: synthesis, structure, properties and applications. Springer Science & Business Media, 2012.

[21] LONGWORTH, R.; VAUGHAN, Daniel J. Physical structure of ionomers. Nature, v. 218, n. 5136, p. 85-87, 1968.

[22] PINERI, Michel; EISENBERG, Adi (Ed.). Structure and properties of ionomers. Springer Science & Business Media, 2012.

[23] CARVALHO, Antonio JF; CURVELO, Antonio AS. Effect of sulfonation levelon solubility and viscosity behavior of low to medium charged sulfonated polystyrenes. Macromolecules, v. 36, n. 14, p. 5304-5310, 2003.

[24] ANDRADE, Bruna Torres Negreiros Cordeiro; BEZERRA, Augusto Cesar da Silva; CALADO, Claudinei Rezende. Adding value to polystyrene waste bychemically transforming it into sulfonated polystyrene. Matéria (Rio de Janeiro), v. 24, 2019.

[25] KIM, Sung-Kon et al. Manipulating the glass transition behavior of sulfonated polystyrene by functionalized nanoparticle inclusion. Nanoscale, v. 7, n. 19,p. 8864-8872, 2015.

[26] KUCERA, F.; JANCAR, J. Homogeneous and heterogeneous sulfonation of polymers: a review. Polymer Engineering and Science, v.38, n.5, p.783-792,1998.

[27] Andrade, B.T.N.C. Síntese de poliestireno parcialmente sulfonado a partir de resíduos de poliestireno para aplicação como aditivo superplastificante em concretos e argamassas 2017. Dissertação (mestrado) – Centro Federal de Educação Tecnológica de Minas Gerais, Programa de Pós-Graduação em

Engenharia de Materiais, Belo Horizonte, 2017.

[28] SOLOMONS, T.W.G.; FRYHLE, C.B. Química Orgânica, Vol. I. 10. Ed. Rio de Janeiro: LCT, 2012. 648p.

[29] M. B. Smith and J. March, March's Advanced Organic Chemistry: Reactions, Mechanisms, and Structure, John Wiley & Sons, 2007.

[30] RUBATAT, Laurent et al. Structure− properties relationship in proton conductive sulfonated polystyrene− polymethyl methacrylate block copolymers (sPS−PMMA). Macromolecules, v. 41, n. 21, p. 8130-8137, 2008.

[31] PIÑÓN-BALDERRAMA, Claudia et al. Self-Assembly Investigations of Sulfonated Poly (methyl methacrylate-block-styrene) Diblock Copolymer Thin Films. Advances in Polymer Technology, v. 2019, 2019.

[32] KROTO, Harold W. et al. C60: Buckminsterfullerene. nature, v. 318, n. 6042, p.162-163, 1985.

[33] SHERIGARA, Bailure S.; KUTNER, Wlodzimierz; D'SOUZA, Francis. Electrocatalytic properties and sensor applications of fullerenes and carbon nanotubes. Electroanalysis: An International Journal Devoted toFundamental and Practical Aspects of Electroanalysis, v. 15, n. 9, p. 753- 772, 2003.

[34] PAN, Yuan et al. Advances in photocatalysis based on fullerene C60 and its derivatives: Properties, mechanism, synthesis, and applications. AppliedCatalysis B: Environmental, v. 265, p. 118579, 2020.

[35] TAOURI, Lydia et al. Fullerene-MWCNT nanostructured-based electrochemical sensor for the detection of Vanillin as food additive. Journalof Food Composition and Analysis, v. 100, p. 103811, 2021.

[36] RUOFF, R. S. et al. Solubility of fullerene (C60) in a variety of solvents. The Journal of Physical Chemistry, v. 97, n. 13, p. 3379-3383, 1993.

[37] SIVARAMAN, N. et al. Solubility of C70 in organic solvents. Fullerenes, Nanotubes, and Carbon Nanostructures, v. 2, n. 3, p. 233-246, 1994.

[38] SARICIFTCI, Niyazi S. et al. Photoinduced electron transfer from a conducting polymer to buckminsterfullerene. Science, v. 258, n. 5087, p. 1474-1476, 1992

[39] YU, Gang et al. Polymer photovoltaic cells: enhanced efficiencies via a networkof internal donor-acceptor heterojunctions. Science, v. 270, n. 5243, p. 1789-1791, 1995.

[40] GU, Jinan; YUAN, Jianyu; MA, Wanli. Correlation between polymer molecular weight and optimal fullerene content in efficient polymer solar cells. Organic Electronics, v. 34, p. 229-236, 2016.

[41] DANG, Minh Trung; HIRSCH, Lionel; WANTZ, Guillaume. P3HT: PCBM, best seller in polymer photovoltaic research. Advanced Materials, v. 23, n. 31, p. 3597-3602, 2011.

[42] LI, Fei et al. Complementary hydrogen bonding and block copolymer self- assembly in cooperation toward stable solar cells with tunable morphologies.Macromolecules, v. 46, n. 22, p. 9021-9031, 2013.

[43] GUO, Fei et al. High-performance semitransparent perovskite solar cells with solution-processed silver nanowires as top electrodes. Nanoscale, v. 7, n. 5,p. 1642-1649, 2015.

[44] CHEN, Dian et al. P3HT/PCBM bulk heterojunction organic photovoltaics: correlating efficiency and morphology. Nano letters, v. 11, n. 2, p. 561-567,2010.

[45] CAMPOY-QUILES, Mariano et al. Morphology evolution via self-organizationand lateral and vertical diffusion in polymer: fullerene solar cell blends. Nature materials, v. 7, n. 2, p. 158, 2008.

[46] PIERSIMONI, Fortunato et al. Influence of fullerene photodimerization on the PCBM crystallization in polymer: Fullerene bulk heterojunctions under thermal stress. Journal of Polymer Science Part B: Polymer Physics, v. 51, n. 16, p. 1209-1214, 2013.

[47] YANG, Yingkui et al. Graphene-based materials with tailored nanostructures for energy conversion and storage. Materials Science and Engineering: R:Reports, v. 102, p. 1-72, 2016.

[48] CHOE, Hochull et al. Patent citation network analysis for the domain of organic photovoltaic cells: Country, institution, and technology field. Renewable and Sustainable Energy Reviews, v. 26, p. 492-505, 2013.

[49] ASSUNÇÃO, Ivan Carlos Cruz. Desenvolvimento de dispositivos orgânicos de óxido de grafeno para conversão de energia solar. 2016. Tese de Doutorado.

[50] PRATO, Maurizio. Fullerene polymers: synthesis, properties and applications. John Wiley & Sons, 2009.

[51] HARRIS, Peter JF. Fullerene polymers: a brief review. C, v. 6, n. 4, p. 71, 2020.

[52] GIACALONE, Francesco; MARTIN, Nazario. Fullerene polymers: synthesis and

properties. Chemical reviews, v. 106, n. 12, p. 5136-5190, 2006.

[53] HIORNS, Roger C. et al. Main-chain fullerene polymers for photovoltaicdevices. Macromolecules, v. 42, n. 10, p. 3549-3558, 2009.

[54] HIORNS, Roger C. et al. Synthesis of donor− acceptor multiblock copolymers incorporating fullerene backbone repeat units. Macromolecules, v. 43, n. 14,p. 6033-6044, 2010.

[55] RAMANITRA, Hasina H. et al. Increased thermal stabilization of polymer photovoltaic cells with oligomeric PCBM. Journal of Materials Chemistry C, v. 4, n. 34, p. 8121-8129, 2016.

[56] APICELLA, A. et al. Poly (ethylene oxide) (PEO) and different molecular weight PEO blends monolithic devices for drug release. Biomaterials, v. 14,n. 2, p. 83-90, 1993.

[57] COLLAZOS, Stephanie Ortiz. Filmes de Langmuir de Ésteres de Polietilenoglicol derivados de ácidos graxos. 2015. Tese de Doutorado. PUC-Rio.

[58] DAI, Sheng; TAM, Kam Chiu. Laser light scattering and isothermal titration calorimetric studies of poly (ethylene oxide) aqueous solution in presence ofsodium dodecyl sulfate. Journal of colloid and interface science, v. 292, n. 1, p. 79-85, 2005.

[59] BURGAZ, Engin. Poly (ethylene-oxide) /clay/silica nanocomposites: Morphology and thermomechanical properties. Polymer, v. 52, n. 22, p. 5118-5126, 2011.

[60] YAU, Hin Chun et al. Diamond Rings or Dumbbells: Controlling the Structure of Poly (ethylene glycol)–Fullerene [60] Adducts by Varying Linking ChainLength. Macromolecules, v. 47, n. 15, p. 4870-4875, 2014.

[61] HUIQIU, Zhang et al. Photoelectric properties of C60-poly (ethylene glycol) andpoly (3, 4-ethylenedioxythiophene) composite gel prepared via a low- temperature organic-solvent process. Polymer Journal, v. 48, n. 2, p. 163- 168, 2016.

[62] MOSELEY, Pat T. Solid state gas sensors. Measurement Science and technology, v. 8, n. 3, p. 223, 1997.

[63] FENG, Shaobin et al. Review on smart gas sensing technology. Sensors, v. 19, n. 17, p. 3760, 2019.

[64] MAHMOOD, Lubna; GHOMMEM, Mehdi; BAHROUN, Zied. Smart Gas Sensors: Materials, Technologies, Practical Applications, and Use of Machine Learning–A Review. Journal of Applied and Computational Mechanics, v. 9, n. 3, p. 775-

803,2023.

[65] SCHALLER, Emmanuelle; BOSSET, Jacques O.; ESCHER, Felix. 'Electronic noses' and their application to food. LWT-Food Science and Technology, v. 31, n. 4, p. 305-316, 1998.

[66] VADALA, Rohit et al. A review on electronic nose for diagnosis and monitoring treatment response in lung cancer.Journal of Breath Research, 2023.

[67] S.-W. Chiu, H.-C. Wu, T.-I. Chou, H. Chen, and K.-T. Tang, "A miniature electronic nose system based on an MWNT–polymer microsensor array and a low-power signal-processing chip," Anal. Bioanalytical Chem., vol. 406, no. 16, pp. 3985–3994, 2014.

[68] K.-T. Tang et al., "24.5 A 0.5 v 1.27 mW nose-on-a-chip for rapid diagnosis of ventilator-associated Pneumonia," in Proc. IEEE Int. Solid-State Circuits Conf. Dig. Tech. Papers, 2014, pp. 420–421

[69] S. Zhang, X. Li, M. Zong, X. Zhu, and R. Wang, "Efficient kNN classification with different numbers of nearest neighbors," IEEE Trans. neural Netw. Learn. Syst., vol. 29, no. 5, pp. 1774–1785, May 2018

[70] K.-T. Tang, S.-W. Chiu, M.-F. Chang, C.-C. Hsieh, and J.-M. Shyu, "A low-power electronic nose signal-processing chip for a portable artificial olfaction system," IEEE Trans. Biomed. Circuits Syst., vol. 5, no. 4, pp. 380–390, Aug. 2011.

[71] WANG, Huaping et al. Gas sensing materials roadmap. Journal of Physics: Condensed Matter, v. 33, n. 30, p. 303001, 2021.

[72] BHATTACHARYA, Shantanu et al. Introduction to sensors for aerospace and automotive applications. Sensors for automotive and aerospace applications,p. 1-6, 2019.

[73] NASIRI, Noushin; CLARKE, Christian. Nanostructured chemiresistive gassensors for medical applications. Sensors, v. 19, n. 3, p. 462, 2019.

[74] RÓDENAS GARCÍA, Milagros et al. Review of low-cost sensors for indoor air quality: Features and applications. Applied Spectroscopy Reviews, v. 57, n.9-10, p. 747-779, 2022.

[75] DAS, Om Prakash et al. Development and Performance Analysis of a Portable NO x Gas Sensor for Environmental Monitoring Applications. In: 2023 International Conference in Advances in Power, Signal, and InformationTechnology (APSIT).

IEEE, 2023. p. 499-504.

[76] KOROTCENKOV, Ghenadii. Handbook of gas sensor materials. Conventional approaches, v. 1, 2013.

[77] LIU, Xiao et al. A survey on gas sensing technology. Sensors, v. 12, n. 7, p.9635-9665, 2012.

[78] PREETHICHANDRA, D. M. G. et al. Conducting Polymer Based Ammonia and Hydrogen Sulfide Chemical Sensors and Their Suitability for Detecting Food Spoilage. Advanced Materials Technologies, v. 8, n. 4, p. 2200841, 2023.

[79] OLIVEIRA, Matheus Dias et al. Ammonia emission in poultry facilities: a review for tropical climate areas. Atmosphere, v. 12, n. 9, p. 1091, 2021.

[80] MACATANGAY, Ariel V.; PROKHOROV, Kimberlee S.; SWETERLITSCH, Jeffrey J. Strategies to mitigate ammonia release on the International SpaceStation. SAE Transactions, p. 344-355, 2007.

[81] TIMMER, Björn; OLTHUIS, Wouter; VAN DEN BERG, Albert. Ammonia sensors and their applications—a review. Sensors and Actuators B:Chemical, v. 107, n. 2, p. 666-677, 2005.

[82] HURTADO, JL Martinez; LOWE, C. R. Ammonia-sensitive photonic structures fabricated in nafion membranes by laser ablation. ACS Applied Materials & Interfaces, v. 6, n. 11, p. 8903-8908, 2014.

[83] MCGRATH, Michael J. et al. Sensing and sensor fundamentals. Sensor technologies: Healthcare, wellness, and environmental applications, p. 15- 50, 2013.

[84] CELIESIUTE, Raimonda et al. Electrochromic sensors based on conducting polymers, metal oxides, and coordination complexes. Critical Reviews in Analytical Chemistry, v. 49, n. 3, p. 195-208, 2019.

[85] TIMMER, Björn; OLTHUIS, Wouter; VAN DEN BERG, Albert. Ammonia sensors and their applications—a review. Sensors and Actuators B:Chemical, v. 107, n. 2, p. 666-677, 2005.

[86] YOON, Hyeonseok; JANG, Jyongsik. Conducting-polymer nanomaterials for high-performance sensor applications: issues and challenges. Advanced Functional Materials, v. 19, n. 10, p. 1567-1576, 2009

[87] KUSHWAHA, Chandra Shekhar et al. Advances in conducting polymer nanocomposite based chemical sensors: An overview. Materials Science and Engineering: B, v. 284, p. 115856, 2022.

[88] YAQOOB, Usman; YOUNIS, Mohammad I. Chemical gas sensors: Recent developments, challenges, and the potential of machine learning—A review. Sensors, v. 21, n. 8, p. 2877, 2021.

[89] RAJU, Parameswari; LI, Qiliang. Semiconductor materials and devices for gas sensors. Journal of The Electrochemical Society, v. 169, n. 5, p. 057518, 202

[90] SHARMA, Asha et al. Recent advances in tin oxide nanomaterials as electrochemical/chemiresistive sensors. Journal of the Electrochemical Society, v. 168, n. 2, p. 027505, 2021.

[91] BAI, Hua; SHI, Gaoquan. Gas sensors based on conducting polymers. Sensors, v. 7, n. 3, p. 267-307, 2007.

[92] SAXENA, Vibha et al. Room temperature operated ammonia gas sensor using polycarbazole Langmuir–Blodgett film. Sensors and Actuators B: Chemical,v. 107, n. 1, p. 277-282, 2005.

[93] A. G. MacDiarmid, Angewandte Chemie International Edition, 40(14), 2581 (2001).

[94] S. A. Waghuley, S. M. Yenorkar, S. S. Yawale, and S. P. Yawale, Sensor Actuat B-Chem, 128(2), 366 (2008).

[95] C. M. Hangarter, N. Chartuprayoon, S. C. Hernandez, Y. Choa, and N. V. Myung, Nano Today, 8(1), 39 (2013).

[96] WONG, Yung Cheng et al. Conducting polymers as chemiresistive gas sensing materials: A review. Journal of the Electrochemical Society, v. 167, n. 3, p. 037503, 2020.

[97] Y. F. Wang, M. Hu, J. R. Liang, X. C. Liu, and Z. S. Wang, J Electrochem Soc, 163(14), B732 (2016)- N. H. Al-Hardan, M. J. Abdullah, A. A. Aziz, H. Ahmad, and L. Y. Low, Vacuum, 85(1), 101 (2010).]

[98] H. Bai and G. Q. Shi, Sensors-Basel, 7(3), 267 (2007).

[99] J. L. Bredas and G. B. Street, Accounts Chem Res, 18(10), 309 (1985)

[100] N. V. Bhat, A. P. Gadre, and V. A. Bambole, J Appl Polym Sci, 88(1), 22 (2003)

[101] X. Yan, Z. Han, Y. Yang, and B. Tay, Sensors and Actuators B: Chemical, 123(1), 107 (2007).

[102] M. M. Arafat, B. Dinan, S. A. Akbar, and A. S. Haseeb, Sensors (Basel), 12(6), 7207 (2012)

[103] E. Espid, B. Adeli, and F. Taghipour, J Electrochem Soc, 166(5), H3223 (2019).

[104] S. Q. Li, P. F. Lin, L. P. Zhao, C. Wang, D. Y. Liu, F. M. Liu, P. Sun, X. S. Liang, F. M. Liu, X. Yan, Y. Gao, and G. Y. Lu, Sensor Actuat B-Chem, 259 505 (2018).

[105] A. T. Mane, S. T. Navale, S. Sen, D. K. Aswal, S. K. Gupta, and V. B. Patil, Org Electron, 16, 195 (2015).

[106] YAN, Fadong et al. Semitransparent OPV modules pass environmental chambertest requirements. Solar energy materials and solar cells, v. 114, p. 214-218,2013.

[107] KUMAR, Archana Kaliyaraj Selva et al. A mini-review: How reliable is the drop casting technique. Electrochemistry Communications, v. 121, p. 106867, 2020.

[108] HALL, David B.; UNDERHILL, Patrick; TORKELSON, John M. Spin coatingof thin and ultrathin polymer films. Polymer Engineering & Science, v. 38, n. 12, p. 2039-2045, 1998.

[109] SHARMA, Sandeep K. et al. Lactose biosensor based on Langmuir–Blodgett films of poly (3-hexyl thiophene). Biosensors and Bioelectronics, v. 20, n. 3, p. 651-657, 2004

[110] SILVA, Edilene Assunção da. Effect of the addition of amphiphilic moleculeson the formation of Langmuir and Langmuir-Blodgett films of alkylated polythiophene derivatives: application in sensors. 2014

[111] MCCULLOUGH, Richard D. The chemistry of conducting polythiophenes. Advanced materials, v. 10, n. 2, p. 93-116, 1998.

[112] GUIMARAES, Juliana Aguilar. Study of Langmuir and Langmuir-Blodgett films aiming at the development of cholesterol biosensor. UFRJ-COPPE, Rio de Janeiro, 2009.

[113] BONARDI, Claudia; OLIVEIRA JUNIOR, Osvaldo Novais de. Surface potential of langmuir and langmuir-blodgett films. 1995.

[114] Mattoso, L. H. C., Ferreira, M., Oliveira Jr, O. N. (1994). Langmuir Films of

Conductive Polymers. *Polymers: Science and Technology*. 23–34. Taken from http://revistapolimeros.org.br/files/v4n2/v4n2a02.pdf.

[115] H. S. Makowski, R. D. Lundberg and G. H. Singhal, U.S. Pat. 3,870,841, (1975).

[116] CARVALHO, Antonio JF et al. Synthesis of Poly (styrene-co-methyl methacrylate)-Based Ionomers and Their Langmuir and Langmuir− Blodgett (LB) Film Formation. The Journal of Physical Chemistry B, v. 108, n. 22, p. 7033-7039, 2004.

[117] YU, Xinyue; CAO, Xiao; CHEN, Quan. Rheological properties of sulfonated polystyrene ionomers at high-ion contents. Rheologica Acta, v. 60, p. 241-249, 2021.

[118] MÜLLER-BUSCHBAUM, P. et al. Solvent-induced surface morphology of thin polymer films. Macromolecules, v. 34, n. 5, p. 1369-1375, 2001.

[119] CHOI, Mi-Ri et al. Polyaniline-based conducting polymer compositions with ahigh work function for hole-injection layers in organic light-emitting diodes:

[120] KHAN, Mohd Taukeer et al. Effect of traps on the charge transport in semiconducting polymer PCDTBT. Solid-State Electronics, v. 145, p. 49- 53, 2018.

[121] OLIVEIRA, Vinicius Jessé Rodrigues de. Fabricação e caracterização de plataformas sensoriais baseadas em polímeros conjugados e nanotubos de carbono para detecção de gases. 2023.

[122] VOLPATI, Diogo. Filmes nanoestruturados aplicados ao sistema de língua eletrônica: um estudo de interfaces. 2012.

[123] PAYAMYAR, Payam et al. Synthesis of a covalent monolayer sheet by photochemical anthracene dimerization at the air/water interface and its mechanical characterization by AFM indentation.Advanced materials, v. 26, n. 13, p. 2052-2058, 2014.

[124] MURRAY, Daniel J. et al. Large area synthesis of a nanoporous two-dimensional polymer at the air/water interface.Journal of the American Chemical Society, v. 137, n. 10, p. 3450-3453, 2015.

[125] SAHABUDEEN, Hafeesudeen et al. Wafer-sized multifunctional polyimine-based two-dimensional conjugated polymers with high mechanical stiffness.Nature Communications, v. 7, n. 1, p. 13461, 2016.

[126] DEY, Kaushik et al. Selective molecular separation by interfacially crystallized covalent organic framework thin films. Journal of the American Chemical Society, v. 139, n. 37, p. 13083-13091, 2017.

[127] MÜLLER, Vivian et al. A two-dimensional polymer synthesized at the air/water interface. Angewandte Chemie International Edition, v. 57, n. 33, p. 10584-10588, 2018.

[128] LIU, Kejun et al. On-water surface synthesis of crystalline, few-layer two-dimensional polymers assisted by surfactant monolayers. Nature chemistry, v. 11, n. 11, p. 994-1000, 2019.

[129] Interfacial Polymerization: From Chemistry to Functional Materials', Feilong Zhang, Jun-bing Fan, and Shutao Wang, Angew. Chem. Int. Ed., 2020, 59, 21840.

[130] WANG, Meihui et al. Single-crystal, large-area, fold-free monolayer graphene.Nature, v. 596, n. 7873, p. 519-524, 2021.

[131] E. F. Lutz, 'The Cyclic Trimerization of Acetylenes Over a Ziegler Catalyst'*J. Chem. Am. Soc.*, 1961, *83*, 2551.

[132] Jockusch, S.; Landis, M. S.; Freiermuth, B.; Turro, N. J., Photochemistry and photophysics of α-hydroxy ketones. Macromolecules 2001, 34 (6), 1619- 1626.